A NOVEL FRAMEWORK FOR SYSTEM IDENTIFICATION, SIMULATION AND CONTROL

A Dissertation

by

YULING SHEN

Submitted to the Graduate and Professional School of
Texas A&M University
in partial fulfillment of the requirements for the degree of

DOCTOR OF PHILOSOPHY

Chair of Committee,	Robert E. Skelton
Co-Chair of Committee,	Majji Manoranjan
Committee Members,	Raktim Bhattacharya
	Dileep Kalathil
Head of Department,	Ivett Leyva

December 2021

Major Subject: Aerospace Engineering

Copyright 2021 Yuling Shen

ABSTRACT

This research is aimed at making contributions in three fundamental problems in systems and control. The problems are broadly known as system identification, optimal simulation and data-based control. The system identification problem involves the inverse problem of developing the dynamics model of a system from input/output experimental data. The system simulation problem pertains to the use of numerical simulations in predicting model response for a complex dynamical system, while the data-based control problem is aimed at deriving certain control inputs based on empirical response data to direct the system to elicit a desired response from it.

Q-Markov covariance equivalent realization (QMC) is a system identification approach that matches exactly the first q Markov parameters and covariance parameters of a system with a pre-specified positive scalar q. Existing QMC methods possess two deficiencies. First, they are not applicable system identification of unstable systems. Second, they find infinite numbers of solutions and do not provide a means to choose the best solution. The first result of this research develops a new QMC formulation that extends the existing QMC methods for identification of unstable systems. This new QMC formulation is derived over closed-loop dynamics as an observer and does not pose any constraints on the stability of the system to identify. In addition, this research presents a methodology to determine an efficient QMC solution and a general algorithm for system identification applications using the QMC method.

When dynamic systems are simulated on the computer, the numerical values of the outputs and states are corrupted by round-off errors. The second set of results of this research aims at finding the simulation model that gives optimal performance under finite precision computing. This research provides two approaches to tackle this problem. The first approach formulates the problem into three linear matrix inequalities (LMIs) plus a non-convex constraint and transforms it into a feedback control problem. It becomes solvable numerically via the LMI toolbox after convexification and guarantees convergence to a local optimum. The second approach focuses on simulation applications of flexible structures in modal coordinates. It finds the simulation model

with the optimal size via truncation of modes.

A data-based control law for reference tracking applications is developed as the third result of this research. This control law finds an optimal input sequence that minimizes a quadratic weighted cost function consisting of tracking errors and input increments. Its effectiveness is demonstrated using an application involving the morphing control of a tensegrity airfoil.

DEDICATION

This dissertation is dedicated to my family and my fiancée for all the patience and love.

ACKNOWLEDGMENTS

I am a lucky person. Born in a family that doesn't have to worry about food and clothing, I have parents who have always supported me, grandparents who thought of me, and the right person at the right age to spend my life with. At the same time, I went to school with smooth sailing. Occasionally encountered some minor difficulties, I could always solve the problems smoothly with the help of the people around me. In the road of life, I did not take too many detours. I have seen primarily kind human beings and a wonderful world.

However, I fully realize that the world is not as good as I have seen. In the past two years, many disasters, such as the raging covid-19 epidemic, the widespread Australian fire, and the unprecedented explosion in Lebanon, have destroyed the lives of many unfortunate people. Nearly 3.4 billion people live on less than $6 a day, wars and riots occur, and many other issues are changing the world in ways that we don't even know how they will end, sometimes for the better or worse.

I am writing this down to alert me of my responsibility. I am about to leave the campus and enter the complicated but real world. I shall not take for granted what I obtained today or what I will achieve in the future. I shall keep in mind that there are people that are more deserving than me. They are not as lucky as I am since they may not have access to my opportunities. Also, I shall keep in mind that no act of kindness is ever wasted, no matter how small. The present determines the future. To make the world a better place requires every action and every bit of determination in the present.

In addition, I would like to thank the following people who have been crucial to me in doctoral education.

I wish to express my sincere appreciation to my advisor, Prof. Robert E. Skelton. He is a role model in both life and work. From him, I understood that the education of a Ph.D. is not only about research but also the ways of thinking and discovering. As he always said, most of the up-to-date knowledge will expire within five years, but the method of acquiring knowledge will not. Eight

years ago, Prof. Skelton offered me the first project that introduced me to academic research when I was still an undergraduate student. Four years ago, Prof. Skelton invited me to his research team, where I eventually completed my education. This long journey is lovely and meaningful that I will never forget.

I also wish to thank my co-advisor, Prof. Manoranjan Majji. He is an acute and knowledgeable scholar. He can easily distinguish if a problem is worthwhile and foresee possible applications. His diligence in work and time management skills has set an excellent example for me. Beyond that, Prof. Majji is a great teacher who explains complex concepts clearly. Techniques that he taught in lectures are practical. Some of them have benefited me in research till now. Prof. Majji advises two key chapters in this dissertation. I will not be able to complete this dissertation without assistance from him.

I want to thank Prof. Raktim Bhattacharya and Prof. Dileep Kalathil for serving as my committee members. I audited his lecture, Design of Advanced Flight Control Systems, in my second year as a Ph.D. student. This lecture laid the foundation for my future research in system theory. Prof. Kalathil is an expert in computer science who always provides insights from different perspectives. He suggested career planning during our first meeting, which has been influential to me till now.

I want to thank Mrs. Gail Rowe, who has always been available whenever I needed help and solved real problems for me. There was a period that I traveled to China, and it took five months to receive my US visa. Everything needed to start over when I returned. Gail has been accommodating at that time in the employment continuum, getting me reacquainted with the program, exemption from the AESS seminar attendances while I was away, etc. She has made my life as a Ph.D. student much comfortable.

I want to express special gratitude to my family. My parents, Mr. Wenzhong Shen and Mrs. Chunmei Chen have supported me as an international student to study in the United States, both financially and emotionally. My Grandparents, Mr. Tonggen Shen and Mrs. Qinbao Jiang, loved me selflessly. My grandma, Mrs. Fengbao Chen, who is currently suffering from cancer, told

me not to return halfway but to complete my study. My fiancée, Miss Qian Wang, is the one I sincerely feel sorry for. We have been separated in different countries for seven years. I am glad we are always warmly connected from daily calls and sharing of joys. It is my fortune to have earned her support and love.

Last but not least, I would like to thank the great colleagues that I have been working with. Dr. Muhao Chen has been very helpful in the discussion of research problems. Dr. Roman Goyal provided decent feedbacks during group meetings. Mr. Ran Wang is beneficial not only in academics but also in life. Mr. Jiacheng Zhang is a great programmer from whom I learned a lot.

CONTRIBUTORS AND FUNDING SOURCES

Contributors

This work was supported by a dissertation committee consisting of Professors Robert E. Skelton, Prof. Manoranjan Majji and Prof. Raktim Bhattacharya of the Department of Aerospace Engineering and Professor Dileep Kalathil of the Department of Electrical & Computer Engineering.

Part of this research was conducted as a collaborative work. The topology and dynamic description of the tensegrity airfoil depicted in Chapter 5 was conducted by Dr. Muhao Chen.

All other work conducted for the dissertation was completed by the student independently.

Funding Sources

Graduate study was supported by a graduate research assistantship and AERO Grad Excellence fellowship from the Department of Aerospace Engineering, Texas A&M University.

NOMENCLATURE

QMC	q-Markov Covariance Equivalent Realization
ERA	Eigensystem Realization Algorithm
ERA/DC	Eigensystem Realization Algorithm Using Data Correlations
ZOH	Zero Order Hold
LQG	Linear Quadratic Gaussian
m	Number of Outputs
r	Number of Inputs
n	Effective State Dimension of System of Interest
γ	Simulation Model Size
β	Fractional Bit Number
α	Error Covariance Scalar
$\{A, B, C, D\}$	System of Interest
$\{\hat{A}, \hat{B}, \hat{C}, \hat{D}\}$	QMC System
$\{\bar{A}, \bar{B}, C, D\}$	Observer QMC System
$\{A_e, B_e, C_e, D_e\}$	ERA System
$\{A_d, B_d, C_d, D_d\}$	ERA/DC System
$\{A_s, B_s, C_s, D_s\}$	Simulation System
$\{\tilde{A}, \tilde{B}, \tilde{C}, \tilde{D}\}$	Error Assembly System
$\{A_l, B_l, C_l, D_l\}$	Modal Coordinate System

TABLE OF CONTENTS

Page

LIST OF FIGURES

LIST OF TABLES

TABLE Page

1. INTRODUCTION AND LITERATURE REVIEW

The interaction of dynamical systems and data poses three distinct sets of problems of interest to the analyst. The knowledge of the inputs and outputs (I/O) associated with a dynamic system enables us to discover the system's dynamics via the I/O signal relationships. The set of inverse problems are known as system identification approaches. With the knowledge of the system's dynamics and input signals, one may predict the system responses. This is the system simulation problem. Alternatively, based on the data analytic relationships between output and input signals, control algorithms may be designed to make the system behave as expected, which is the data-based control problem. A relationship among these three key elements is depicted in Figure 1.1. These three problems, and their relationships via signal analysis are the subject of this work.

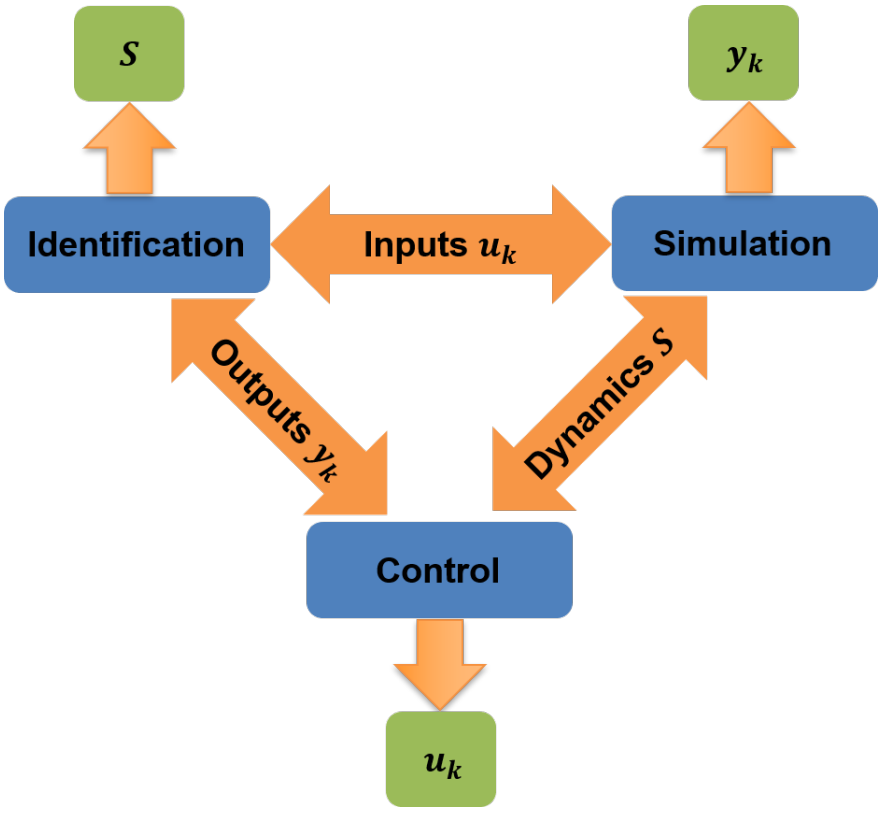

Figure 1.1: Three fundamental problems in systems and control.

1.1 System Identification Problem

System identification explorations were desired during the 1960s after Kalman introduced the state-space realization. Extensive research on system identification methods is documented in the literature [1, 2]. Ho and Kalman presented the first solution to find the minimal state-space representation using impulse response data in 1966 [3]. This approach paved the way for the subspace identification technique, one of the prevailing techniques to date. General system identification approaches for a black box system fall into two categories: those that seek a least square solution of all measurements, such as Eigensystem Realization Algorithm (ERA) [4] or Dynamic Mode Decomposition (DMD) [5], and those seek an exact match of some but not all properties, such as q-Markov Covariance Equivalent Realization (QMC) [6, 7]. Frequency domain approaches also exist in the literature [8].

Based upon Ho-Kalman's method, the ERA became popular in the identification of flexible structures ever since its appearance in 1985 [4]. It finds a least square solution that minimizes the error norms between two sequential Hankel matrices, constructed using input-output cross-correlations. An extension of that called ERA/DC considers data correlation was developed in 1987 [9].

Instead of finding a least square solution, the QMC method [10, 11] finds all state-space realizations that exactly match the first several cross-correlations and auto-correlations, or namely Markov parameters and covariance parameters, up to a positive scalar q. Markov parameters and covariance parameters characterize the transient and steady-state properties of a system respectively. Therefore a QMC realization maintains both transient and steady-state properties of the system one aims to identify. QMC is particularly useful in system identification applications of non-minimum phase physics [12–14]. Model reduction applications of the QMC approach that have performance requirements on steady-state output covariance, such as pointing control or vibration control, have also been studied [13, 15].

A comparison among the ERA, ERA/DC, QMC, and another method developed by Moonen *et al.* was conducted to identify a Mini-Mast structure [16, 17]. This study concluded that ERA/DA

gives the best results of the four methods. This comparison found that ERA and ERA/DC are perfect identification for a noise-free system, while QMC demands more computation time to approach the same accuracy. This added computation is mainly used in finding converged auto-correlations and cross-correlations. However, the computation cost is not as significant these days with advances in microelectronics and embedded computing.

The QMC method is significantly developed over the past decades. Figure 1.2 shows the general concept of system identification using the QMC method, and Figure 1.3 shows the key ideas of the QMC formulation. Liu and Skelton [6, 7] present their new formulation of QMC to parameterize QMC solutions. Skelton and Shi show how to determine a weighted QMC model with noisy measurements [18]. This approach was applied to the identification and control of NASA'S ACES structure [13]. Zhu *et al.* show the method to find QMC systems using pseudo-random binary signals [19]. Li and Skelton extended the QMC method for finite precision implementations by introducing round-off errors into the QMC parameterization [20]. Majji studied the time-varying applications for QMC systems [21]. Although many efforts have been made, two problems remain unsolved in the current formulation of the QMC method.

The first problem is "how to find a QMC approximation model for an unstable system?" Existing QMC methods use the steady state discrete algebraic Lyapunov stability equation governing state covariance during derivations. A steady solution exists for this equation only for stable dynamical systems. The QMC approach finds all stable linear models whose state covariance is the identity matrix that matches the given set of data. Therefore, an identified system estimated by existing QMC methods is always stable. A stable approximation can hardly capture the majority of information associated with the unstable part of the system. If the given data comes from an unstable system, existing QMC methods may not recognize the physics well. This problem is solved in the second chapter of this dissertation.

The second problem is "how to find the most efficient QMC solution among the set of infinite solutions?" Existing QMC methods contain a free unitary variable, and find all linear stable systems that match the given set of Markov and covariance parameters up to q. Unfortunately there is no

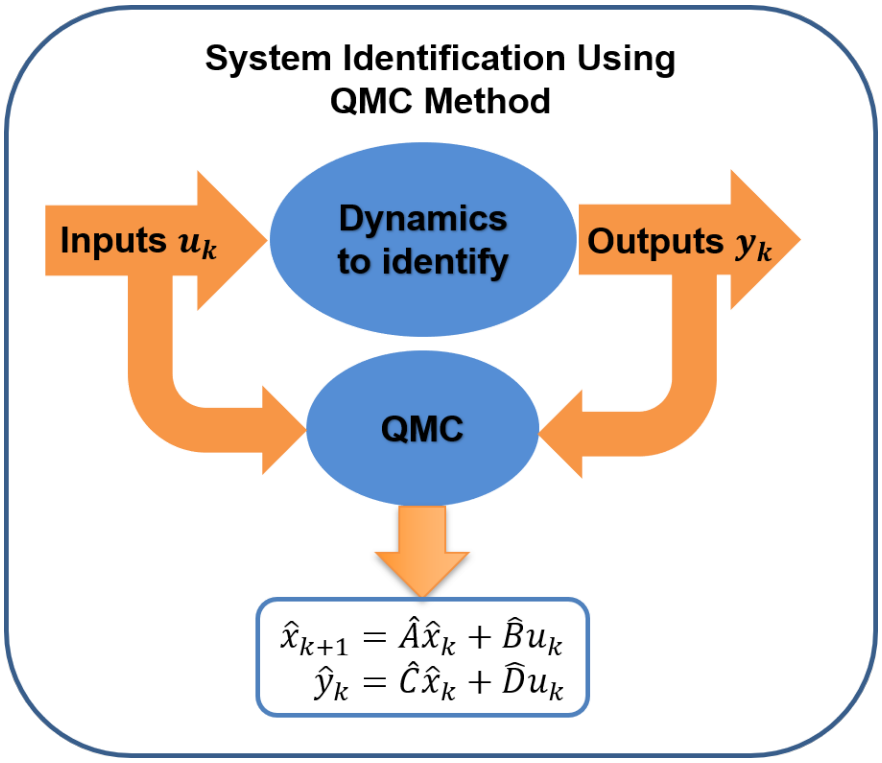

Figure 1.2: System identification using the QMC method.

clear measure to define the free unitary variable. Matching q parameters does not guarantee to match the parameters associated with the physics model. The problem of finding the QMC solution that matches the transfer function of the physics is detailed in the third chapter of this dissertation.

1.2 System Simulation Problem

We describe this world using mathematical models for purposes of estimation and control. The disciplines we learned from universities suggest that we should put more and more physics in the model to get the most accurate model. Well, if we look at physics, we might say yes. Modeling is not just about the physics. The world is infinitely complex, but our ability to predict or explain the world comes through imperfect laws of physics, imperfect models of physical laws, and imperfect computations of the model. Suppose we have got the best model from physics, the computer is going to make errors: round-off errors and truncation errors. A system simulation based upon round-off errors and truncation errors is inaccurate. Figure 1.4 depicts this fact. We

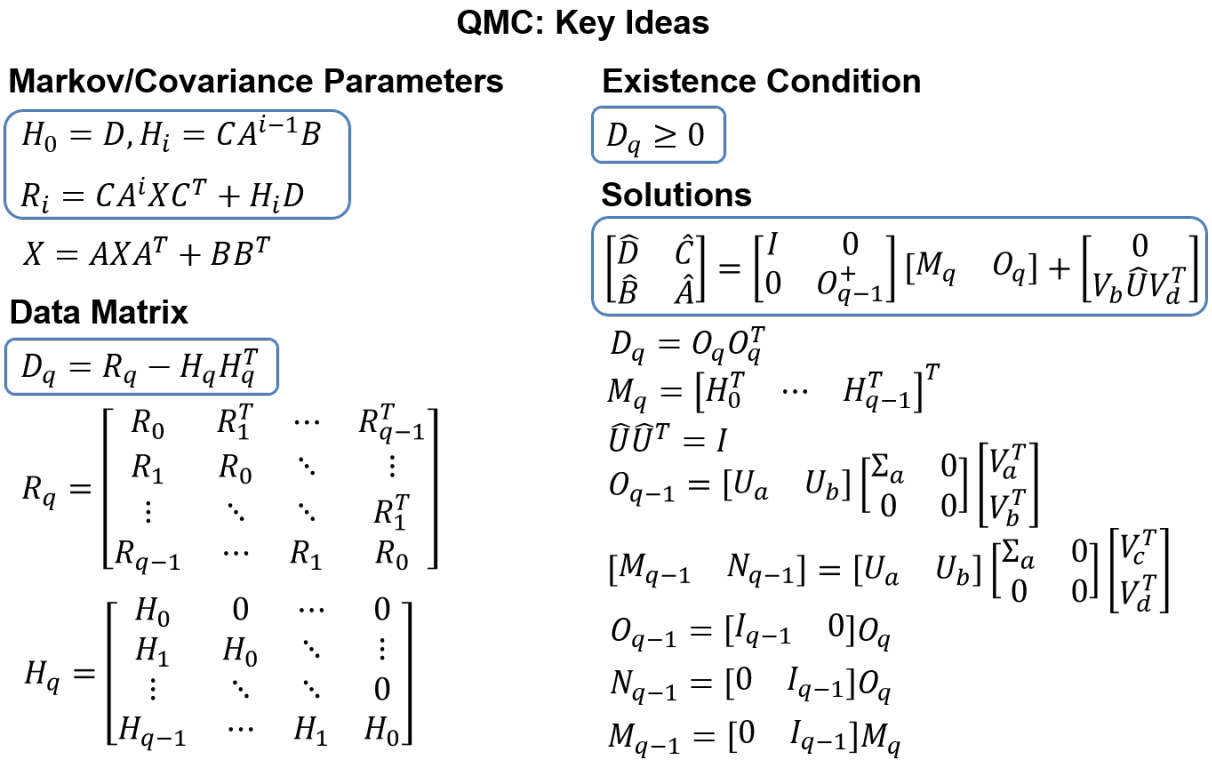

Figure 1.3: Key ideas of the QMC method.

have to integrate signal processing to derive an adequate model of any engineering system, in addition to respecting the physical laws.

Emerges in the 1960s, finite precision computing is as old as the computer itself. Some researchers focused on reducing the effects of finite word length effects by seeking an optimal realization of the exact physics. In 1976 and 1977, Mulis and Roberts and Hwung first revealed the influence of round-off errors on digital filter performance and proved that there exists a coordinate transformation matrix that minimizes round-off noise effects [22, 23]. Williamson and Kadiman included arithmetic errors in the linear quadratic regulator (LQR) controllers [24]. Some other researchers focused on reducing model sizes to match key parameters. The reduced basis method, balancing method, and q-Markov cover are several of them [2, 6, 25, 26]. The work by Li and Skelton presented a methodology to compute all the linear state-space models matching input/output cross-correlations and output auto-correlations up to a specified positive scalar q in finite precision

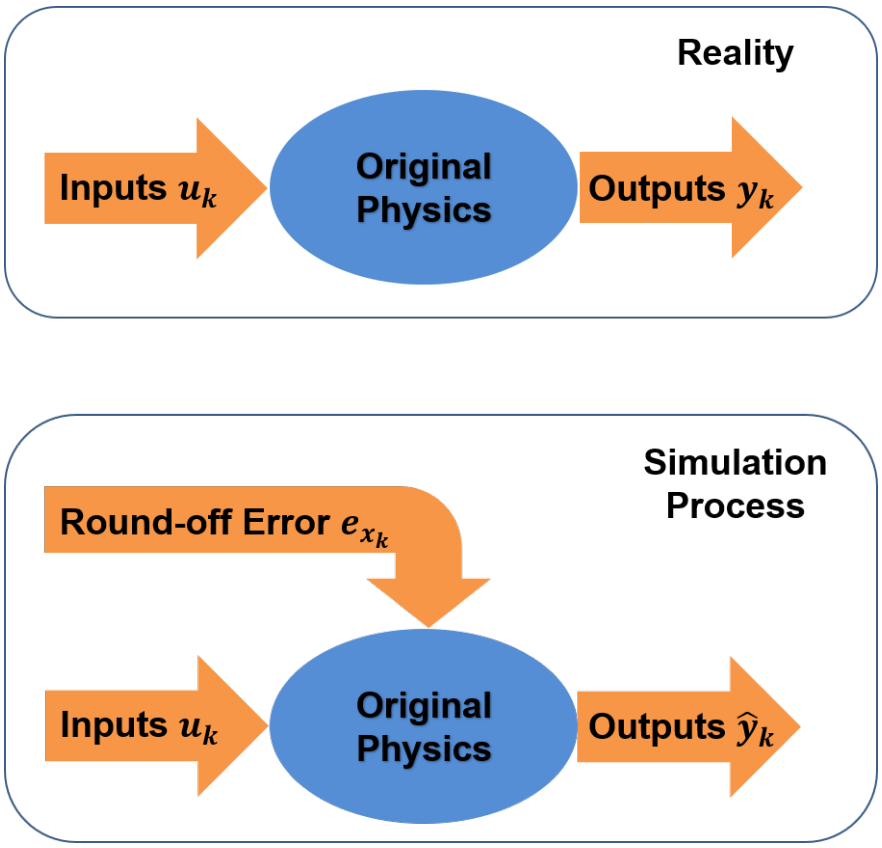

Figure 1.4: System simulation process with finite precision effects.

environments, yet sometimes it is impossible to find one with a large q [20].

However, sufficient attention to signal processing techniques was not paid by the control engineers. For example, the original Hubble Space Telescope (HST, launched on April 25, 1990) controller was designed assuming infinite precision computing. The pointing accuracy (ratio of pointing variance to control variance) of HST was not better than any earth-based space telescopes, which means five billion dollars wasted. A redesign by Skelton *et al.* improved two orders of magnitude in pointing accuracy without increasing control complexity (update coefficients within the existing algorithm) [27, 28]. This work does not contribute significantly to either control theories or signal processing disciplines but is a great attempt to integrate the two fields.

Finite precision errors consist of the following: quantization of coefficients, quantization of signals, overflow, and accumulated computational errors [29]. Coefficient errors can be observed

and compensated during implementations. In this dissertation the other three errors are addressed. Dynamics error comes from the model size and coefficient differences between the simulation model and physical system. Computational error comes from the accumulation of round-off errors during the computer simulation process. The minimization of dynamics error reduces to a model reduction problem [30]. The minimization of round-off error reduces to a minimum round-off noise realization problem [22, 23]. Extensive research has been conducted on them as two different problems [31, 32]. However, few trials have been made to combine these two problems to minimize total errors. As the model size grows, the dynamics error decreases monotonically, but computational error increases. While the total error is the sum of two, a threshold of model size should exist where total error reaches the minimum. A conceptual representation is shown in Figure 1.5. As a result, one may intentionally introduce dynamics error by reducing simulation model size for overall superior simulation performance. Li and Skelton present their work to find the optimal simulation system implementing finite precision effects [33, 34]. However, their designs are limited to linear systems only. This dissertation will present an approach applicable to nonlinear systems that seeks the simulation model that gives the most optimal simulation performance within a pre-specified finite-precision environment.

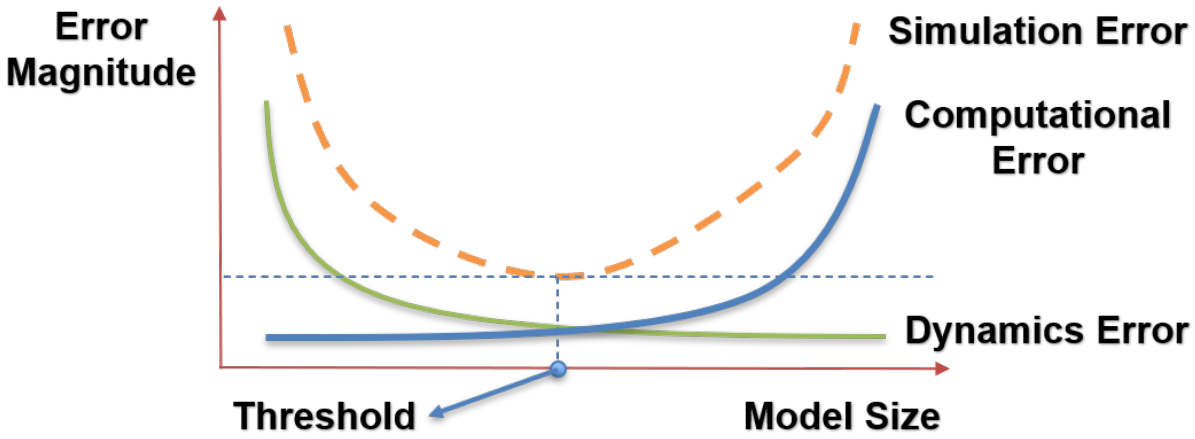

Figure 1.5: A conceptual representation of simulation error which combines dynamics error and computational error

1.3 System Control Problem

Researchers typically formulate the control problems of dynamic systems by starting with their equations of motions. Appropriate linearizations for a nonlinear system are used to apply the principles of linear system theory. However, we cannot write down the dynamics of systems of interest every time (such as black box systems) or sometimes do not trust the dynamics that we already have.

The development of modern technology enables the vast storage and fast processing of big data. Consequently, data-driven approaches relying on input-output (I/O) data have emerged. Lim and Phan developed an observer from I/O data, which estimates the system's states at some future step [35]. Safonov and Taso developed a method to determine a validated control law that meets given performance specifications from I/O data [36]. Zhang *et al.* developed a data-driven control approach that recognizes a neural network model from I/O data and then applies adaptive dynamic programming [37]. Proctor *et al.* used the technique of regression that identifies a model from I/O data [38]. Wang *et al.* found an optimal control policy for unknown systems using a dynamic programming approach [39]. However, most of these approaches seek the best fit for input-output data, which may have no explicit physical explanations.

On the other hand, a few attempts have been made to control a system with interpreted physical properties from I/O data. Markov parameters are impulse responses of a system. They are evaluated from the knowledge of input-output data, step response, or well-conditioned time response [1,40]. The work by Furuta *et al.* solved the finite horizon linear quadratic gaussian (LQG) problem using an infinite number of Markov parameters [41]. Building upon that, Shi and Skelton proposed their Markov data-based control design, solving the finite horizon LQG problem but reducing the required information to the first N +1 Markov parameters only [42]. Aangenent further extends this data-based LQG design to applications of infinite horizon applications [43].

Reference tracking control is essential in modern control applications. Wildly used in robot manipulation, aircraft control, manufacturing, etc, the purpose of reference tracking control is to tune the control inputs such that the system's outputs follow a pre-specified reference signal.

Figure 1.6 shows the general idea of reference tracking control. While most of these data-based controller designs are limited to regulation, few efforts have been made on reference tracking applications. Admittedly, it is possible to design a tracking controller by first preparing a regulator then adding feed-forward compensators [44]. However, a tracking controller like this is of no utility. It often requires additional information of derivatives of the reference signal, and is not robust to uncertainties in models [45]. This dissertation presents a new data-based controller design for reference tracking applications. The controller used minimizes a quadratic cost consisting of tracking errors and input increments.

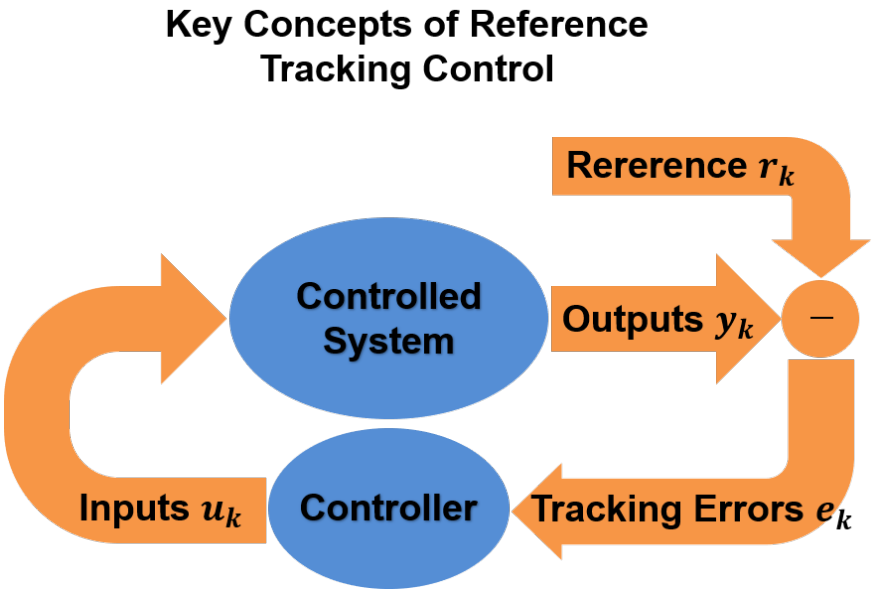

Figure 1.6: The concept of the reference tracking control.

1.4 Contribution of this Dissertation

This dissertation contains innovative work on system identification, simulation, and control. Major contributions of this work are:

1. A unique formation of the q-Markov covariance equivalent realization (QMC) problem using closed-loop observer dynamics. This formulation does not require the true system to be

stable, thereby extends the current QMC methods to identification of unstable or marginally stable systems.

2. A QMC solution selection, and proof that this solution matches the transfer function of the system dynamics.

3. A general algorithm for system identification of linear timer varying systems using the QMC method.

4. A general approach for non-linear dynamic system simulation with finite-precision effects that minimizes the norm of simulation error through integration signal processing and model reduction.

5. A new data-based controller design for reference tracking applications. This design finds the optimal control sequence which minimizes a quadratic cost function consisting of tracking error and input increments over a finite horizon.

1.5 Outline of this Dissertation

Chapter 1 introduces the main contributions of this dissertation: the system identification problem using q-Markov Covariance Equivalent Realization (QMC) methods, the dynamic system simulation problem considering finite precision effects, and the data-based system control problem. In short, the system identification problem finds an approximation system that is the closest to the system to identify, the dynamic system simulation problem finds the optimal simulation model to implement in a finite precision environment to deliver the most accurate simulation result, and the system control problem finds an optimal control sequence that minimizes a quadratic cost function consisting of tracking error and input increments over a finite horizon.

Chapter 2 addresses the system identification problem that extends the current QMC methods to identify unstable or marginally stable systems. First, we formulate the QMC problem using closed-loop observer dynamics, then define and find observer Markov parameters matching the given Markov and covariance parameters. Next, we provide the existence conditions of the observer

QMC system and parameterize all observer QMC models that match the given set of data. A method to reconstruct the state-space realizations from observer dynamics is also provided.

Chapter 3 addresses the system identification problem to find the best QMC solution that matches the pre-specified data. A QMC solution selection criterion using finite data of Markov and covariance parameters up to q is presented. This solution is then shown to be equivalent to a QMC solution that matches Matkov and covariance parameters up to ∞ . Next, we present an algorithm to apply the QMC method in system identification problems. A specific comparison among the QMC and two other widely-recognized system identification methods is also provided.

Chapter 4 addresses the system simulation problem from two aspects that find the most optimal simulation model that minimizes simulation error with finite precision effects. We first mathematically formulate the problem and transform it into linear matrix inequalities along with a coupling non-convex constraint. After convexification, we can numerically solve the problem using the LMI toolbox with a guaranteed local optimum. By integrating the QMC method, both approaches are extended to the simulation of non-linear systems.

Chapter 5 addresses the system control problem that finds an optimal control sequence that minimizes a weighted quadratic cost function for reference control applications. First, the model-based control law is derived. The parameters of the model-based controllers using Markov parameters is then constructed. An application on control of a 2D tensegrity morphing airfoil is implemented to demonstrate the method.

Chapter 6 summarizes the major accomplishments of this dissertation.

2. Q-MARKOV COVARIANCE EQUIVALENT REALIZATIONS FOR UNSTABLE SYSTEMS

Existing q-Markov covariance equivalent realization (QMC) methods do not apply to unstable systems. This chapter develops a unique QMC formulation that extends the current QMC methods to the identification of unstable systems. This unique QMC formulation is derived over a closed-loop dynamics of an observer, which is guaranteed asymptotically stable by pole assignment. All linear state-space models in an observer form that match a prespecified set of input/output cross-correlation and output auto-correlation data are computed. A method to reconstruct all solutions of general state-space models that match the prespecified data is also provided.

2.1 Introduction

Suppose we have access to the inputs and outputs (I/O) data of a system to identify. In that case, we may evaluate the system's dynamics by solving the inverse problem from I/O experimental data, which is the system identification problem. Q-Markov Covariance Equivalent Realization (QMC) is a system identification technique that finds all state-space realizations that exactly match the Markov and covariance parameters of the system to identify up to q. Markov parameters are defined as the cross-correlations between the series of I/O data, and covariance parameters as the auto-correlations between the output data [46–48]. Both parameters are obtainable from a white noise experiment to the system to identify. Since the Markov parameters represent and transient property and covariance parameters the steady-state property of a system, matching these two parameters gives a sound approximation system.

Existing QMC methods use the steady state discrete algebraic Lyapunov equation during its formulation [6, 7]. However, a steady-state solution does not exist for the dynamics with an unstable origin. Accordingly, existing QMC methods do not apply to system identification applications of unstable or marginally stable systems. This chapter introduces a unique formulation for the QMC method using the state-space observer dynamics to address this deficiency.

A state-space observer model is a closed-loop auto-regressive model that feeds output signals to states during propagation [49]. A typical application of the state-space observer model is to find the least square solution of Markov parameters from a given set of I/O data [50, 51]. The closed-loop dynamics is guaranteed to be asymptotically stable by pole assignment when observable [52]. The discrete algebraic Lyapunov equation for the state-space observer dynamics always exists a steady-state solution, thus extending the existing QMC methods for unstable system applications.

The outline of this chapter is as follows: Section 2.2 formulates the mathematical problem statement. Section 2.3 defines and finds observer Markov parameters that will be used in the calculation of observer QMC systems. Section 2.4 gives the existence condition of the observer QMC systems. Section 2.5 presents the parameterization of all observer QMC solutions and shows a method to reconstruct the state-space realizations from observer dynamics. Section 2.6 presents illustrate examples that demonstrate this formulation.

2.2 Problem Statement

Let us assume an unknown system of interest:

$$x_{k+1} = Ax_k + Bu_k, \tag{2.1a}$$

$$y_k = Cx_k + Du_k, \tag{2.1b}$$

where $x_k \in \mathbb{R}^n$, $y_k \in \mathbb{R}^m$, $u_k \in \mathbb{R}^r$, are the state, output, and input signals, and A, B, C, D are matrices of proper dimensions. We are assumed to have access to input u_k and output y_k only. If exciting the system (2.1) with a zero-mean independent white noise sequence with variance I, we experimentally evaluate its Markov parameters (H_i) and covariance parameters (R_i) using the following formulas:

$$H_i = E(y_{k+i}u_k^T) = \lim_{N\to\infty} \frac{1}{N} \sum_{k=0}^{N} y_{k+i}u_k^T, \tag{2.2a}$$

$$R_i = E(y_{k+i}y_k^T) = \lim_{N\to\infty} \frac{1}{N} \sum_{k=0}^{N} y_{k+i}y_k^T. \tag{2.2b}$$

Suppose a QMC solution is a statet space realization in the form (2.3):

$$\hat{x}_{k+1} = \hat{A}\hat{x}_k + \hat{B}u_k, \tag{2.3a}$$

$$\hat{y}_k = \hat{C}\hat{x}_k + \hat{D}u_k, \tag{2.3b}$$

Deterministic definitions for corresponding Markov parameters ($\hat{H}_i$) and covariance parameters ($\hat{R}_i$) of the QMC solution (2.3) are given in (2.4a,2.4b) where $\hat{X}$ is the steady state solution of the discrete algebraic Lyapunov equation (2.4c):

$$\hat{H}_0 = 0, \hat{H}_i = \hat{C}\hat{A}^{i-1}\hat{B}, i = 1, 2, \ldots \tag{2.4a}$$

$$\hat{R}_i = \hat{C}\hat{A}^i\hat{X}\hat{C}^T + \hat{H}_i H_0^T, i = 0, 1, 2, \ldots \tag{2.4b}$$

$$\hat{X} = \hat{A}\hat{X}\hat{A}^T + \hat{B}\hat{B}^T. \tag{2.4c}$$

Existing QMC methods solve the following problem: "Suppose an unknown system (2.1) produces $\{H_i, R_i | i = 0, 1, \cdots, q-1\}$ where q is a pre-specified positive scalar, find all finite-dimensional linear time-invariant (FDLTI) models (2.3) whose $\{\hat{H}_i, \hat{R}_i | i = 0, 1, \cdots, q-1\}$ matches the data $\{H_i, R_i | i = 0, 1, \cdots, q-1\}$ [6, 7, 20]."

Existing QMC theories assume that (2.1) is asymptotically stable. However, a steady state solutions of $(2.4c)$ does not exist when (2.3) is unstable or marginally stable [53]. As a result, existing QMC methods cannot find an approximation system (2.3) that is unstable or marginally stable. In this chapter, We attack this problem with a unique formulation by implementing the state-space observer dynamics during the derivation of the QMC method.

First, we introduce an output feedback gain sequence by adding and subtracting the term Gy_k to the right hand side of equation (2.3), which would give the equation (2.5):

$$\hat{x}_{k+1} = \hat{A}\hat{x}_k + \hat{B}u_k + G\hat{y}_k - G\hat{y}_k. \tag{2.5}$$

Here, $G \in \mathbb{R}^{n \times m}$ is an arbitrary matrix of proper dimension. Rearrangement would give us the

state-space observer model (2.6) :

$$\hat{x}_{k+1} = \bar{A}\hat{x}_k + \bar{B}v_k, \tag{2.6a}$$

$$\hat{y}_k = \hat{C}\hat{x}_k + \hat{D}u_k, \tag{2.6b}$$

where $\bar{A} = \hat{A} + G\hat{C}$, $\bar{B} = \begin{bmatrix} \hat{B} + G\hat{D} & -G \end{bmatrix}$, $v_k = \begin{bmatrix} u_k \\ \hat{y}_k \end{bmatrix} \in \mathbb{R}^{r+m}$. If (2.3) is observable, there exists a G that can place the pole of $\bar{A}$ as desired, and a positive scalar p that $\bar{A}^p \approx 0$ [54]. This guarantees the closed-loop dynamics (2.6) is asymptotically stable. We can construct the discrete algebraic Lyapunov equation where the steady state solution $\hat{X}$ exists as the following:

$$\hat{X} = \begin{bmatrix} \bar{B} & \bar{A} \end{bmatrix} \begin{bmatrix} U & U\hat{H}_0^T & 0 \\ \hat{H}_0 U & \hat{R}_0 & \hat{C}\hat{X} \\ 0 & \hat{X}\hat{C} & \hat{X} \end{bmatrix} \begin{bmatrix} \bar{B} & \bar{A} \end{bmatrix}^T. \tag{2.7}$$

Deriving QMC methods over the observer dynamics, we find all stable linear systems in observer form (2.6) that match the given data $\{H_i, R_i | i = 0, 1, \cdots, q-1\}$. Notice that a steady-state solution to the discrete algebraic Lyapunov equation (2.7) always exists. This avoids the constraint of (2.4c) thereby poses no requirement on the stability of the system to identify. With this new formulation, we can find an unstable approximation system when given data is from unstable physics.

It is our intention to find all observer QMC solutions (2.6) that up to q Markov and covariance parameters generated by (2.6) match the given data $\{H_i, R_i | i = 0, 1, \cdots, q-1\}$ for a pre-specified positive scalar q.

2.3 Observor-Based Markov Parameters

In this section we define the observer Markov parameters $\bar{h}_i$ of the state-space observer model (2.6), and shows how to evaluate them using given information of $\{H_i, R_i | i = 0, 1, \cdots, q-1\}$. These observer Markov parameters are essential for computation of observer QMC model of (2.6).

Define $\bar{h}_i$ as the following:

$$\bar{h}_0 = \hat{D}, \bar{h}_i = \hat{C}\bar{A}^{i-1}\bar{B}, i = 1, 2, \cdots. \tag{2.8}$$

Notice that:

$$\bar{h}_i = \begin{bmatrix} \hat{C}\bar{A}^{i-1}(\hat{B} + G\hat{D}) & -\hat{C}\bar{A}^{i-1}G \end{bmatrix} \tag{2.9a}$$

$$= \begin{bmatrix} \bar{h}_i^{(1)} & \bar{h}_i^{(2)} \end{bmatrix}. \tag{2.9b}$$

The superscripts $^{(1)}$ and $^{(2)}$ will be used to distinguish inputs u and outputs y from the observer inputs v during later derivations.

Before we proceed with the main theorem of this section which computes the observer markov parameters ($\bar{h}_i$) using information of Markov parameters (H_i) and Covariance paremeters (R_i), we shall introduce a linear algebra tool first [55, 56]. The following lemma leads to the existence condition and all the solutions of the observer markov parameters.

Lemma 2.3.1. *Let $A \in \mathbb{R}^{a\times b}$ and $B \in \mathbb{R}^{a\times c}$ be given matrices. Then the following statements are equivalent:*

1. *The equation*

$$AX = B \tag{2.10}$$

has a solution,

2. *A and B satisfy*

$$AA^{+}B = B, \tag{2.11}$$

3. A and B satisfy

$$(I - AA^{+})B = 0. \tag{2.12}$$

In this case, all such X are parameterized by:

$$X = A^{+}B + Z - A^{+}AZ, \tag{2.13}$$

where Z is an arbitrary $b \times c$ matrix and A^{+} denotes the Moore-Penrose inverse of A.

Proof. The implication $1 \to 2$ can be verified by multiplying both sides of (2.10) by AA^{+} from the left. To prove the converse, suppose (2.11) holds. Then using (2.13)

$$\begin{aligned} AX &= A(A^{+}B + Z - A^{+}AZ), \\ &= AA^{+}B + AZ - AA^{+}AZ, \\ &= B \end{aligned} \tag{2.14}$$

which holds by virtue of the pseudo-inverse property $AA^{+}A = A$ and (2.11). Thus we have $1 \to 2$ and it has been shown that any X given by (2.13) is a solution of (2.10).

To prove that any solution X to (2.10) can be generated by (2.13), we must show that for any solutions of (2.10), there exists a Z satisfying (2.13). That is, solve

$$X = A^{+}(AX) + Z - A^{+}AZ, \tag{2.15}$$

for Z. Obviously, a choice $Z = X$ works.

To prove the equivalence of 2 and 3, suppose (2.11) holds. Replace B in (2.12) by the left-hand side of (2.11) to get

$$(I - AA^{+})(AA^{+}B) = 0. \tag{2.16}$$

Hence (2.11) implies (2.12). This completes the proof. □

Theorem 2.3.2. *Suppose an unknown (not necessarily stable) system generates data* $\{H_i, R_i | i = 0, 1, \cdots, q-1\}$. *There exists at least a sequence of* $\{\bar{h}_i | i = 0, 1, \cdots, p\}$ *that matches the given data if* $p \geq q$. *All solutions of observer Markov parameters* $\bar{h}_i$ *are given by the following:*

$$\begin{bmatrix} \bar{h}_p^{(1)} & \bar{h}_{p-1}^{(1)} & \dots & \bar{h}_0 & \bar{h}_p^{(2)} & \bar{h}_{p-1}^{(2)} & \dots & \bar{h}_1^{(2)} \end{bmatrix} = \begin{bmatrix} L_q & K_q \end{bmatrix} V_q^+ + Z(I - V_q V_q^+), \tag{2.17}$$

where p *is a positive scalar that satisfies* $p \geq q$, V_q^+ *is the pseudo inverse of matrix* V_q, Z *is an arbitrary matrix of proper dimension, matrices* V_q, L_q, K_q *are defined as*

$$V_q = \begin{bmatrix} \bar{U} & \bar{H}_l \\ \bar{H}_r & \bar{R} \end{bmatrix}, \tag{2.18a}$$

$$L_q = \begin{bmatrix} H_0 & H_1 & \cdots & H_{q-1} \end{bmatrix}, \tag{2.18b}$$

$$K_q = \begin{bmatrix} R_0 & R_1 & \cdots & R_{q-1} \end{bmatrix}, \tag{2.18c}$$

where

$$\bar{U} = \begin{bmatrix} 0 & \cdots & \cdots & 0 \\ \vdots & \iddots & \iddots & U \\ \vdots & \iddots & \iddots & 0 \\ 0 & U & \iddots & \vdots \\ U & 0 & \cdots & 0 \end{bmatrix}, \tag{2.18d}$$

$$\bar{H}_l = \begin{bmatrix} H_p^T & \cdots & \cdots & H_1^T \\ \vdots & \iddots & \iddots & H_0^T \\ \vdots & \iddots & \iddots & 0 \\ H_1^T & H_0^T & \iddots & \vdots \\ H_0^T & 0 & \cdots & 0 \end{bmatrix}, \tag{2.18e}$$

$$\bar{H}_r = \begin{bmatrix} 0 & \cdots & \cdots & 0 \\ \vdots & \iddots & \iddots & H_0 \\ \vdots & \iddots & \iddots & 0 \\ 0 & H_0 & \iddots & H_{q-2} \end{bmatrix}, \tag{2.18f}$$

$$\bar{R} = \begin{bmatrix} R_p^T & \cdots & \cdots & R_1^T \\ \vdots & \iddots & \iddots & R_0^T \\ \vdots & \iddots & \iddots & R_1 \\ R_1^T & R_0^T & \iddots & \vdots \\ R_0^T & R_1 & \cdots & R_{q-2} \end{bmatrix}. \tag{2.18g}$$

Proof. The consecutive outputs of (2.6) can be written as the following:

$$\hat{y}_0 = \hat{C}\hat{x}_0 + \hat{D}u_0, \tag{2.19a}$$

$$\hat{y}_1 = \hat{C}\bar{A}\hat{x}_0 + \hat{C}\bar{B}v_0 + \hat{D}u_1, \tag{2.19b}$$

$$\vdots$$

$$\hat{y}_p = \hat{C}\bar{A}^p\hat{x}_0 + \hat{C}\bar{A}^{p-1}\bar{B}v_0 + \cdots + \hat{C}\bar{B}v_{p-1} + \hat{D}u_p, \tag{2.19c}$$

$$\vdots$$

$$\begin{aligned} \hat{y}_{p+q-1} = {} & \hat{C}\bar{A}^{p+q-1}\hat{x}_0 + \hat{C}\bar{A}^{p+q-2}\bar{B}v_0 + \cdots \\ & + \hat{C}\bar{B}v_{p+q-2} + \hat{D}u_{p+q-1}. \end{aligned} \tag{2.19d}$$

Using the property that $\bar{A}^p \approx 0$, the following expression can be formulated:

$$\begin{bmatrix} \hat{y}_p & \hat{y}_{p+1} & \dots & \hat{y}_{p+q-1} \end{bmatrix} =$$

$$\begin{bmatrix} \bar{h}_p^{(1)} & \bar{h}_{p-1}^{(1)} & \dots & \bar{h}_1^{(1)} & \bar{h}_0 \end{bmatrix} \begin{bmatrix} u_0 & u_1 & \dots & u_{q-1} \\ u_1 & u_2 & \dots & u_q \\ \vdots & \vdots & \ddots & \vdots \\ u_p & u_{p+1} & \dots & u_{p+q-1} \end{bmatrix} +$$

$$\begin{bmatrix} \bar{h}_p^{(2)} & \bar{h}_{p-1}^{(2)} & \dots & \bar{h}_1^{(2)} \end{bmatrix} \begin{bmatrix} \hat{y}_0 & \hat{y}_1 & \dots & \hat{y}_{q-1} \\ \hat{y}_1 & \hat{y}_2 & \dots & \hat{y}_q \\ \vdots & \vdots & \ddots & \vdots \\ \hat{y}_{p-1} & \hat{y}_p & \dots & \hat{y}_{p+q-2} \end{bmatrix}. \tag{2.20}$$

Taking outer-product with u_p^T and $\hat{y}_p^T$ on both sides of (2.20) yields the following two equations:

$$L_q = \begin{bmatrix} \bar{h}_p^{(1)} & \bar{h}_{p-1}^{(1)} & \dots & \bar{h}_0 \end{bmatrix} \bar{U} + \begin{bmatrix} \bar{h}_p^{(2)} & \bar{h}_{p-1}^{(2)} & \dots & \bar{h}_1^2 \end{bmatrix} \bar{H}_r \tag{2.21a}$$

$$K_q = \begin{bmatrix} \bar{h}_p^{(1)} & \bar{h}_{p-1}^{(1)} & \dots & \bar{h}_0 \end{bmatrix} \bar{H}_l + \begin{bmatrix} \bar{h}_p^{(2)} & \bar{h}_{p-1}^{(2)} & \dots & \bar{h}_1^2 \end{bmatrix} \bar{R}, \tag{2.21b}$$

Assembling (2.21a) and (2.21b) gives the following:

$$\begin{bmatrix} L_q & K_q \end{bmatrix} = \begin{bmatrix} \bar{h}_p^{(1)} & \bar{h}_{p-1}^{(1)} & \dots & \bar{h}_0 & \bar{h}_p^{(2)} & \bar{h}_{p-1}^{(2)} & \dots & \bar{h}_1^{(2)} \end{bmatrix} V_q. \tag{2.22}$$

Notice that equation (2.22) follows the pattern of a typical linear algebra problem "$AX = B$". Equation (2.22) exists a solution if and only if V_q is full column rank, where the dimension of V_q shall satisfy:

$$qm + qr \leq pr + r + pm, \tag{2.23}$$

which is

$$p \geq q - \frac{r}{m+r}. \tag{2.24}$$

Thus, the lower bound of p is q, and all solutions of (2.22) are given by (2.17). This completes the proof. □

2.4 Existence Conditions of QMC for Unstable Systems

In this section we will discuss the existence condition of the observer QMC solution (2.6).

Theorem 2.4.1. *Suppose an unknown (but not necessarily stable) system generates data* $\{H_i, R_i | i = 0, 1, \cdots, q-1\}$*, and its observer Markov parameter sequence* $\{\bar{h}_i | i = 0, 1, \cdots, p\}$ *for* $p \geq q$ *is computed using Theorem 2.3.2. There exists a linear system (2.6) that matches the data iff* $\bar{D}_q \geq 0$ *where*

$$\bar{D}_q = \bar{H}_q^{(2)} R_q \bar{H}_q^{(2)^T} - \bar{H}_q^{(1)} \bar{H}_q^{(1)^T}, \tag{2.25a}$$

$$\bar{H}_q^{(1)} = \begin{bmatrix} \bar{h}_0 & 0 & \cdots & 0 \\ \bar{h}_1^{(1)} & \bar{h}_0 & \vdots & 0 \\ \vdots & \ddots & \ddots & \vdots \\ \bar{h}_{q-1}^{(1)} & \cdots & \bar{h}_1^{(1)} & \bar{h}_0 \end{bmatrix}, \tag{2.25b}$$

$$\bar{H}_q^{(2)} = \begin{bmatrix} 1 & 0 & \cdots & 0 \\ -\bar{h}_1^{(2)} & 1 & \vdots & 0 \\ \vdots & \ddots & \ddots & \vdots \\ -\bar{h}_{q-1}^{(2)} & \cdots & -\bar{h}_1^{(2)} & 1 \end{bmatrix}, \tag{2.25c}$$

$$R_q = \begin{bmatrix} R_0 & R_1^T & \cdots & R_q^T \\ R_1 & R_0 & \ddots & \vdots \\ \vdots & \ddots & \ddots & R_1^T \\ R_{q-1} & \cdots & R_1 & R_0 \end{bmatrix}. \tag{2.25d}$$

Proof. One may notice that equations (2.19a) - (2.19d) can be re-formulated as the following:

$$\hat{y}_0 = \hat{C}\hat{x}_0 + \bar{h}_0 u_0, \tag{2.26a}$$

$$\hat{y}_1 = \hat{C}\bar{A}\hat{x}_0 + \bar{h}_1^{(1)} u_0 + \bar{h}_1^{(2)}\hat{y}_0 + \bar{h}_0 u_1, \tag{2.26b}$$

$$\hat{y}_2 = \hat{C}\bar{A}^2\hat{x}_0 + \bar{h}_2^{(1)} u_0 + \bar{h}_2^{(2)}\hat{y}_0 + \bar{h}_1^{(1)} u_1 + \bar{h}_1^{(2)}\hat{y}_1 + \bar{h}_0 u_2, \tag{2.26c}$$

$$\vdots$$

$$\hat{y}_q = \hat{C}\bar{A}^{q-1}\hat{x}_0 + \bar{h}_q^{(1)} u_0 + \bar{h}_q^{(2)}\hat{y}_0 + \bar{h}_{q-1}^{(1)} u_1 + \bar{h}_{q-1}^{(2)}\hat{y}_1 + \cdots + \bar{h}_1^{(1)} u_{q-1} + \bar{h}_1^{(2)}\hat{y}_{q-1} + \bar{h}_0 u_q. \tag{2.26d}$$

Augment equations (2.26a) - (2.26d) to get the following expression:

$$\bar{H}_q^{(2)}\mathbf{y_q} = \bar{O}_q\hat{x}_0 + \bar{H}_q^{(1)}\mathbf{u}_q, \tag{2.27a}$$

where

$$\bar{O}_q = \begin{bmatrix} \hat{C} \\ \hat{C}\bar{A} \\ \hat{C}\bar{A}^2 \\ \vdots \\ \hat{C}\bar{A}^q \end{bmatrix}, \mathbf{y_q} = \begin{bmatrix} y_0 \\ y_1 \\ y_2 \\ \vdots \\ y_q \end{bmatrix}, \mathbf{u}_q = \begin{bmatrix} u_0 \\ u_1 \\ u_2 \\ \vdots \\ u_q \end{bmatrix}. \tag{2.27b}$$

Taking outer product on both sides of (2.27a) yields:

$$\bar{H}_q^{(2)} R_q \bar{H}_q^{(2)^T} = \bar{O}_q\hat{X}\bar{O}_q^T + \bar{H}_q^{(1)} U_q \bar{H}_q^{(1)^T}. \tag{2.28}$$

If $\bar{D}_q \geq 0$ is satisfied, there exists at least one observer system (2.6) that satisfies the equality (2.28). This completes the proof. □

2.5 Parameterizing All QMC Solutions

In this section we find all parameterization of the observer QMC models. Before proceeding with the main theorem, we shall introduce another linear algebra tool that leads to the existence condition and all the solutions of the observer QMC models [55].

Lemma 2.5.1. *Let $A \in \mathbb{R}^{a\times b}$ and $B \in \mathbb{R}^{a\times c}$ be given matrices, where $c \geq b$. Then the following statements are equivalent:*

1. *There exists X satisfying*

$$AX = B, XX^T = I, \tag{2.29}$$

2. *A and B satisfy*

$$AA^T = BB^T, \tag{2.30}$$

In this case, all such X are parameterized by:

$$X = \begin{bmatrix} V_{A1} & V_{A2} \end{bmatrix} \begin{bmatrix} I & 0 \\ 0 & U \end{bmatrix} \begin{bmatrix} V_{B1}^T \\ V_{B2}^T \end{bmatrix}, \tag{2.31}$$

where U is an arbitrary matrix such that $UU^T = I$ and V_{A1}, V_{A2}, V_{B1} and V_{B2} are defined from the SVD of A and B as follow:

$$A = \begin{bmatrix} U_{A1} & U_{A2} \end{bmatrix} \begin{bmatrix} \Sigma_A & 0 \\ 0 & 0 \end{bmatrix} \begin{bmatrix} V_{A1}^T \\ V_{A2}^T \end{bmatrix} = U_A \Sigma_A V_A^T, \tag{2.32a}$$

$$B = \begin{bmatrix} U_{A1} & U_{A2} \end{bmatrix} \begin{bmatrix} \Sigma_A & 0 \\ 0 & 0 \end{bmatrix} \begin{bmatrix} V_{B1}^T \\ V_{B2}^T \end{bmatrix} = U_A \Sigma_A V_B^T. \tag{2.32b}$$

Proof. Square both sides of $AX = B$ to get:

$$AX(AX)^T = AXX^TA^T = AA^T = BB^T. \tag{2.33}$$

This proves necessity of (2.30). For sufficiency, recall from the SVD of A that U_A satisfies

$$AA^TU_A = U_A \begin{bmatrix} \Sigma_A^2 & 0 \\ 0 & 0 \end{bmatrix}. \tag{2.34}$$

From (2.30) and (2.34) it is clear that we can choose $U_A = U_B$, $\Sigma_A = \Sigma_B$. Hence (2.34). Now define

$$Z^T \triangleq \begin{bmatrix} Z_1^T \\ Z_2^T \end{bmatrix} \triangleq \begin{bmatrix} V_{A1}^T \\ V_{A2}^T \end{bmatrix} X, \tag{2.35}$$

then (2.29) becomes

$$\begin{bmatrix} U_{A1} & U_{A2} \end{bmatrix} \begin{bmatrix} \Sigma_A & 0 \\ 0 & 0 \end{bmatrix} \begin{bmatrix} Z_1^T \\ Z_2^T \end{bmatrix} = \begin{bmatrix} U_{A1} & U_{A2} \end{bmatrix} \begin{bmatrix} \Sigma_A & 0 \\ 0 & 0 \end{bmatrix} V_b^T, \tag{2.36a}$$

$$Z^TZ = I, \tag{2.36b}$$

which is

$$\Sigma_A Z_1^T = \Sigma_A V_{B1}^T, Z_2^TZ_2 = I, Z_2Z_1 = 0, \tag{2.37}$$

which is (using the fact $V_{B2}V_{B1} = 0$)

$$Z_1 == V_{B1}, Z_2 = V_{B2}U^T, UU^T = I, \tag{2.38}$$

which is (since $X = V_A Z^T$)

$$X = V_A \begin{bmatrix} I & 0 \\ 0 & U \end{bmatrix} V_b^T, UU^T = I. \tag{2.39}$$

This completes the proof. □

Theorem 2.5.2. *Given the data $\{H_i, R_i | i = 0, 1, \cdots, q-1\}$ generated by a system (not necessarily stable) with white noise excitation of variance U. Let integers $p \geq q > 0$ be specified. Suppose $\bar{D}_q \geq 0$. Then all linear stable models (2.6) with $\hat{X} = I$ that match the given data are parameterized by (2.40); their corresponding linear models (2.3) that match the given data are parameterized by (2.49).*

$$\hat{D} = H_0, \tag{2.40a}$$

$$\hat{C} = \begin{bmatrix} I_m & 0 \end{bmatrix} \bar{O}_q, \tag{2.40b}$$

$$\begin{bmatrix} \bar{B} & \bar{A} \end{bmatrix} = \bar{O}_{q-1}^{+} \begin{bmatrix} \bar{M}_{q-1} & \bar{O}_{q-1} \end{bmatrix} + V_b \hat{U} V_d^T V^{-1}, \tag{2.40c}$$

where $\bar{O}_q \bar{O}_q^T = \bar{D}_q$ is the minimal rank factorization of $\bar{D}_q$, $\hat{U}$ is an arbitrary matrix of proper dimension satisfying $\hat{U}\hat{U}^T = I$, and V_b, V_d are given by the following SVD:

$$\bar{O}_{q-1} = \begin{bmatrix} U_a & U_b \end{bmatrix} \begin{bmatrix} \Sigma_a & 0 \\ 0 & 0 \end{bmatrix} \begin{bmatrix} V_a^T \\ V_b^T \end{bmatrix}, \tag{2.40d}$$

$$\begin{bmatrix} \bar{M}_{q-1} V^{-1} & \bar{N}_{q-1} V^{-1} \end{bmatrix} = \begin{bmatrix} U_a & U_b \end{bmatrix} \begin{bmatrix} \Sigma_a & 0 \\ 0 & 0 \end{bmatrix} \begin{bmatrix} V_c^T \\ V_d^T \end{bmatrix}, \tag{2.40e}$$

where

$$VV^T = \begin{bmatrix} U & UH_0^T & 0 \\ H_0 U & R_0 & \hat{C} \\ 0 & \hat{C}^T & I \end{bmatrix}, \tag{2.40f}$$

$$\bar{O}_{q-1} = \begin{bmatrix} I_{q-1} & 0 \end{bmatrix} \bar{O}_q, \tag{2.40g}$$

$$\bar{N}_{q-1} = \begin{bmatrix} 0 & I_{q-1} \end{bmatrix} \bar{O}_q, \tag{2.40h}$$

$$\bar{M}_{q-1} = \begin{bmatrix} \bar{h}_1 \\ \bar{h}_2 \\ \vdots \\ \bar{h}_{q-1} \end{bmatrix}. \tag{2.40i}$$

Proof. Assume an observed-based qmc model exists whose state covariance is $\hat{X} = I$. The two governing equations of the new QMC method are the following:

$$I = \begin{bmatrix} \bar{B} & \bar{A} \end{bmatrix} V V^T \begin{bmatrix} \bar{B} & \bar{A} \end{bmatrix}^T, \tag{2.41a}$$

$$\bar{O}_{q-1} \begin{bmatrix} \bar{B} & \bar{A} \end{bmatrix} = \begin{bmatrix} \bar{M}_{q-1} & \bar{O}_{q-1} \end{bmatrix}. \tag{2.41b}$$

Rearrangement yields the following expressions:

$$I = \begin{bmatrix} \bar{B}V & \bar{A}V \end{bmatrix} \begin{bmatrix} \bar{B}V & \bar{A}V \end{bmatrix}^T, \tag{2.42a}$$

$$\bar{O}_{q-1} \begin{bmatrix} \bar{B}V & \bar{A}V \end{bmatrix} = \begin{bmatrix} \bar{M}_{q-1}V & \bar{O}_{q-1}V \end{bmatrix}. \tag{2.42b}$$

Equations (2.42a) and (2.42b) can be represented as the standard linear algebra problem of $\{\mathbf{AX} = \mathbf{B};\ \mathbf{XX^T} = \mathbf{I}\}$ [55] by the change of variables. The existence condition is the following:

$$\bar{O}_{q-1}\bar{O}_{q-1}^T = \begin{bmatrix} \bar{M}_{q-1}V & \bar{O}_{q-1}V \end{bmatrix} \begin{bmatrix} \bar{M}_{q-1}V & \bar{O}_{q-1}V \end{bmatrix}^T. \tag{2.43}$$

We will show that (2.43) is always true. Notice the left hand side of (2.43) is the following:

$$\bar{O}_{q-1}\bar{O}_{q-1}^T = \begin{bmatrix} I_{m(q-1)} & 0 \end{bmatrix} \bar{O}_q \bar{O}_q^T \begin{bmatrix} I_{m(q-1)} \\ 0 \end{bmatrix}$$

$$= \begin{bmatrix} I_{m(q-1)} & 0 \end{bmatrix} (\bar{H}_q^{(2)} R_q \bar{H}_q^{(2)^T} - \bar{H}_q^{(1)} U_q \bar{H}_q^{(1)^T}) \begin{bmatrix} I_{m(q-1)} \\ 0 \end{bmatrix}$$

$$= \bar{H}_{q-1}^{(2)} R_{q-1} \bar{H}_{q-1}^{(2)^T} - \bar{H}_{q-1}^{(1)} U_{q-1} \bar{H}_{q-1}^{(1)^T}. \tag{2.44}$$

The right hand side of (2.43) is the following:

$$\begin{bmatrix} \bar{M}_{q-1} V & \bar{O}_{q-1} V \end{bmatrix} \begin{bmatrix} \bar{M}_{q-1} V & \bar{O}_{q-1} V \end{bmatrix}^T$$

$$= \begin{bmatrix} \bar{M}_{q-1}^{(1)} & \bar{M}_{q-1}^{(2)} & \bar{N}_{q-1} \end{bmatrix} \begin{bmatrix} U & UH_0^T & 0 \\ H_0 U & R_0 & C \\ 0 & C^T & I \end{bmatrix} \begin{bmatrix} \bar{M}_{q-1}^{(1)} & \bar{M}_{q-1}^{(2)} & \bar{N}_{q-1} \end{bmatrix}^T$$

$$= \bar{M}_{q-1}^{(1)} U \bar{M}_{q-1}^{(1)^T} + \bar{M}_{q-1}^{(2)} H_0 U \bar{M}_{q-1}^{(1)^T} + \bar{M}_{q-1}^{(1)} U H_0^T \bar{M}_{q-1}^{(2)^T}$$

$$+ \bar{M}_{q-1}^{(2)} R_0 \bar{M}_{q-1}^{(2)^T} + \bar{N}_{q-1} C^T \bar{M}_{q-1}^{(2)^T} + \bar{M}_{q-1}^{(2)} C \bar{N}_{q-1}^T + \bar{N}_{q-1} \bar{N}_{q-1}^T, \tag{2.45}$$

where

$$\bar{M}_{q-1}^{(1)} = \begin{bmatrix} 0 & I_{m(q-1)} \end{bmatrix} \bar{H}_q^{(1)} \begin{bmatrix} I_r \\ 0 \end{bmatrix}, \tag{2.46a}$$

$$\bar{M}_{q-1}^{(2)} = -\begin{bmatrix} 0 & I_{m(q-1)} \end{bmatrix} \bar{H}_q^{(2)} \begin{bmatrix} I_r \\ 0 \end{bmatrix}, \tag{2.46b}$$

$$\bar{N}_{q-1} = \begin{bmatrix} 0 & I_{m(q-1)} \end{bmatrix} \bar{O}_q. \tag{2.46c}$$

Notice that:

$$\bar{N}_{q-1} C^T \bar{M}_{q-1}^{(2)^T} + \bar{M}_{q-1}^{(1)} U H_0^T \bar{M}_{q-1}^{(2)^T} =$$

$$-\begin{bmatrix}0 & I_{m(q-1)}\end{bmatrix}(\bar{H}_q^{(2)}\begin{bmatrix}R_0 & 0 & \cdots & 0\\ R_1 & 0 & \ddots & 0\\ \vdots & \ddots & \ddots & \vdots\\ R_{q-1} & 0 & \cdots & 0\end{bmatrix}H_q^{(2)^T})\begin{bmatrix}0\\ I_{m(q-1)}\end{bmatrix}, \tag{2.47a}$$

$$\bar{M}_{q-1}^{(2)}C\bar{N}_{q-1}^T + \bar{M}_{q-1}^{(2)}H_0U\bar{M}_{q-1}^{(1)^T} =$$
$$-\begin{bmatrix}0 & I_{m(q-1)}\end{bmatrix}(\bar{H}_q^{(2)}\begin{bmatrix}R_0 & R_1^T & \cdots & R_{q-1}^T\\ 0 & 0 & \ddots & 0\\ \vdots & \ddots & \ddots & \vdots\\ 0 & 0 & \cdots & 0\end{bmatrix}H_q^{(2)^T})\begin{bmatrix}0\\ I_{m(q-1)}\end{bmatrix}, \tag{2.47b}$$

$$\bar{N}_{q-1}\bar{N}_{q-1}^T =$$
$$\begin{bmatrix}0 & I_{m(q-1)}\end{bmatrix}(\bar{H}_q^{(2)}R_q\bar{H}_q^{(2)^T} - \bar{H}_q^{(1)}U_q\bar{H}_q^{(1)^T})\begin{bmatrix}0\\ I_{m(q-1)}\end{bmatrix}, \tag{2.47c}$$

$$\bar{M}_{q-1}^{(1)}U\bar{M}_{q-1}^{(1)^T} =$$
$$\begin{bmatrix}0 & I_{m(q-1)}\end{bmatrix}\bar{H}_q^{(1)}\begin{bmatrix}I_r\\ 0\end{bmatrix}U\begin{bmatrix}I_r & 0\end{bmatrix}\bar{H}_q^{(1)^T}\begin{bmatrix}0\\ I_{m(q-1)}\end{bmatrix}, \tag{2.47d}$$

$$\bar{M}_{q-1}^{(2)}R_0\bar{M}_{q-1}^{(2)^T} =$$
$$\begin{bmatrix}0 & I_{m(q-1)}\end{bmatrix}\bar{H}_q^{(2)}\begin{bmatrix}I_r\\ 0\end{bmatrix}U\begin{bmatrix}I_r & 0\end{bmatrix}\bar{H}_q^{(2)^T}\begin{bmatrix}0\\ I_{m(q-1)}\end{bmatrix}. \tag{2.47e}$$

The right hand side of (2.43), which is the sum of terms (2.47a) to (2.47e), is given as:

$$\begin{aligned} RHS &= \begin{bmatrix} 0 & I_{m(q-1)} \end{bmatrix} (\bar{H}_q^{(2)} \begin{bmatrix} 0 \\ I_{m(q-1)} \end{bmatrix} R_q \begin{bmatrix} 0 & I_{m(q-1)} \end{bmatrix} \bar{H}_q^{(2)^T} \\ &- \bar{H}_q^{(1)} \begin{bmatrix} 0 \\ I_{m(q-1)} \end{bmatrix} U_q \begin{bmatrix} 0 & I_{m(q-1)} \end{bmatrix} \bar{H}_q^{(1)^T}) \begin{bmatrix} 0 \\ I_{m(q-1)} \end{bmatrix} \\ &= \bar{H}_{q-1}^{(2)} R_{q-1} \bar{H}_{q-1}^{(2)^T} - \bar{H}_{q-1}^{(1)} U_{q-1} \bar{H}_{q-1}^{(1)^T} \\ &= LHS. \end{aligned} \tag{2.48}$$

Thus, we have shown that the existence condition (2.43) is satisfied, and a solution to (2.42a) and (2.42b) always exists. The solution is given by (2.40). □

Lemma 2.5.3. *The QMC solution (2.3) can be constructed using its observer form (2.6) as follows:*

$$G = -\bar{B} \begin{bmatrix} 0 \\ I_m \end{bmatrix}, \tag{2.49a}$$

$$\hat{A} = \bar{A} - G\hat{C}, \tag{2.49b}$$

$$\hat{B} = \bar{B} \begin{bmatrix} I_r \\ 0 \end{bmatrix} - G\hat{D}. \tag{2.49c}$$

where m and r represents the numbers of outputs and inputs respectively.

Proof. This is a direct result from the composition of (2.6) where

$$\bar{A} = \hat{A} + G\hat{C}, \tag{2.50a}$$

$$\bar{B} = \begin{bmatrix} \hat{B} + G\hat{D} & -G \end{bmatrix}. \tag{2.50b}$$

□

2.6 Illustrative Examples

In this section, we show two illustrative examples to demonstrate the QMC for unstable systems. The first case is an oscillator. It is marginally stable. A solution to the discrete algebraic Lyapunov equation does not exist, therefore it is not well-recognized by existing QMC methods. The second case is a non-minimum phase system, which has a zero on the right half-plane. Such a system may go in the wrong direction when applied inputs initially and cannot be well-recognized by most system identification approaches. We found approximation systems employing the QMC method developed in this chapter for both cases.

2.6.1 An Oscillator Example

Consider the system of interest (2.1) with the following parameters:

$$A = \begin{bmatrix} -0.5918 & 0.8061 \\ -0.8061 & -0.5918 \end{bmatrix}, \; B = \begin{bmatrix} 1.5918 \\ 0.8061 \end{bmatrix},$$
$$C = \begin{bmatrix} -1 & 0 \end{bmatrix}, \qquad D = 1. \tag{2.51}$$

It is easy to verify that this system is marginally stable. Choose $p = q = 3$. The QMC solution (2.3) is found as the following:

$$\hat{A} = \begin{bmatrix} -0.5918 & 0.8061 \\ -0.8061 & -0.5918 \end{bmatrix}, \; \hat{B} = \begin{bmatrix} 0.0085 \\ 0 \end{bmatrix},$$
$$\hat{C} = \begin{bmatrix} -187.2703 & 94.8310 \end{bmatrix}, \; \hat{D} = 1. \tag{2.52}$$

Tables 2.1 and 2.2 compare the parameters generated by the system to identify, and the QMC system. H_i and R_i are the Markov and covariance parameters of the oscillator system (2.51), while $\hat{H}_i$ and $\hat{R}_i$ are the Markov and covariance parameters recovered by the QMC system (2.52). Their errors are defined in (2.53).

$$\Delta H_i \triangleq \hat{H}_i - H_i, \tag{2.53a}$$

$$\Delta R_i \triangleq \hat{R}_i - R_i. \tag{2.53b}$$

Figures 2.1 and 2.2 show the error percentages of Markov and covariance parameters. It is noticed that the first $q = 3$ of both parameters are matched exactly. Proceeding parameters have some errors but are at insignificant scales. The two systems are related via the following transformation matrix:

$$T = \begin{bmatrix} 187.2703 & -94.8310 \\ 94.8410 & 187.2721 \end{bmatrix}, \tag{2.54}$$

where

$$\hat{A} = T^{-1}AT,\ \hat{B} = T^{-1}B,\ \hat{C} = CT. \tag{2.55}$$

It is reasonable to claim that the oscillator system (2.51) and the QMC system (2.52) are simimar in kinematics.

Table 2.1: Comparing the Covariance Parameters of the System to Identify and the QMC System for the Oscillator Example.

Index	H_i	$\hat{H}_i$	$\frac{\Delta H_i}{H_i}$
0	1	1	0.00%
1	−1.5918	−1.5918	0.00%
2	0.2923	0.2923	0.00%
3	1.2458	1.2458	−0.00%
4	−1.7669	−1.7668	−0.01%
5	0.8455	0.8454	−0.02%
6	0.7661	0.7662	0.00%
7	−1.7523	−1.7521	−0.01%
8	1.3080	1.3077	−0.02%
9	0.2042	0.2044	0.09%

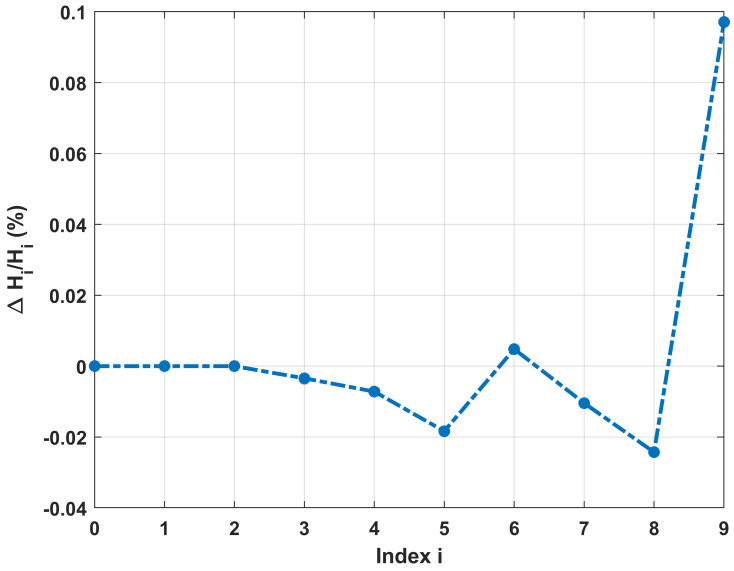

Figure 2.1: Error percentage in Markov parameters for the oscillator example.

Table 2.2: Comparing the Covariance Parameters of the System to Identify and the QMC System for the Oscillator Example.

Index	R_i	$\hat{R}_i$	$\frac{\Delta R_i}{R_i}$
0	$4.4064E^4$	$4.4064E^4$	-0.00%
1	$-2.6077E^4$	$-2.6077E^4$	-0.00%
2	$-1.3199E^4$	$-1.3199E^4$	0.00%
3	$4.1698E^4$	$4.1698E^4$	0.00%
4	$-3.6153E^4$	$-3.6154E^4$	0.00%
5	$0.1094E^4$	$0.1094E^4$	0.04%
6	$3.4858E^4$	$3.4858E^4$	0.00%
7	$-4.2350E^4$	$-4.2351E^4$	0.00%
8	$1.5268E^4$	$1.5269E^4$	0.01%
9	$2.4278E^4$	$2.4277E^4$	-0.00%

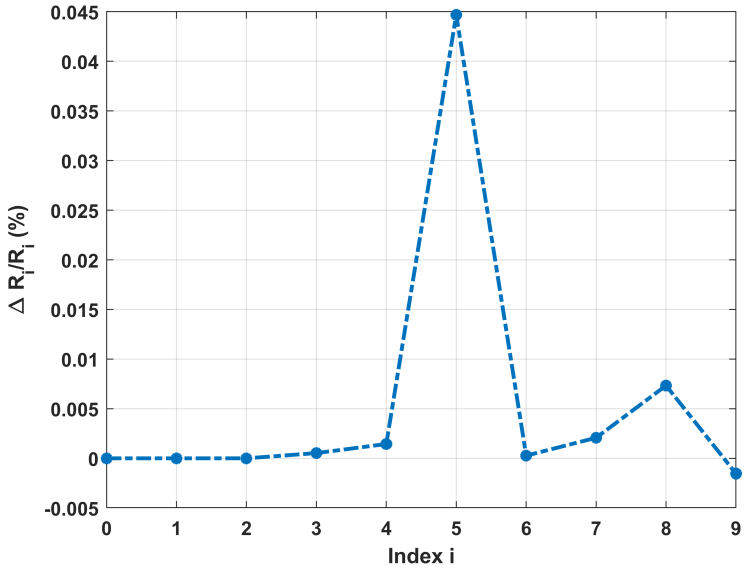

Figure 2.2: Error percentage in Covariance parameters for the oscillator example.

2.6.2 A Non-Minimum Phase Example

A system is in its minimum phase if the system and its inverse are both causal and stable, while a non-minimum system is the one whose inverse is not stable [57, 58]. Compared to minimum phase systems, non-minimum phase systems are generally harder to identify and control. Consider the system with the following transfer function (2.56). It has two poles and one positive zero, which is a non-minimum phase system.

$$G(s) = \frac{s-1}{s^2+2s+4}. \tag{2.56}$$

Discretizing (2.56) at a sampling time of 0.1s gives the following parameters:

$$A = \begin{bmatrix} 0.8013 & -0.3601 \\ 0.0900 & 0.9813 \end{bmatrix}, \; B = \begin{bmatrix} 0.0900 \\ 0.0047 \end{bmatrix},$$
$$C = \begin{bmatrix} 1 & -1 \end{bmatrix}, \qquad D = 0. \tag{2.57}$$

One may verify that this system is non-minimum phase. Choose $p = q = 3$. The QMC solution (2.3) is found as the following:

$$\hat{A} = \begin{bmatrix} 0.8339 & 0.2505 \\ -0.1109 & 0.9487 \end{bmatrix}, \; \hat{B} = \begin{bmatrix} -0.4919 \\ 0.2962 \end{bmatrix},$$
$$\hat{C} = \begin{bmatrix} -0.1760 & 0.0040 \end{bmatrix}, \; \hat{D} = 0. \tag{2.58}$$

Tables 2.3 and 2.4 compare the parameters generated by the original system and the QMC system. H_i and R_i are the Markov and covariance parameters of the non-minimum phase system (2.57), while $\hat{H}_i$ and $\hat{R}_i$ are the Markov and covariance parameters recovered by the QMC system (2.58). It is noticed that the first $q = 3$ of both parameters are matched exactly. Proceeding parameters are matched well too. Their error percentages are plotted in Figures 2.3 and 2.4, where the

magnitude are 10^{-12}. The two systems are related via the following transformation:

$$T = \begin{bmatrix} -0.1424 & 0.0674 \\ 0.0335 & 0.0714 \end{bmatrix}, \tag{2.59}$$

where

$$\hat{A} = T^{-1}AT,\ \hat{B} = T^{-1}B,\ \hat{C} = CT. \tag{2.60}$$

Therefore, the non-minimum phase system (2.57) and the QMC system (2.58) are simimar in kinematics.

Table 2.3: Comparing the parameters of physics/QMC systems for non-minimum Phase System.

Index	H_i	$\hat{H}_i$	$\frac{\Delta H_i}{H_i}$
0	0	0	0.00%
1	0.0854	0.0854	0.00%
2	0.0578	0.0578	0.00%
3	0.0331	0.0331	−0.00%
4	0.0117	0.0117	0.00%
5	−0.0062	−0.0062	0.00%
6	−0.0207	−0.0207	0.00%
7	−0.0318	−0.0318	0.00%
8	−0.0397	−0.0397	0.00%
9	−0.0448	−0.0448	0.00%

2.7 Conclusion

This chapter developed a unique formulation of the QMC method, which extends the existing QMC methods to system identification applications of unstable or marginally stable systems. Existing QMC methods only apply to system identification of asymptotically systems. This unique formulation, which is derived using a closed-loop dynamics of state-space observer model, does

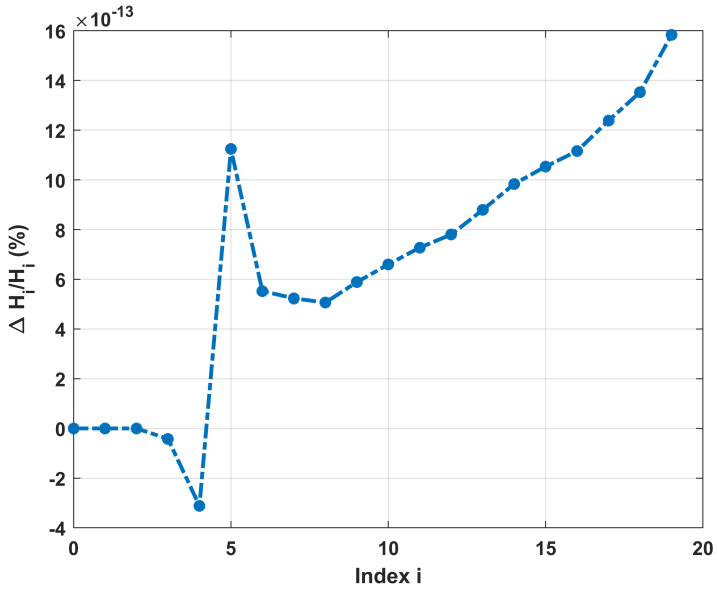

Figure 2.3: Error percentage in Markov parameters for the non-minimum phase example.

Table 2.4: Comparing the parameters of physics/QMC systems for non-minimum phase system.

Index	R_i	$\hat{R}_i$	$\frac{\Delta R_i}{R_i}$
0	0.0310	0.0310	0.00%
1	0.0259	0.0259	0.00%
2	0.0209	0.0209	0.00%
3	0.0160	0.0160	−0.00%
4	0.0114	0.0114	−0.00%
5	0.0072	0.0072	−0.00%
6	0.0035	0.0035	−0.00%
7	0.0004	0.0004	−0.00%
8	−0.0022	−0.0022	0.00%
9	−0.0042	−0.0042	0.00%

not pose any constraints on the stability of the system to identify. Two illustrative examples, a marginally stable oscillator system and a non-minimum phase system, have been conducted, and their results are presented to demonstrate the unique QMC formulation.

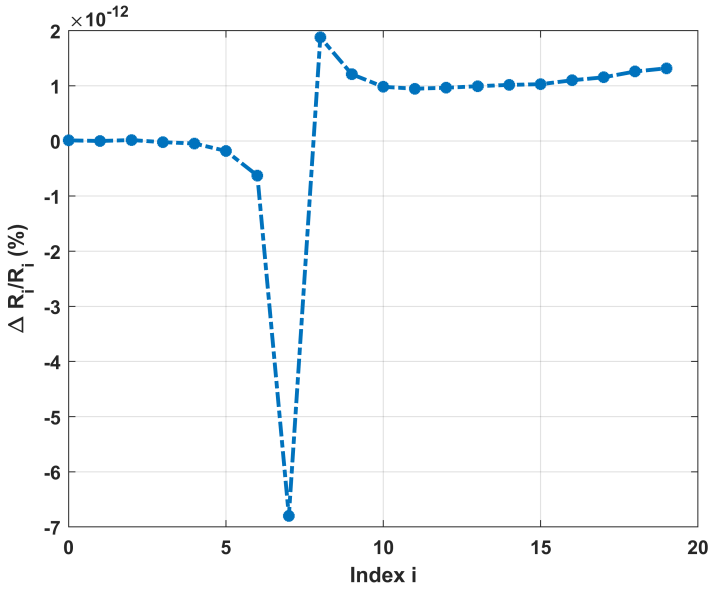

Figure 2.4: Error percentage in Covariance parameters for the non-minimum phase example.

3. THE EFFICIENT Q-MARKOV COVARIANCE EQUIVALENT REALIZATION

This chapter provides a method that finds an efficient q-Markov covariance equivalent realization (QMC) system that matches the first Markov parameters and covariance parameters up to ∞ with a finite number of data. It further presents a generalized QMC theory to find the efficient QMC solution for stable/unstable systems and an algorithm for system identifications using the QMC method. A comparison of the QMC approach with Eigensystem Realization Algorithm (ERA) and Eigensystem Realization Algorithm using Data Correlations (ERA/DC) is presented. Compared to the other two, the efficient QMC method finds an approximation system with the least errors in frequency responses.

3.1 Introduction

The system simulation problem determines the dynamics of an unknown system from its input/output data. General system identification techniques fall into two categories: those that seek a least-square solution that minimizes the norms of errors for all data or those who seek an exact match to some but not all of the data. The least square methods are prevalent in today's system identification applications because it gives a solution under all circumstances. However, there is no guarantee on the performance of the least square solution, whereas the solution can be as bad as possible. Inversely, exact match methods guarantee the matching of some parameters and are especially useful in applications with specific requirements of certain parameters.

Q-Markov covariance equivalent realization (QMC) is an exact match method that finds all state-space realizations that exactly match the Markov and covariance parameters up tp q of the system one aims to identify. Since Markov and covariance parameters characterize the transient and steady-state proprieties, an exact match of these two parameters produces a reasonable approximation system. The parameterization of existing QMC methods contains a free unitary variable. Accordingly, it finds infinite solutions that match the given data when its existence condition is met. Unfortunately, a criterion for selecting the best QMC solution is not available, and matching

these two parameters up to q does not guarantee to match the physics system's parameters. This chapter provides a criterion to select the particular QMC solution that matches the Markov and covariance parameters up to infinity using minimal data. We call it "the efficient QMC".

The outline of this chapter is as follows: Section 3.2 formulates the mathematical problem statement. Section 3.3 gives the existence condition and solution of the efficient QMC and proves that it matches Markov and covariance parameters up to infinity. Section 3.4 gives a generalized QMC theory to find the efficient QMC solution for stable/unstable system and an algorithm for system identifications using the QMC method. Section 3.5 presents a comparison among the efficient QMC and two other popular system identification techniques, Eigensystem Realization Algorithm (ERA) and Eigensystem Realization Algorithm using Data Correlations (ERA/DC).

3.2 Problem Statement

Let us assume an unknown system of interest:

$$x_{k+1} = Ax_k + Bu_k, \tag{3.1a}$$

$$y_k = Cx_k + Du_k, \tag{3.1b}$$

where $x_k \in \mathbb{R}^n$, $y_k \in \mathbb{R}^m$, $u_k \in \mathbb{R}^r$, are the state, output, and input signals, and A, B, C, D are matrices of proper dimensions. We are assumed to have access to input u_k and output y_k only. If exciting the system (3.1) with a zero-mean independent white noise sequence with variance I, we experimentally evaluate its Markov parameters (H_i) and covariance parameters (R_i) using the following formulas:

$$H_i = E(y_{k+i}u_k^T) = \lim_{N\to\infty} \frac{1}{N} \sum_{k=0}^{N} y_{k+i}u_k^T, \tag{3.2a}$$

$$R_i = E(y_{k+i}y_k^T) = \lim_{N\to\infty} \frac{1}{N} \sum_{k=0}^{N} y_{k+i}y_k^T. \tag{3.2b}$$

Suppose a QMC solution is a state-space realization in the form (3.3):

$$\hat{x}_{k+1} = \hat{A}\hat{x}_k + \hat{B}u_k, \tag{3.3a}$$

$$\hat{y}_k = \hat{C}\hat{x}_k + \hat{D}u_k, \tag{3.3b}$$

Deterministic definitions for corresponding Markov parameters ($\hat{H}_i$) and covariance parameters ($\hat{R}_i$) of the QMC solution (3.3) are given in (3.4a,3.4b) where $\hat{X}$ is the steady state solution of the Lyapunov stability equation (3.4c):

$$\hat{H}_0 = 0, \hat{H}_i = \hat{C}\hat{A}^{i-1}\hat{B}, i = 1, 2, \ldots \tag{3.4a}$$

$$\hat{R}_i = \hat{C}\hat{A}^i\hat{X}\hat{C}^T + \hat{H}_i H_0^T, i = 0, 1, 2, \ldots \tag{3.4b}$$

$$\hat{X} = \hat{A}\hat{X}\hat{A}^T + \hat{B}\hat{B}^T. \tag{3.4c}$$

Existing QMC methods solve the following problem: "Suppose an unknown system (3.1) produces $\{H_i, R_i | i = 0, 1, \cdots, q-1\}$ where q is a pre-specified positive scalar. Find all finite-dimensional linear time-invariant (FDLTI) models (3.3) whose $\{\hat{H}_i, \hat{R}_i | i = 0, 1, \cdots, q-1\}$ matches the data $\{H_i, R_i | i = 0, 1, \cdots, q-1\}$ [6, 7, 20]."

Construct matrices H_q and R_q using Markov parameters and covariance parameters as (3.5a) and (3.5b), and define the data matrix D_q as (3.5c):

$$H_q = \begin{bmatrix} H_0 & 0 & \cdots & 0 \\ H_1 & H_0 & \vdots & 0 \\ \vdots & \ddots & \ddots & \vdots \\ H_{q-1} & \cdots & H_1 & H_0 \end{bmatrix}, \tag{3.5a}$$

$$R_q = \begin{bmatrix} R_0 & R_1^T & \cdots & R_q^T \\ R_1 & R_0 & \ddots & \vdots \\ \vdots & \ddots & \ddots & R_1^T \\ R_{q-1} & \cdots & R_1 & R_0 \end{bmatrix}, \tag{3.5b}$$

$$D_q = R_q - H_q U_q H_q^T. \tag{3.5c}$$

If $D_q \geq 0$ is satisfied, all linear systems that match the given set of data are parameterized as the following [6, 7]:

$$\begin{bmatrix} \hat{D} & \hat{C} \\ \hat{B} & \hat{A} \end{bmatrix} = \begin{bmatrix} I & 0 \\ 0 & O_{q-1}^{+} \end{bmatrix} \begin{bmatrix} M_q & O_q \end{bmatrix} + \begin{bmatrix} 0 \\ V_b \hat{U} V_d^T \end{bmatrix}, \tag{3.6a}$$

where $M_q = \begin{bmatrix} H_0 \\ \vdots \\ H_{q-1} \end{bmatrix}$, $O_q O_q^T = D_q$ is the minimal rank factorization of D_q, $\hat{U}$ is an arbitrary matrix of proper dimension satisfying $\hat{U}\hat{U}^T = I$, and V_b, V_d are given by the following decomposition:

$$O_{q-1} = \begin{bmatrix} U_a & U_b \end{bmatrix} \begin{bmatrix} \Sigma_a & 0 \\ 0 & 0 \end{bmatrix} \begin{bmatrix} V_a^T \\ V_b^T \end{bmatrix}, \tag{3.6b}$$

$$\begin{bmatrix} K_{q-1} & N_{q-1} \end{bmatrix} = \begin{bmatrix} U_a & U_b \end{bmatrix} \begin{bmatrix} \Sigma_a & 0 \\ 0 & 0 \end{bmatrix} \begin{bmatrix} V_c^T \\ V_d^T \end{bmatrix}, \tag{3.6c}$$

where $K_{q-1} = \begin{bmatrix} 0 & I_{q-1} \end{bmatrix} M_q$, and $N_{q-1} = \begin{bmatrix} 0 & I_{q-1} \end{bmatrix} O_q$.

Equation (3.6) shows the set of all solutions that matches the data $\{H_i, R_i | i = 0, 1, \cdots, q-1\}$. It is our intention to find the efficient QMC solution that matches the data $\{H_i, R_i | i = 0, 1, \cdots, \infty\}$.

3.3 The Efficient QMC

In this section we show the selection of the efficient QMC solution, and prove that this solution matches parameters $\{H_i, R_i | i = 0, 1, \cdots, \infty\}$ using finite data.

Theorem 3.3.1. *Suppose an unknown system generates data $\{H_i, R_i | i = 0, 1, \cdots, q-1\}$, and $D_q > 0$. Let n be the effective state dimension and m be the output size of the unknown system. The following two statements are equivalent:*

1. $q \geq \frac{n}{m} + 1$

2. *There exists an efficient QMC solution (3.3) with $X = I$ that matches $\{H_i, R_i | i = 0, 1, \cdots, q-$*

1}

Under this circumstance, the efficient QMC solution is given by the following:

$$\begin{bmatrix} \hat{D} & \hat{C} \\ \hat{B} & \hat{A} \end{bmatrix} = \begin{bmatrix} I & 0 \\ 0 & O_{q-1}^{+} \end{bmatrix} \begin{bmatrix} M_q & O_q \end{bmatrix}. \tag{3.7}$$

Proof. Expanding the system (3.3) over the horizon $[0, q-1]$ yields the following:

$$\hat{y}_0 = \hat{C}\hat{x}_0 + \hat{D}u_0, \tag{3.8a}$$

$$\hat{y}_1 = \hat{C}\hat{A}\hat{x}_0 + \hat{C}\hat{B}u_0 + \hat{D}u_1, \tag{3.8b}$$

$$\hat{y}_2 = \hat{C}\hat{A}^2\hat{x}_0 + \hat{C}\hat{A}\hat{B}u_0 + \hat{C}\hat{B}u_1 + \hat{D}u_2, \tag{3.8c}$$

$$\vdots$$

$$\hat{y}_{q-1} = \hat{C}\hat{A}^{q-1}\hat{x}_0 + \hat{C}\hat{A}^{q-2}\hat{B}u_0 + \cdots + \hat{C}\hat{B}u_{q-1} + \hat{D}u_q. \tag{3.8d}$$

Augment equations (3.8a) - (3.8d) to get the following expression:

$$\begin{bmatrix} \hat{y}_0 \\ \hat{y}_1 \\ \hat{y}_2 \\ \vdots \\ \hat{y}_{q-1} \end{bmatrix} = \begin{bmatrix} \hat{C} \\ \hat{C}\hat{A} \\ \hat{C}\hat{A}^2 \\ \vdots \\ \hat{C}\hat{A}^{q-1} \end{bmatrix} \hat{x}_0 + \begin{bmatrix} \hat{H}_0 & 0 & \cdots & \cdots & 0 \\ \hat{H}_1 & \hat{H}_0 & \ddots & \ddots & \vdots \\ \hat{H}_2 & \hat{H}_1 & \ddots & \ddots & \vdots \\ \vdots & \ddots & \ddots & \ddots & \vdots \\ \hat{H}_{q-1} & \cdots & \hat{H}_2 & \hat{H}_1 & \hat{H}_0 \end{bmatrix} \begin{bmatrix} u_0 \\ u_1 \\ u_2 \\ \vdots \\ u_q \end{bmatrix}, \tag{3.9}$$

Notice that if a QMC solution (3.3) exists, $\hat{H}_i$ and $\hat{R}_i$ match the parameters H_i and R_i up to q. Take outer products on both sides of (3.9) yields:

$$R_q = O_q O_q^T + H_q H_q^T, \tag{3.10}$$

If $D_q \geq 0$ is satisfied, there exists at least one QMC solution 3.3 that matches the given data.

Under this condition, two governing equations of the QMC algorithm are below:

$$O_{q-1}\begin{bmatrix}\hat{B} & \hat{A}\end{bmatrix} = \begin{bmatrix}K_{q-1} & N_{q-1}\end{bmatrix}, \tag{3.11a}$$

$$\begin{bmatrix}\hat{B} & \hat{A}\end{bmatrix}\begin{bmatrix}\hat{B} & \hat{A}\end{bmatrix}^T = I. \tag{3.11b}$$

Equation (3.11a) can be easily verified by observation; equation (3.11b) comes from the Lyapunov stability equation of (3.3) by setting $\hat{X} = I$ and $U = I$. Equation (3.11a) and (3.11b) forms the standard linear algebra problem of $\mathbf{AX} = \mathbf{B}, \mathbf{XX^T} = \mathbf{I}$. Its solution is given as (3.6) which involves a pseudo inverse of O_{q-1}.

Notice that the dimension of O_{q-1} is $(q-1)m \times n$, where q is the number of parameters to match, and m is the dimension of outputs. Under the condition that $(q-1)m \geq n$, the singular value decomposition of O_{q-1}, which is equation (3.6b), becomes the following:

$$O_{q-1} = \begin{bmatrix}U_a & U_b\end{bmatrix}\begin{bmatrix}\Sigma_a \\ 0\end{bmatrix}\begin{bmatrix}V_a^T\end{bmatrix}, \tag{3.12}$$

Notice that V_b vanishes in the decomposition above. This means the term $V_b\hat{U}V_d^T$ vanishes, and the variable $\hat{U}$ does not have an impact on the qmc solution. The qmc solution becomes unique as (3.7). □

Lemma 3.3.2. *If Markov parameters H_i and covariance parameters R_i are fully converged, the efficient QMC solution (3.7) matches $\{H_i, R_i | i = 0, 1, \ldots, \infty\}$.*

Proof. We just prove that the efficient QMC solution (3.7) matches $\{H_i, R_i | i = 0, 1, \ldots, q+k-1\}$ for any positive scalar k.

Define $D_{q+k} > 0$ to be the data matrix constructed by $\{H_i, R_i | i = 0, 1, \ldots, q+k-1\}$, and $\{A_{q+k}, B_{q+k}\}$ is the unique $q+k$-MC plant that matches D_{q+k}:

$$D_{q+k} \triangleq \begin{bmatrix}D_q & D_{12} \\ D_{12}^T & D_{22}\end{bmatrix}, \tag{3.13a}$$

$$A_{q+k} \triangleq \begin{bmatrix} \hat{A} & A_{12} \\ A_{21} & A_{22} \end{bmatrix}, \tag{3.13b}$$

$$B_{q+k} \triangleq \begin{bmatrix} \hat{B} \\ B_2 \end{bmatrix}, \tag{3.13c}$$

From the decomposition of D_{q+k}, we have:

$$D_{q+k} = O_{q+k} O_{q+k}^T, \tag{3.14a}$$

where

$$O_{q+k} = \begin{bmatrix} O_q & 0 \\ O_{21} & O_{22} \end{bmatrix}. \tag{3.14b}$$

Expand O_{q+k} as the following:

$$O_{q+k} = \begin{bmatrix} \hat{C} & 0 \\ \vdots & \vdots \\ \hat{C}\hat{A}^{q-1} & 0 \\ O_{q,1} & O_{q,2} \\ O_{q+1,1} & O_{q+1,2} \\ \vdots & \vdots \\ O_{q+k-1,1} & O_{q+k-1,2} \end{bmatrix}. \tag{3.15a}$$

where

$$O_{21} = \begin{bmatrix} O_{q,1} \\ O_{q+1,1} \\ \vdots \\ O_{q+k-1,1} \end{bmatrix}, O_{22} = \begin{bmatrix} O_{q,2} \\ O_{q+1,2} \\ \vdots \\ O_{q+k-1,2} \end{bmatrix}. \tag{3.15b}$$

The governing equation that $\{A_{q+k}, B_{q+k}\}$ satisfies the following:

$$\begin{bmatrix} \hat{C} & 0 \\ \vdots & \vdots \\ \hat{C}\hat{A}^{q-1} & 0 \\ O_{q,1} & O_{q,2} \\ O_{q+1,1} & O_{q+1,2} \\ \vdots & \vdots \\ O_{q+k-2,1} & O_{q+k-2,2} \end{bmatrix} \begin{bmatrix} \hat{A} & A_{12} & \hat{B} \\ A_{21} & A_{22} & B_2 \end{bmatrix} = \begin{bmatrix} \hat{C}\hat{A} & 0 & H_1 \\ \vdots & \vdots & \vdots \\ O_{q,1} & O_{q,2} & H_q \\ O_{q+1,1} & O_{q+1,2} & H_{q+1} \\ O_{q+2,1} & O_{q+2,2} & H_{q+2} \\ \vdots & \vdots & \\ O_{q+k-1,1} & O_{q+k-1,2} & H_{q+k-1} \end{bmatrix} \tag{3.16}$$

Notice

$$\begin{bmatrix} \hat{O}_{q-1} & 0 \end{bmatrix} \begin{bmatrix} A_{12} \\ A_{22} \end{bmatrix} = 0, \tag{3.17a}$$

The matrix $\hat{O}_{q-1}$ is of full column rank because of the dimension requirement $q \geq \frac{n}{m} + 1$. The only solution for (3.17a) is

$$A_{12} = 0. \tag{3.17b}$$

Notice

$$\begin{bmatrix} \hat{C}\hat{A}^{q-1} & 0 \end{bmatrix} \begin{bmatrix} A_{12} \\ A_{22} \end{bmatrix} = O_{q,2}, \tag{3.17c}$$

Using (3.17b) makes

$$O_{q,2} = 0. \tag{3.17d}$$

Notice

$$\begin{bmatrix} O_{q,1} & O_{q,2} \end{bmatrix} \begin{bmatrix} A_{12} \\ A_{22} \end{bmatrix} = O_{q+1,2}, \tag{3.17e}$$

Using (3.17b) and (3.17d) makes

$$O_{q+1,2} = 0. \tag{3.17f}$$

Keep this iteration and one can conclude:

$$O_{22} = 0, \tag{3.18}$$

Notice that O_{q-1} is of full column rank, thus

$$rank(O_{q+k}) = rank(O_{q-1}). \tag{3.19}$$

As a result, we have

$$A_{21} = 0, \tag{3.20a}$$

$$A_{22} = 0, \tag{3.20b}$$

$$B_2 = 0. \tag{3.20c}$$

Consequently, the efficient QMC solution (3.7) is equivalent to a QMC solution that matches the data matrix D_{q+k} for any positive scalar k.

□

3.4 A Generalized QMC Theory

In Chapter 2 section 2.5 we develop a formulation that extends the QMC method to system identification of unstable systems. In Chapter 2 section 3.2 we develop a formulation that finds the efficient QMC solution. In this section we combine the two formulations to a generalized QMC theory that finds an efficient QMC solution for system identification applications, regardless of the stability of the system to identify.

Theorem 3.4.1. *Given the data $\{H_i, R_i | i = 0, 1, \cdots, q-1\}$ generated by a system (not necessarily stable) with white noise excitation of variance U. Suppose $\bar{D}_q \geq 0$ is satisfied. Let m, r and n represent the numbers of outputs, inputs and effective state dimension of the unknown system respectively, where where $(q-1)m \geq n$ is satisfied. Let integers $p \geq q > 0$ be specified. The efficient QMC solution in form of (2.6) with $\hat{X} = I$ that matches the given data is the following:.*

$$\hat{D} = H_0, \tag{3.21a}$$

$$\hat{C} = \begin{bmatrix} I_m & 0 \end{bmatrix} \bar{O}_q, \tag{3.21b}$$

$$\begin{bmatrix} \bar{B} & \bar{A} \end{bmatrix} = \bar{O}_{q-1}^{+} \begin{bmatrix} \bar{M}_{q-1} & \bar{O}_{q-1} \end{bmatrix}, \tag{3.21c}$$

where $\bar{O}_q \bar{O}_q^T = D_q$ is the minimal rank factorization of D_q, $\hat{U}$ is an arbitrary matrix of proper dimension satisfying $\hat{U}\hat{U}^T = I$. Its corresponding QMC system in form of (3.3) is given as:

$$G = -\bar{B} \begin{bmatrix} 0 \\ I_m \end{bmatrix}, \tag{3.22a}$$

$$\hat{A} = \bar{A} - G\hat{C}, \tag{3.22b}$$

$$\hat{B} = \bar{B}\begin{bmatrix} I_r \\ 0 \end{bmatrix} - G\hat{D}. \tag{3.22c}$$

Proof. This theorem is a direct result from Theorem 2.5.2 and Theorem 3.3.1. □

Consider recognizing a physics system whose effective state dimension n is unknown. We summarize a general algorithm for system identification using the QMC method.

Algorithms 3.4.1. *Let $k \leq n$ be specified.*

1. *Select q and m such that $(q-1)m \geq k$.*
2. *Construct $\bar{D}_q$ using data $\{H_i, R_i | i = 0, 1, \cdots, q-1\}$.*
3. *If $rank(D_q) < qm$, declare convergence and proceed to Step 4; otherwise, set $k \leftarrow k+1$ and return to Step 1.*
4. *Find the approximation system using Theorem 3.4.1.*

Remark: In reality, we deal with sensors and actuators with noise. When checking the rank of data matrix $\bar{D}_q$, it is typical to observe that some small eigenvalues close to 0, but not exactly 0. One needs to determine the threshold for such truncations.

3.5 Illustrative Examples

In this section, we introduce a cantilever beam example to demonstrate our method. We find approximation systems of the beam example using methods of q-Markov Covariance Equivalent Realization (QMC), Eigensystem Realization Algorithm (ERA) and Eigensystem Realization Algorithm Considering Data Correlations (ERA/DC), then compare their results.

3.5.1 The Euler Bernoulli Beam

Consider a cantilever beam as shown in Figure 3.1. The beam has deflection $\mu(r,t)$, where r is the spatial displacement from the clamped end, and t is the time variable. Consider the damped

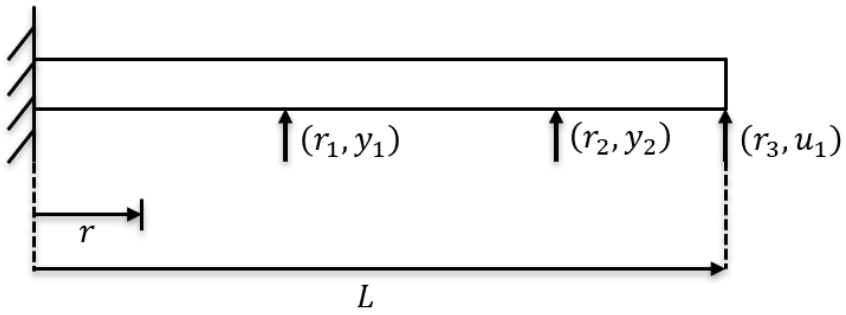

Figure 3.1: A conceptual drawing of a cantilever beam.

flexible structure with N degrees of freedom:

$$\mathcal{M}\ddot{q} + \mathcal{D}\dot{q} + \mathcal{K}q = \mathcal{B}u, \tag{3.23}$$

where $q = [q_1, \ldots, q_N]$ is the time-varying displacement, $u = [u_1, \ldots, u_r]$ is the input vector, matrices $\mathcal{M}, \mathcal{D}$ and $\mathcal{K}$ are the mass, damping and stiffness matrix respectively. Matrix $\mathcal{B}$ determines the locations of actuators. With the normalization of the mass matrix $\mathcal{M}$, the governing equation (3.23) may be reduced to the following modal form:

$$\ddot{q} + 2c\Omega\dot{q} + \Omega^2 q = \mathcal{H}u, \tag{3.24}$$

where $\Omega = diag(\omega_1, \ldots, \omega_N)$, $\mathcal{H} = \left[\mathcal{H}_1, \ldots, \mathcal{H}_N\right]^T$. Here, ω_i^2 are the mode frequencies where:

$$\omega_i = (\beta_i L)^2 \sqrt{\frac{EI}{\rho L^4}}, \tag{3.25}$$

where EI, ρ, and L are the moduli of elasticity, mass density, and beam length, respectively. They are assumed constant. For force inputs, $\mathcal{H}_i$ are defined as:

$$\mathcal{H}_i = [\Phi_i(r_1), \ldots, \Phi_i(r_p)], \tag{3.26}$$

where p is the number of force inputs, and $r_1, \ldots, r_p$ are locations of force actuators. The function $\Phi_i(r)$ is the spatial mode shape function that satisfies specified boundary conditions. Its solution for a cantilever beam is given below [59]:

$$\Phi_i(r) = \mathcal{C}[cosh(\beta_i r) - cos(\beta_i r) - k_i\{sinh(\beta_i r) - sin(\beta_i r)\}], \tag{3.27}$$

where the constant $\mathcal{C}$ is determined by the initial condition at $t = 0$, and constant k_i is defined as:

$$k_i = \frac{cosh(\beta_i L) + cos(\beta_i L)}{sinh(\beta_i L) + sin(\beta_i L)}. \tag{3.28}$$

Define the state vector as follows:

$$x = \left[q_1, \dot{q}_1, \ldots, q_N, \dot{q}_N\right]^T, \tag{3.29a}$$

the corresponding state equation may be constructed below:

$$A = diag\left(\left[\begin{array}{cc} 0 & 1 \\ -\omega_1^2 & -2c\omega_1 \end{array}\right], \ldots, \left[\begin{array}{cc} 0 & 1 \\ -\omega_N^2 & -2c\omega_N \end{array}\right]\right), \tag{3.29b}$$

$$B = \left[\begin{array}{ccc} 0 & \ldots & 0 \\ \Phi_1(r_1) & \ldots & \Phi_1(r_p) \\ \vdots & \ldots & \vdots \\ 0 & \ldots & 0 \\ \Phi_N(r_1) & \ldots & \Phi_N(r_p) \end{array}\right], \tag{3.29c}$$

Define outputs as the accelerations of deflections below:

$$y = \left[\ddot{\mu}_1, \ldots, \ddot{\mu}_m\right]^T, \tag{3.29d}$$

the corresponding output equation may be constructed below:

$$C = \begin{bmatrix} \Phi_1(r_1) & \dots & \Phi_N(r_1) \\ \vdots & \vdots & \vdots \\ \Phi_1(r_m) & \dots & \Phi_N(r_m) \end{bmatrix} diag\left(\begin{bmatrix} -\omega_1^2 & -2c\omega_1 \end{bmatrix}, \dots, \begin{bmatrix} -\omega_N^2 & -2c\omega_N \end{bmatrix}\right), \tag{3.29e}$$

$$D = \begin{bmatrix} \Phi_1(r_1) & \dots & \Phi_N(r_1) \\ \vdots & \vdots & \vdots \\ \Phi_1(r_m) & \dots & \Phi_N(r_m) \end{bmatrix} \begin{bmatrix} \Phi_1(r_1) & \dots & \Phi_1(r_p) \\ \vdots & \dots & \vdots \\ \Phi_N(r_1) & \dots & \Phi_N(r_p) \end{bmatrix}. \tag{3.29f}$$

3.5.2 Eigensystem Realization Algorithm (ERA)

Assume a system may be represented by the state-space realization (3.1) whose Markov parameters (3.2a) are known. Construct the following Hankel matrices:

$$\Psi_1 = \begin{bmatrix} H_1 & H_2 & \cdots & H_b \\ H_2 & H_3 & \cdots & H_{b+1} \\ \vdots & \iddots & \iddots & \vdots \\ H_a & H_{a+1} & \cdots & H_{a+b-1} \end{bmatrix}, \tag{3.30a}$$

$$\Psi_2 = \begin{bmatrix} H_2 & H_3 & \cdots & H_{b+1} \\ H_3 & H_4 & \cdots & H_{b+2} \\ \vdots & \iddots & \iddots & \vdots \\ H_{a+1} & H_{a+2} & \cdots & H_{a+b} \end{bmatrix}, \tag{3.30b}$$

where a and b are arbitrary positive integers. The above two matrices may be decomposed as the following:

$$\Psi_1 = \mathcal{O}\mathcal{C}, \tag{3.31a}$$

$$\Psi_2 = \mathcal{O}A\mathcal{C}, \tag{3.31b}$$

where

$$\mathcal{O} = \begin{bmatrix} C \\ CA \\ \vdots \\ CA^{a-1} \end{bmatrix}, \tag{3.31c}$$

$$\mathcal{C} = \begin{bmatrix} B & AB & \cdots & A^{b-1}B \end{bmatrix}. \tag{3.31d}$$

Evaluate the singular value decomposition of Ψ gives the following:

$$\Psi_1 = \begin{bmatrix} U_n & U_t \end{bmatrix} \begin{bmatrix} \Sigma_n & 0 \\ 0 & \Sigma_t \end{bmatrix} \begin{bmatrix} V_n^T \\ V_t^T \end{bmatrix}, \tag{3.32}$$

where Σ_n is the dominant eigenvalues and Σ_t is the eigenvalues to truncate. An ERA realization of order n that captures the majority eigenvalues of the Hankel matrix Ψ_1 is computed as below:

$$A_e = \Sigma_n^{-\frac{1}{2}} U_n^T \Psi_2 V_n \Sigma_n^{-\frac{1}{2}}, \tag{3.33a}$$

$$B_e = \Sigma_n^{\frac{1}{2}} V_n^T \begin{bmatrix} I_p \\ 0 \end{bmatrix}, \tag{3.33b}$$

$$C_e = \begin{bmatrix} I_m & 0 \end{bmatrix} U_n \Sigma_n^{\frac{1}{2}}, \tag{3.33c}$$

$$D_e = H_0. \tag{3.33d}$$

3.5.3 Eigensystem Realization Algorithm Using Data Correlations (ERA/DC)

Construct the following matrices:

$$\Psi_i = \begin{bmatrix} H_i & H_{i+1} & \cdots & H_{b+i-1} \\ H_{i+1} & H_{i+2} & \cdots & H_{b+i} \\ \vdots & \iddots & \iddots & \vdots \\ H_{a+i-1} & H_{a+i} & \cdots & H_{a+b+i-2} \end{bmatrix}, \tag{3.34a}$$

$$\Theta_i = \Psi_i \Psi_1^T, \tag{3.34b}$$

$$\mathcal{U}_i = \begin{bmatrix} \Theta_i & \Theta_{i+1} & \cdots & \Theta_{\beta+i-1} \\ \Theta_{i+1} & \Theta_{i+2} & \cdots & \Theta_{\beta+i} \\ \vdots & \iddots & \iddots & \vdots \\ \Theta_{\alpha+i-1} & \Theta_{\alpha+i} & \cdots & \Theta_{\alpha+\beta+i-2} \end{bmatrix}, \tag{3.34c}$$

where a, b, and α, β are arbitrary positive integers. The following decomposition may be composed:

$$\mathcal{U}_1 = \mathcal{M}\mathcal{N}, \tag{3.35a}$$

$$\mathcal{U}_2 = \mathcal{M}A\mathcal{N}, \tag{3.35b}$$

where

$$\mathcal{M} = \begin{bmatrix} \mathcal{O} \\ \mathcal{O}A \\ \vdots \\ \mathcal{O}A^{\alpha-1} \end{bmatrix}, \tag{3.35c}$$

$$\mathcal{N} = \begin{bmatrix} \mathcal{P} & A\mathcal{P} & \cdots & A^{\beta-1}\mathcal{P} \end{bmatrix}, \tag{3.35d}$$

$$\mathcal{P} = \mathcal{C}\mathcal{C}^T\mathcal{O}^T, \tag{3.35e}$$

Notice $\mathcal{O}$ and $\mathcal{C}$ are the observability and controllability matrices defined in Equations (3.31c) and (3.31d).

Evaluate the singular value decomposition of $\mathcal{U}$ gives the following:

$$\mathcal{U}_1 = \begin{bmatrix} U_n & U_t \end{bmatrix} \begin{bmatrix} \Sigma_n & 0 \\ 0 & \Sigma_t \end{bmatrix} \begin{bmatrix} V_n^T \\ V_t^T \end{bmatrix}, \tag{3.36}$$

where Σ_n is the dominant eigenvalues and Σ_t is the eigenvalues to truncate. An ERA/DC realization of order n that captures the majority eigenvalues of the Hankel matrix Ψ_1 is computed as below:

$$A_d = \Sigma_n^{-\frac{1}{2}} U_n^T \mathcal{U}_2 V_n \Sigma_n^{-\frac{1}{2}}, \tag{3.37a}$$

$$B_d = \Sigma_n^{-\frac{1}{2}} U_n^T \begin{bmatrix} \Psi_1 \\ \vdots \\ \Psi_{a+i-1} \end{bmatrix} \begin{bmatrix} I_p \\ 0 \end{bmatrix}, \tag{3.37b}$$

$$C_d = \begin{bmatrix} I_m & 0 \end{bmatrix} U_n \Sigma_n^{\frac{1}{2}}, \tag{3.37c}$$

$$D_d = H_0. \tag{3.37d}$$

3.5.4 A Beam Example

In our specific example, we select the cantilever beam with following material properties: $EI = 1, \rho = 1, L = 1$. We consider 4 modes, 2 outputs and 1 input, where $N = 4, m = 2, p = 1$. The corresponding mode frequencies are given as: $\omega_1^2 = 3.5160, \omega_2^2 = 22.0345, \omega_3^2 = 61.6972, \omega_4^2 = 120.9019$. The two acceleration outputs are specified at locations $r_1 = 0.4L, r_2 = 0.8L$ and the force input is specified at location $r_3 = L$. The effective state dimension of this system is $n = 8$. This beam model is assumed to be the physics.

3.5.4.1 A Noise Free Example

In this case we identify this system using fully converged cross-correlations and auto-correlations (defined as (3.2a) and (3.2b)) for QMC, ERA and ERA/DC methods. We select $q = 9$ in the QMC method that uses data $\{H_i, R_i | i = 0, 1, \ldots, 8\}$, $a = 9, b = 9$ in the ERA method that uses data $\{H_i | i = 0, 1, \ldots, 18\}$, and $a = 9, b = 9, \alpha = 4, \beta = 4$ in the ERA/DC that uses data $\{H_i | i = 0, 1, \ldots, 24\}$.

Figures 3.2, 3.3 and 3.4 show the frequency responses for the beam model versus QMC model, ERA model and ERA/DC model respectively. All three methods capture the four modes at specific mode frequencies. However, the ERA and ERA/DC models lose information on magnitude and phase at lower frequency bands for both outputs. Figure 3.5 shows the error in frequency responses, and Figure 3.6 shows the error in eigenvalues between the three methods and physics. Both show that the QMC method generates the least error, while the ERA method generates the biggest error. Using fully converged Markov and covariance parameters, the QMC method recovers the physics of the system to identify.

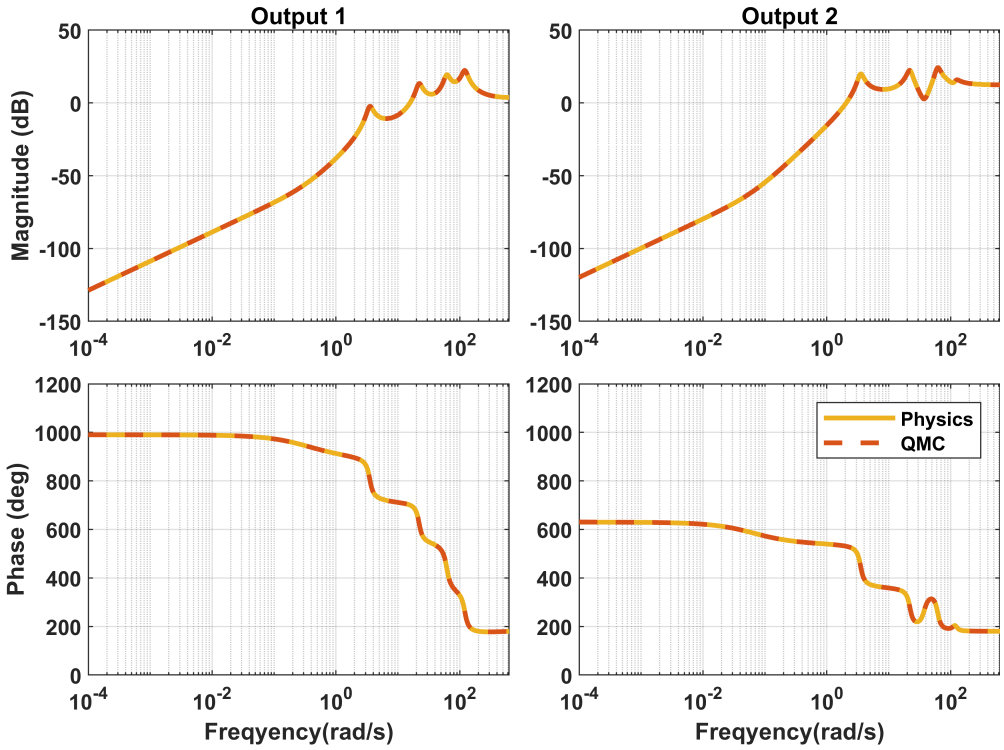

Figure 3.2: Frequency responses of QMC vs physics for a noise-free case.

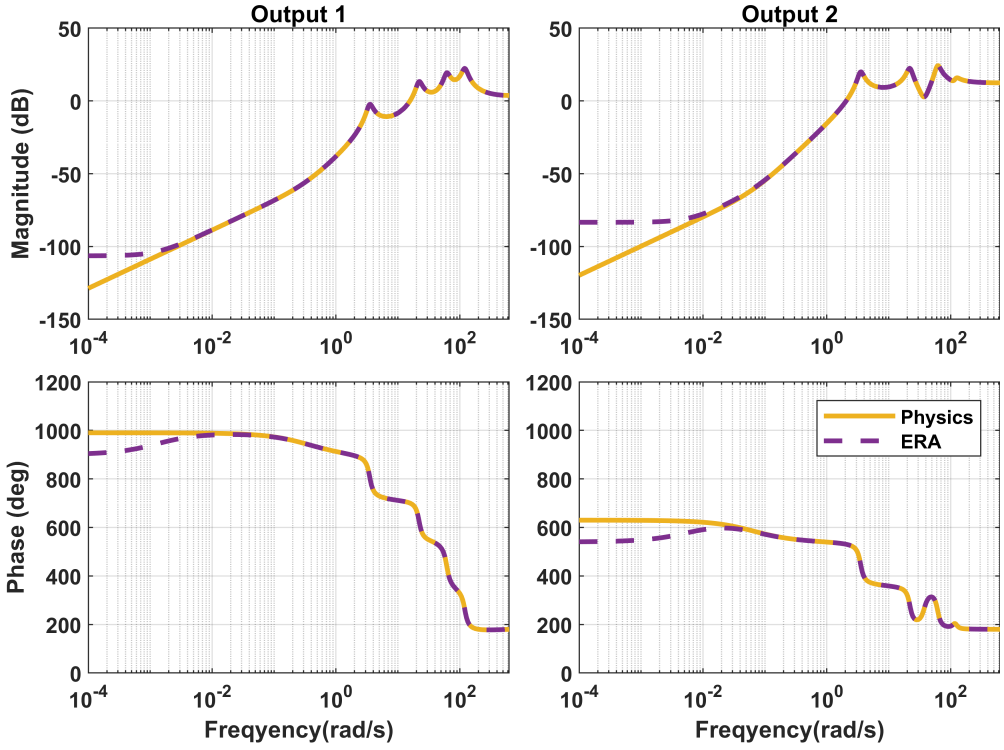

Figure 3.3: Frequency responses of ERA vs physics for a noise-free case.

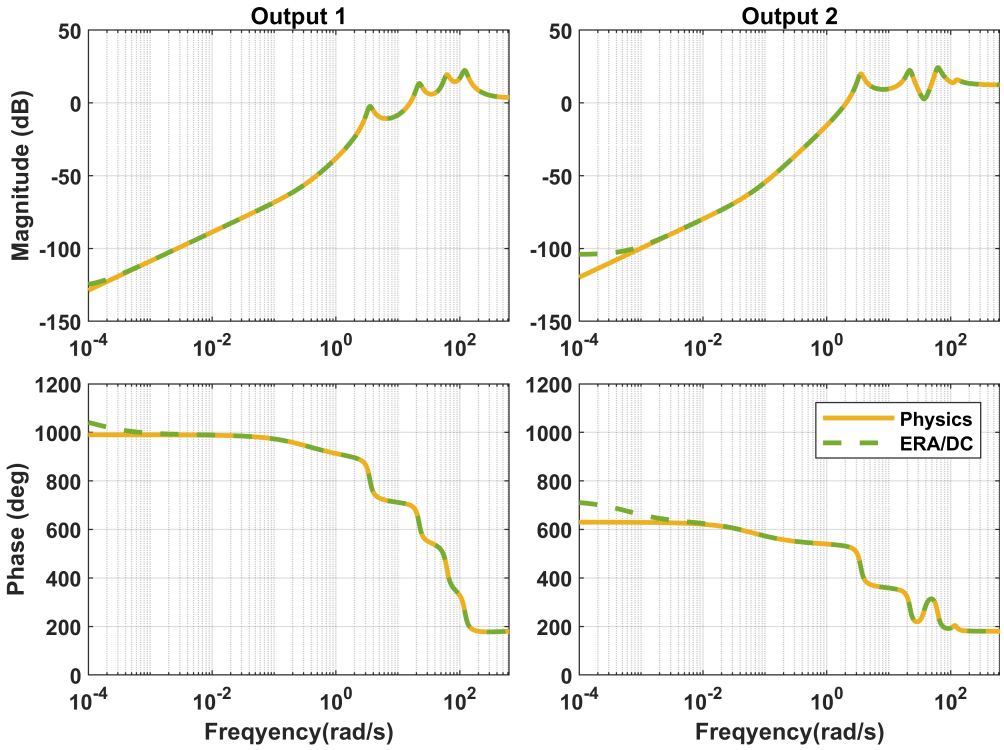

Figure 3.4: Frequency responses of ERA/DC vs physics for a noise-free case.

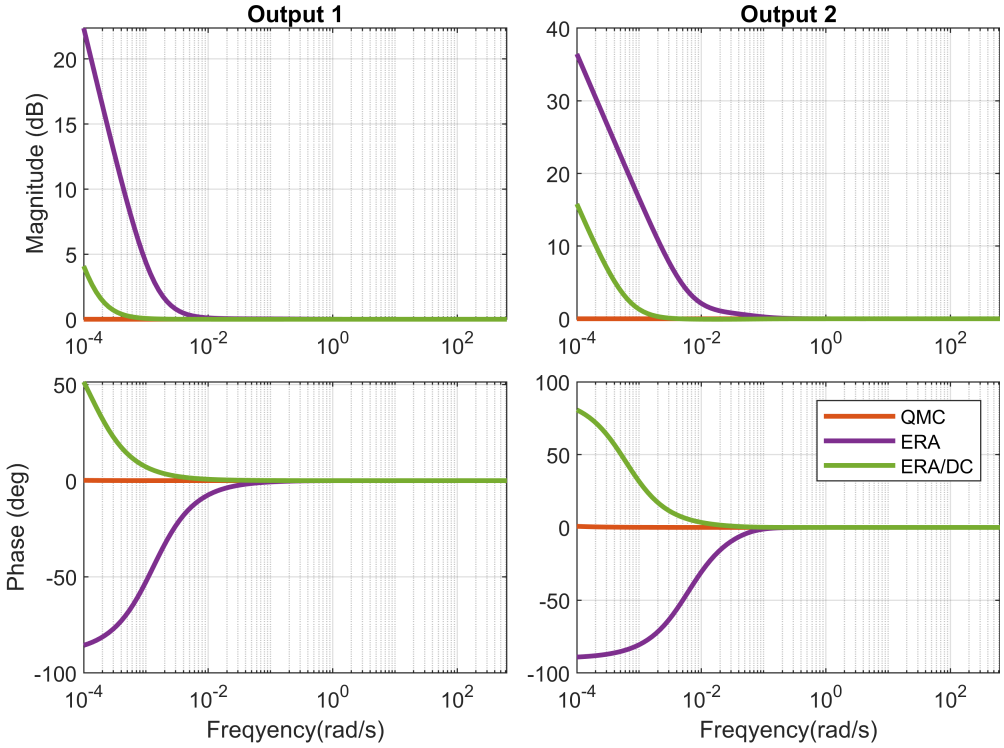

Figure 3.5: Errors in frequency responses for QMC, ERA and ERA/DC for a noise-free case.

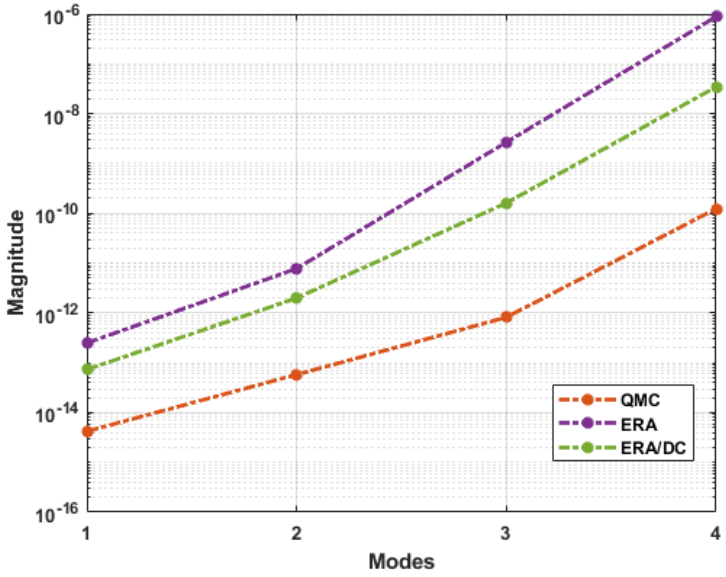

Figure 3.6: Error in eigenvalues for QMC, ERA and ERA/DC at different shape modes for a noise-free case.

3.5.4.2 A Noisy Example

In this case we identify this system cross-correlations and auto-correlations from white noise experiments for QMC, ERA and ERA/DC methods. Additive noises are modelled as zero-mean white Gaussian noise of covariance 1×10^{-7}, and applied on inputs and outputs. With adequate experiment trials, experimentally-determined parameters will eventually converge. In this example, these parameters contain measurement error due to limited computation resources. We select $q = 50$ in the QMC method that uses data $\{H_i, R_i | i = 0, 1, \ldots, 49\}$, $a = 50, b = 50$ in the ERA method that uses data $\{H_i | i = 0, 1, \ldots, 100\}$, and $a = 30, b = 30, \alpha = 20, \beta = 20$ in the ERA/DC that uses data $\{H_i | i = 0, 1, \ldots, 100\}$.

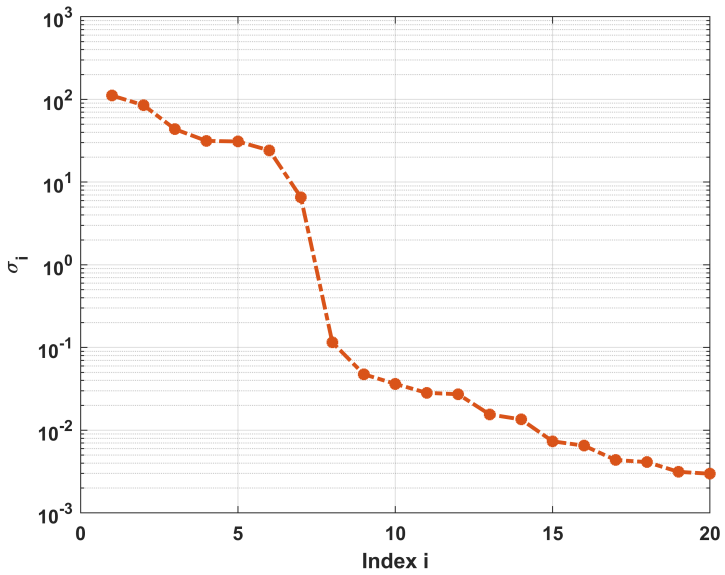

Figure 3.7: Singular values for noisy data matrix D_q of QMC.

Figures 3.7, 3.8 and 3.9 show the singular values of data/measurement matrices of three methods. All three figures show a significant decrease after the $8th$ singular value. Residue singular values are caused by convergence errors, where one needs to determine the threshold of where to truncate. In this case, we keep the first 14 singular values for the QMC method, the first 14 for

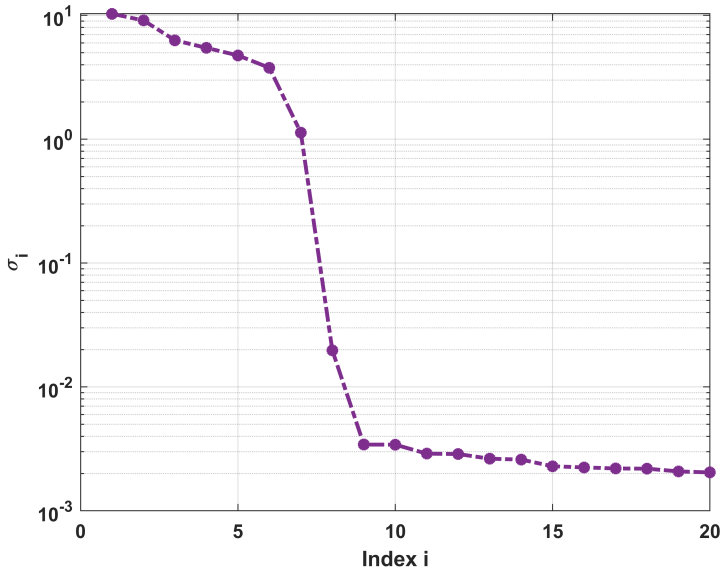

Figure 3.8: Singular values for noisy measurement matrix Φ_1 of ERA.

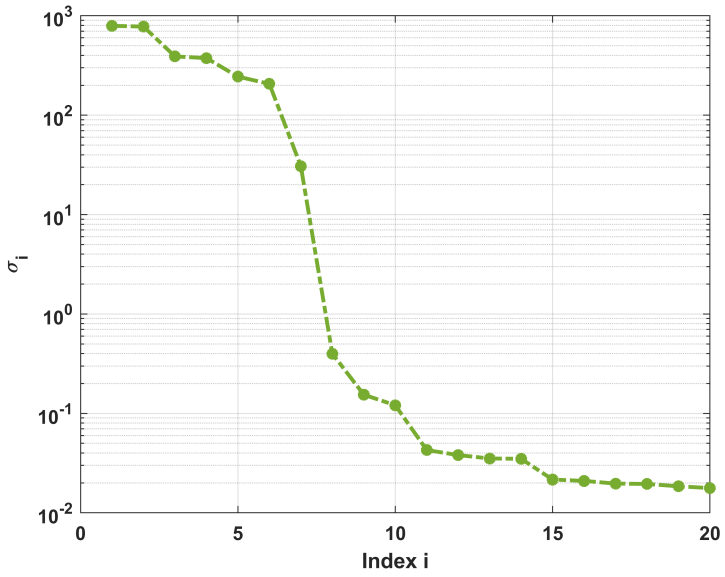

Figure 3.9: Singular values for noisy measurement matrix $\mathcal{U}_1$ of ERA/DC.

the ERA method, and the first 14 for ERA/DC method. Their corresponding frequency responses versus the physics are presented in Figures 3.10, 3.11 and 3.12. One may observe that only the QMC method identifies the four modes at correct frequencies correctly. The ERA method misses

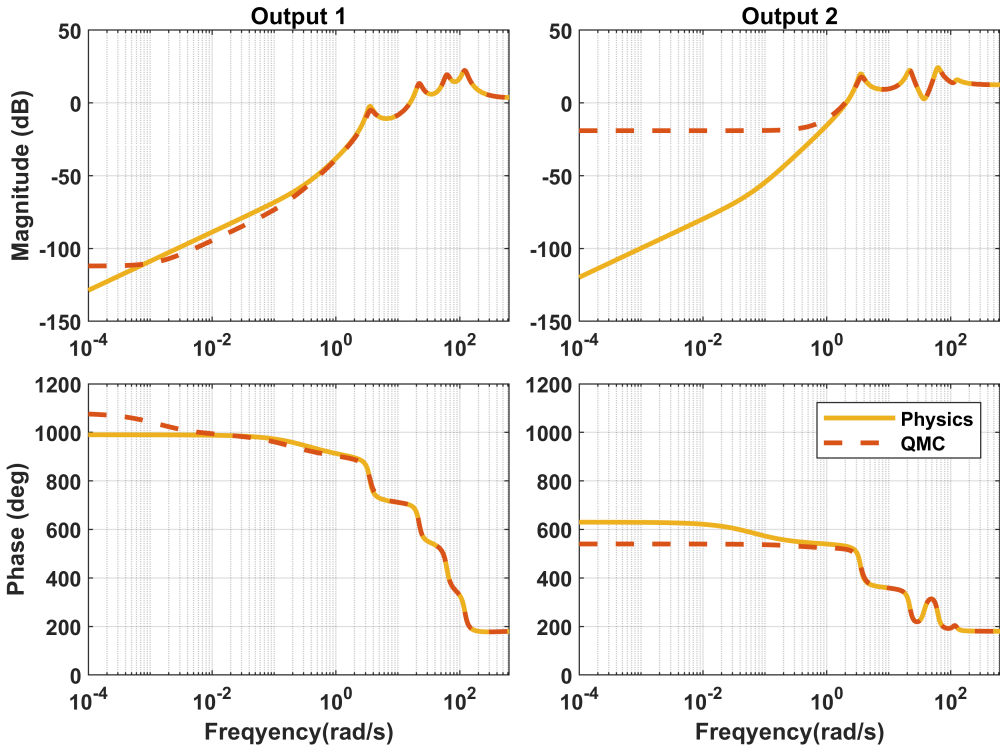

Figure 3.10: Frequency responses of QMC vs Physics for a noisy case.

the phase information for the first mode, and the ERA/DC method misses the magnitude information for the first mode. Figure 3.13 presents the errors in frequency responses of three methods. It shows that the QMC method produces the least magnitude and phase errors during all frequency bands.

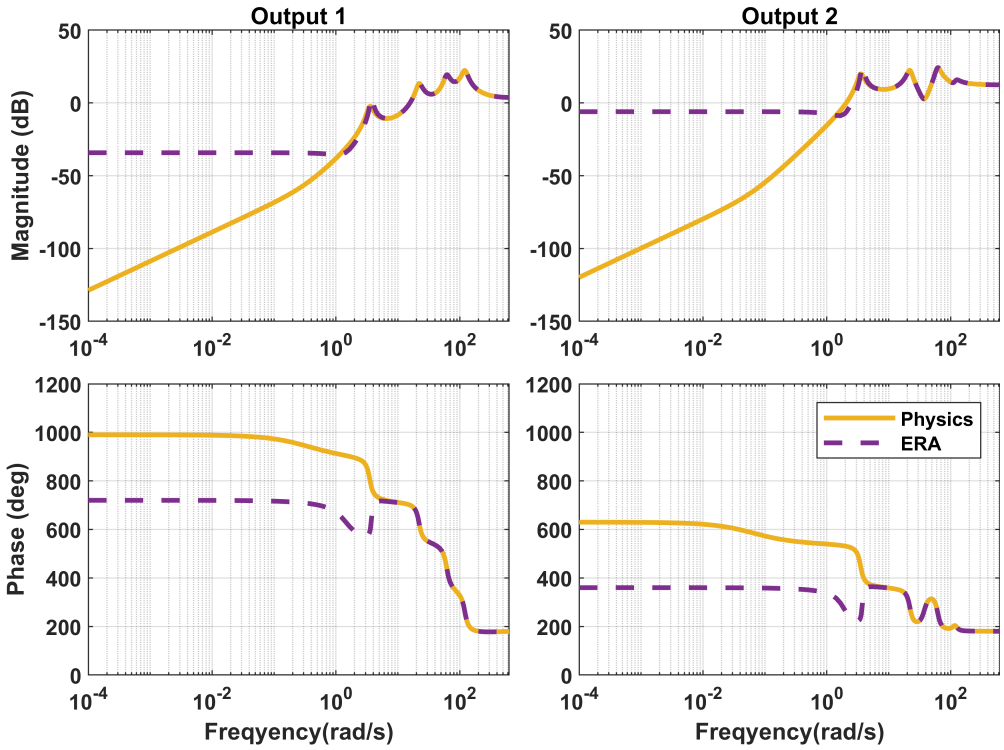

Figure 3.11: Frequency responses of ERA vs Physics for a noisy case.

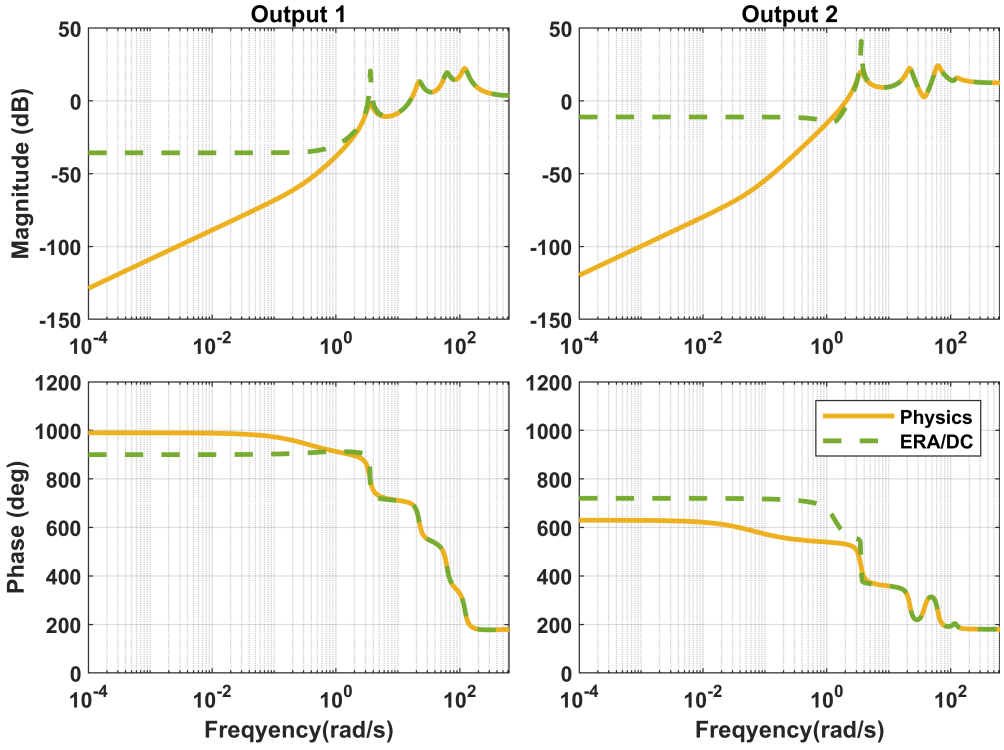

Figure 3.12: Frequency responses of ERA/DC vs Physics for a noisy case.

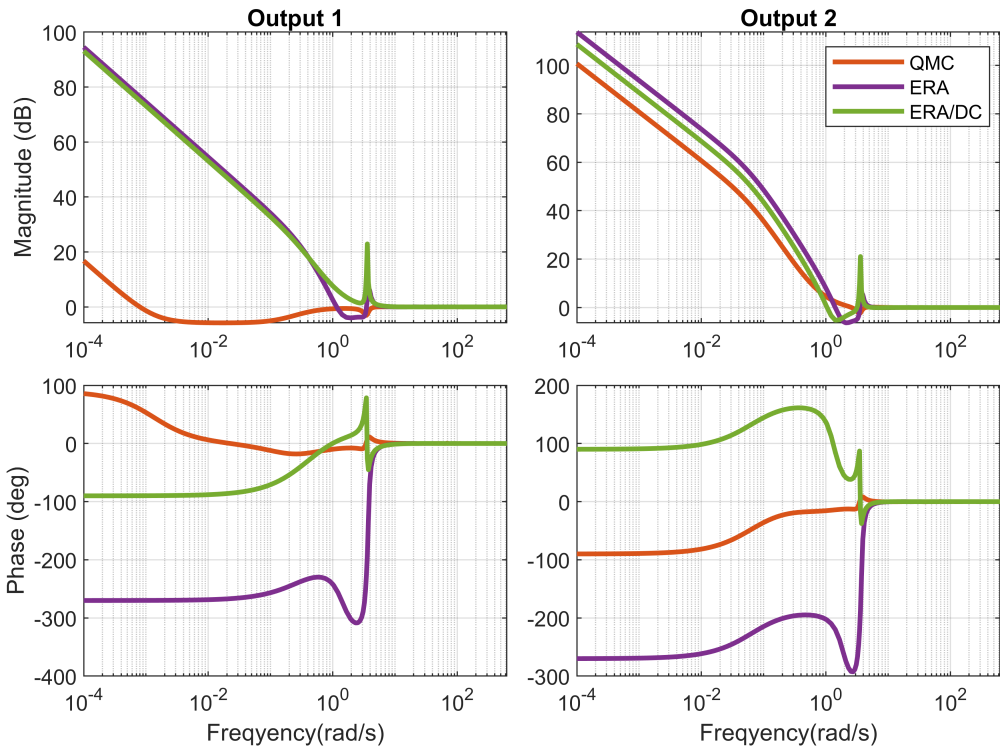

Figure 3.13: Errors in frequency responses of QMC, ERA and ERA/DC for a noisy case.

3.6 Conclusions

A method that finds an efficient q-Markov covariance equivalent realization (QMC) system that matches the first Markov parameters and covariance parameters up to ∞ with a finite number of data is presented. This efficient QMC solution also matches the transfer function and frequency responses of the system to identify. A generalized QMC theory is also provided to find the efficient QMC solution for stable/unstable systems and an algorithm for system identification using the QMC method. A comparison of the QMC approach with Eigensystem Realization Algorithm (ERA) and Eigensystem Realization Algorithm using Data Correlations (ERA/DC) is presented. Compared to the other two, the QMC method finds an approximation system with the least errors in frequency responses.

4. DYNAMIC SYSTEM SIMULATION

The dynamic simulation problem with finite precision computing is studied via signal processing and model reduction integration. This chapter delivers two approaches to attack the simulation problem. The first approach transforms the simulation problem into a feedback control problem, yielding to three linear matrix inequalities (LMIs) along plus a coupling non-convex constraint. It becomes solvable via LMI toolbox, and guarantees a local optimum. The second approach focuses on finding an optimal simulation model for flexible structures via truncation of modes. Extensions to non-linear system simulations are conducted by integration with the q-Markov Covariance Equivalent Realization (QMC) method.

4.1 Problem Statement

In simulation problems, the physics of the system to simulate is normally given. Assume the physics is represented by the following state-space realization:

$$x_{k+1} = Ax_k + Bu_k, \tag{4.1a}$$

$$y_k = Cx_k + Du_k, \tag{4.1b}$$

where the input u_k considered a zero mean, unit variance white noise sequence. When implemented in the finite word-length environment, inputs will involve quantization errors, states and outputs will be twisted by round-off errors, which makes the output inaccurate. A mathematical formation of this effect is the following:

$$\check{x}_{k+1} = A(\check{x}_k + e_{x_k}) + B(u_k + e_{u_k}), \tag{4.2a}$$

$$\check{y}_k = C(\check{x}_k + e_{x_k}) + D(u_k + e_{u_k}) + e_{y_k}, \tag{4.2b}$$

where e_{u_k}, e_{x_k} and e_{y_k} are finite precision errors at inputs, states and outputs. We will quantitatively implement them in Section 4.2. Apparently, the physics output y_k and the simulation output $\check{y}_k$ are

different, and there is no guarantee on the closure between them. We are interested in finding a simulation model that satisfies a covariance constraint on the errors of their outputs.

Denote a linear model in the form of (4.3) that considers finite precision effects:

$$x_{s_{k+1}} = A_s(x_{s_k} + e_{x_k}) + B_s(u_k + e_{u_k}), \tag{4.3a}$$

$$y_{s_k} = C_s(x_{s_k} + e_{x_k}) + D_s(u_k + e_{u_k}) + e_{y_k}, \tag{4.3b}$$

The set of coefficients, $\{A_s, B_s, C_s, D_s\}$, are the model coefficients replacing the physics system $\{A, B, C, D\}$ during computational simulation, where $A \in \mathbb{R}^{n\times n}$, $A_s \in \mathbb{R}^{\gamma\times\gamma}$, n and γ are positive scalars that represent model sizes of the physics system (4.1) and the simulation system (4.3) respectively. Denote $\tilde{y}_k$ as the error between the output of the physical system (4.1) and that of the simulation system (4.3) where

$$\tilde{y}_k = y_k - y_{s_k}, \tag{4.4}$$

We seek to find the set of $\{A_s, B_s, C_s, D_s\}$ that satisfies an upper bound constraint (4.5) where Q is a positive definite diagonal weighting matrix, and α is a given positive scalar. We call α the error covariance scalar.

$$E\{\tilde{y}_k\tilde{y}_k^T\} \leq \alpha Q. \tag{4.5}$$

4.2 Round-off Noise Model and the Scaling Condition

4.2.1 Round-off Noise Model

The round-off error e_k can be modeled as a zero-mean uniform distribution if overflow is not triggered [60]. The quantification of e_k are given below.

1. Fixed-point arithmetic can be expressed as:

$$E\{e_k^2\}_{i,i} = \frac{1}{12}2^{-2\beta_i}, \tag{4.6}$$

where β_i is the word length of the fractional part.

2. Floating-point arithmetic can be modelled as:

$$E\{e_k^2\}_{i,i} = \frac{2}{3}2^{-2\beta_i}b^e, \tag{4.7}$$

where β_i is the word length of the fractional part of the significant, b is the base, and e is the exponent number. In our problem formulation, the round-off noise terms e_{x_k}, e_{u_k} and e_{y_k} are modelled as zero-mean uniform distributions with variance E_x, E_u and E_y as the following:

$$E(e_{x_k}) = 0, E(e_{x_k}e_{x_k}^T) = E_x, \tag{4.8a}$$

$$E(e_{u_k}) = 0, E(e_{u_k}e_{u_k}^T) = E_u, \tag{4.8b}$$

$$E(e_{y_k}) = 0, E(e_{y_k}e_{y_k}^T) = E_y, \tag{4.8c}$$

where E_x, E_u and E_y depends on the type of arithmetic and fractional bits.

4.2.2 Scaling Condition

The round-off error models (4.6) and (4.7) are build upon on the assumption of rare overflow. Additionally, it is possible that the realization of a model may blow up the state covariance and eventually cause overflow [61]. To prevent the overflow, we impose an additional $\mathcal{L}_2$-norm scaling constraint as the following:

$$X_{s_{i,i}} \leq s,\ i = 1, 2, \cdots, n, \tag{4.9}$$

where X_s is the state covariance matrix of (4.3), and s is a given positive scalar. Without loss of generality, let $s = 1$. The scaling condition may be relaxed as the following:

$$X_s \leq I. \tag{4.10}$$

4.3 Simulation Design by Output Feedback Control

4.3.1 The Converted Output Feedback Control Problem

The problem is approached as follows. Augment the two systems (4.1) and (4.3):

$$\tilde{x}_{k+1} = \tilde{A}\tilde{x}_k + \tilde{A}_e e_{x_k} + \tilde{B}u_k + \tilde{B}_e e_{u_k}, \tag{4.11a}$$

$$\tilde{y}_k = \tilde{C}\tilde{x}_k + \tilde{C}_e e_{x_k} + \tilde{D}u_k + \tilde{D}_e e_{u_k} - e_{y_k}. \tag{4.11b}$$

where

$$\tilde{x}_k = \begin{bmatrix} x_k \\ x_{s_k} \end{bmatrix}, \tilde{y}_k = y_k - y_{s_k}, \tag{4.11c}$$

$$\tilde{A} = \begin{bmatrix} A & 0 \\ 0 & A_s \end{bmatrix}, \tilde{A}_e = \begin{bmatrix} 0 \\ A_s \end{bmatrix}, \ \tilde{B} = \begin{bmatrix} B \\ B_s \end{bmatrix}, \tilde{B}_e = \begin{bmatrix} 0 \\ B_s \end{bmatrix}, \tag{4.11d}$$

$$\tilde{C} = \begin{bmatrix} C & -C_s \end{bmatrix}, \tilde{C}_e = -C_s, \tilde{D} = D - D_s, \tilde{D}_e = -D_s, \tag{4.11e}$$

The problem can be solved numerically by reconstructing into an output feedback control problem [33]. Define the following parameter:

$$\boldsymbol{K} = \begin{bmatrix} D_s & C_s \\ B_s & A_s \end{bmatrix}, \tag{4.12a}$$

Parameters of the augmented error system (4.11) may be formulated as the following form:

$$\begin{aligned} \tilde{A} &= \mathcal{A} + \mathcal{F}\boldsymbol{K}\mathcal{M}, \ \tilde{A}_e = \mathcal{F}\boldsymbol{K}\mathcal{J}, \\ \tilde{B} &= \mathcal{B} + \mathcal{F}\boldsymbol{K}\mathcal{E}, \quad \tilde{B}_e = \mathcal{F}\boldsymbol{K}\mathcal{E}, \\ \tilde{C} &= \mathcal{C} + \mathcal{H}\boldsymbol{K}\mathcal{M}, \ \tilde{C}_e = \mathcal{H}\boldsymbol{K}\mathcal{J}, \\ \tilde{D} &= \mathcal{D} + \mathcal{H}\boldsymbol{K}\mathcal{E}, \quad \tilde{D}_e = \mathcal{H}\boldsymbol{K}\mathcal{E}, \end{aligned} \tag{4.12b}$$

where

$$\mathcal{A} = \begin{bmatrix} A & 0 \\ 0 & 0 \end{bmatrix},\ \mathcal{B} = \begin{bmatrix} B \\ 0 \end{bmatrix},\ \mathcal{C} = \begin{bmatrix} C & 0 \end{bmatrix},\ \mathcal{D} = D,$$

$$\mathcal{F} = \begin{bmatrix} 0 & 0 \\ 0 & I \end{bmatrix},\ \mathcal{M} = \mathcal{F}^T,\ \mathcal{J} = \begin{bmatrix} 0 \\ I \end{bmatrix},\ \mathcal{H} = \begin{bmatrix} -I & 0 \end{bmatrix},\ \mathcal{E} = \begin{bmatrix} I \\ 0 \end{bmatrix}.$$

Here $\boldsymbol{K}$ is the only unknown variable among the relations above, which contains parameter information of the simulation system. The problem is transformed into an output feedback control problem where $\boldsymbol{K}$ represents the feedback controller gain.

Theorem 4.3.1. *Let a linear stable system (4.1), a positive definite diagonal matrix Q and a positive scalar α be given. Consider the error system assembly (4.11) with parametrizations (4.12b) where e_u, e_y, and e_x are uniformly distributed random variables with variances of E_u, E_y, and E_x respectively. The following two statements are equivalent*

1. *There exists a simulation model (4.3) of order γ satisfying the scaling condition (4.10). The error system (4.11) consisting of (4.1) and (4.3) is asymptotically stable, and its output covariance satisfies an upper-bound constraint (4.5).*

2. *There exist matrices $\tilde{X} > 0$, $\tilde{X} \in R^{(n+\gamma)\times(n+\gamma)}$, and $\boldsymbol{K} \in R^{(n+n_y)\times(n+n_u)}$ that satisfies the following inequalities*

$$I \geq \begin{bmatrix} 0 & I \end{bmatrix} \boldsymbol{K} \begin{bmatrix} U + E_u & 0 \\ 0 & I + E_x \end{bmatrix} \boldsymbol{K}^T \begin{bmatrix} 0 \\ I \end{bmatrix}, \tag{4.13a}$$

$$\tilde{X} \geq \tilde{A}\tilde{X}\tilde{A}^T + \tilde{A}_e E_x \tilde{A}_e^T + \tilde{B} U \tilde{B}^T + \tilde{B}_e E_u \tilde{B}_e^T, \tag{4.13b}$$

$$\alpha Q \geq \tilde{C}\tilde{X}\tilde{C}^T + \tilde{C}_e E_x \tilde{C}_e^T + \tilde{D} U \tilde{D}^T + \tilde{D}_e E_u \tilde{D}_e^T + E_y. \tag{4.13c}$$

Proof. A linear stable simulation system (4.3) satisfying an output covariance upper bound constraint αQ if the following conditions are satisfied.

1. The simulation system (4.3) is stable to satisfy the Lyapunov stability inequality

$$X_s \geq A_s(X_s + E_x)A_s^T + B_s(U + E_u)B_s^T, \tag{4.14}$$

Notice that the state covariance matrix X_s is constrained by a scaling condition, to prevent overflow, as indicated in Eqn. (4.10). Combining (4.10), (4.14) and (4.12a) formulates the first inequality (4.13a).

2. The integrated error system (4.11) is stable to satisfy its Lyapunov stability inequality, which is the second inequality (4.13b).

3. The error output covariance of (4.11), satisfies an upper bound constraint αQ. Notice that the error output covariance is formulated in (4.15a) and the upper bound constraint is formulated in (4.15b). Combining (4.15a) and (4.15b) formulates the third inequality (4.13c).

$$\tilde{Y} = \tilde{C}\tilde{X}\tilde{C}^T + \tilde{C}_e E_x \tilde{C}_e^T + \tilde{D}U\tilde{D}^T + \tilde{D}_e E_u \tilde{D}_e^T + E_y, \tag{4.15a}$$

$$\tilde{Y} \leq \alpha Q. \tag{4.15b}$$

□

To numerically evaluate the three inequalities (4.13a,4.13b,4.13c), we introduce Schur's complement as a useful linear algebra tool [55, 62, 63]. It is the following lemma that transforms the three inequalities (4.13a,4.13b,4.13c) into three linear matrix inequalities plus one non-convex constraint.

Lemma 4.3.2. *Let* $M = \begin{bmatrix} A & B \\ B^T & C \end{bmatrix}$ *be a symmetrix matrix. The following three statements are equivalent:*

$$(i). \quad M > 0, \tag{4.16}$$

$$(ii). \quad A > 0, C - B^T A^{-1} B > 0, \tag{4.17}$$

$$(iii). \quad C > 0, A - BC^{-1}B^T > 0. \tag{4.18}$$

Proof. Notice that

$$M = \begin{bmatrix} I & 0 \\ B^T A^{-1} & I \end{bmatrix} \begin{bmatrix} A & 0 \\ 0 & C - B^T A^{-1} B \end{bmatrix} \begin{bmatrix} I & A^{-1}B \\ 0 & I \end{bmatrix} = PDP^T, \tag{4.19}$$

where

$$P = \begin{bmatrix} I & 0 \\ B^T A^{-1} & I \end{bmatrix}, \tag{4.20}$$

$$D = \begin{bmatrix} A & 0 \\ 0 & C - B^T A^{-1} B \end{bmatrix}. \tag{4.21}$$

Observe that P is invertable where

$$P^{-1} = \begin{bmatrix} I & 0 \\ -B^T A^{-1} & I \end{bmatrix}. \tag{4.22}$$

Let v be any vector which $v \neq 0$. Then

$$v^T Dv = (v^T P^{-1}) M (P^{-T} v) = w^T M w > 0, \tag{4.23}$$

where

$$w = P^{-T} v. \tag{4.24}$$

One may observe that $M > 0$ guarantees $D > 0$, and vise versa. One may also observe that $D > 0$ guarantees $A > 0, C - B^T A^{-1} B > 0$, and vise versa. Thus, (4.16) and (4.17) are equivalent. Without loss of generality, (4.16), (4.17) and (4.18) are equivalent.

□

Theorem 4.3.3. *The following two statements are equivalent*

1. *There exist matrices* $\tilde{X} > 0$, $\tilde{X} \in R^{(n+\gamma)\times(n+\gamma)}$, *and* $\boldsymbol{K} \in R^{(n+n_y)\times(n+n_u)}$ *that satisfies the inequalities (4.13a-4.13c).*

2. *There exist matrices* $\tilde{X} > 0$, $\tilde{X} \in R^{(n+\gamma)\times(n+\gamma)}$, $Z > 0$, $Z \in R^{(n+\gamma)\times(n+\gamma)}$, *and* $\boldsymbol{K} \in R^{(n+n_y)\times(n+n_u)}$ *that satisfies the matrix inequalities (4.25a-4.25c) and the constraint (4.25d).*

$$\begin{bmatrix} I & \begin{bmatrix} 0 & I \end{bmatrix} \boldsymbol{K} \\ \boldsymbol{K}^T \begin{bmatrix} I \\ 0 \end{bmatrix} & \begin{bmatrix} (U + E_x)^{-1} & 0 \\ 0 & (I + E_x)^{-1} \end{bmatrix} \end{bmatrix} \geq 0, \tag{4.25a}$$

$$\begin{bmatrix} Z^{-1} & \tilde{A} & \tilde{A}_e & \tilde{B} & \tilde{B}_e \\ \tilde{A}^T & Z & 0 & 0 & 0 \\ \tilde{A}_e^T & 0 & E_x^{-1} & 0 & 0 \\ \tilde{B}^T & 0 & 0 & U^{-1} & 0 \\ \tilde{B}_e^T & 0 & 0 & 0 & E_u^{-1} \end{bmatrix} \geq 0, \tag{4.25b}$$

$$\begin{bmatrix} \alpha Q - E_y & \tilde{C} & \tilde{C}_e & \tilde{D} & \tilde{D}_e \\ \tilde{C}^T & Z & 0 & 0 & 0 \\ \tilde{C}_e^T & 0 & E_x^{-1} & 0 & 0 \\ \tilde{D}^T & 0 & 0 & U^{-1} & 0 \\ \tilde{D}_e^T & 0 & 0 & 0 & E_u^{-1} \end{bmatrix} \geq 0, \tag{4.25c}$$

$$\tilde{X} = Z^{-1}. \tag{4.25d}$$

Notice that (4.25a), (4.25b) and (4.25c) are already in linear matrix inequality forms while the inequality (4.25d) is non-convex. The problem can be numerically evaluated using LMI toolbox if we are able to convexify (4.25d).

4.3.2 Convexification

4.3.2.1 Potential Functional

The previous section shows that the dynamic simulation problem is reduced to three LMIs and one non-convex constraint. Similar non-convex constraints appear in structural linear control problems, and an algorithm to convexify using potential functional is given in [64]. A potential functional is defined as Definition 1.

Definition 1. *(Potential matrix functional) A first-order differentiable matrix functional $H(x,z)$ defined for all x and z in a convex set Φ is called a potential functional if*

1. $H(x,z) \geq 0$ *for all* $x, z \in \Phi$,
2. $G(x,x) = 0$ *for all* $x \in \Phi$,
3. $\nabla G(x,x) = 0$ *for all* $x \in \Phi$.

Next, we define a convexifying potential matrix functional for convexification of a non-convex matrix variable as Definition 2.

Definition 2. *(Convexifying potential matrix functional) A first-order differentiable matrix functional $H(x,z)$ is said to be a convexifying potential matrix functional if, given a first order differentiable nonconvex matrix functional $F(x)$ defined for all $x \in \Phi$, $F(x) + H(x,z)$ is a convex matrix functional for all $x, z \in \Phi$.*

We are interested in solving the following nonconvex optimization problem:

$$\min_{x \in \Omega}, \quad \Omega := \{x \in \Phi : F(x) \leq 0\}, \tag{4.26}$$

where $f(x)$ is a scalar and first order differentiable convex function bounded from below on the convex set Ω, and that $F(x)$ is a nonconvex matrix variable to be convexified. The corresponding algorithm to convexify $F(x)$ employing the convexifying potential matrix functional $G(x)$ is attached below.

Algorithms 4.3.1. *Let $\epsilon > 0$, $x_0 \in \Omega$ and a convexifying potential matrix functional $H(x, z)$ be given.*

1. *Solve the convex optimization problem*

$$x_{k+1} := \underset{x}{\operatorname{argmin}}\{f(x) : x \in \Phi_k\}, \tag{4.27a}$$

$$\Omega_k := \{x : F(x) + G(x, x_k) \leq 0\}, \tag{4.27b}$$

2. *If $\|x_{k+1} - x_k\| \geq \epsilon$, stop. Otherwise, set $k \leftarrow k + 1$ and go back to Step 1.*

This algorithm transforms the non-convex optimization problem (4.26) into iterations of a sequence of convex optimization problems, where $F(x)$ is non-convex but $F(x) + G(x)$ is convex. Since the potential functional is driven to 0 at each iteration, the algorithm yields a feasible solution to the original non-convex optimization problem. This algorithm converges to a local optimal solution.

Theorem 4.3.4. *Given a scalar and first order differentiable convex function $f(x)$ and a convexifying potential matrix functional $H(x, z)$ defined for all x, z in the convex set Φ, Algorithm 4.3.1 generates a sequence of feasible points that converges to a solution satisfying the necessary optimality conditions for problem (4.26).*

Proof. We start noticing that every point $x_{k+1} \in \Omega_k$ is also in Ω since from Definition 1, $F(x_{k+1} \leq F(x_{k+1} + G(x_{k+1}, x_k)) \leq 0$. Furthermore, assuming that $x_k \in \Omega$ we can write $F(x_k) + G(x_k, x_k) = F(x_k) \leq 0$ so that $x_k \in \Omega_k$. This proves that when $x_0 \in \Omega$, Algorithm 4.3.1 generates a sequence of feasible solutions. As $x_k \in \Omega_k$, we have immediately that $f(x_{k+1}) \leq f(x_k)$, which holds strictly until $x_{k+1} = x_k, f(x_{k+1} = f(x_k)$, which characterizes the stationary point. Assuming some mild constraint qualification on the definition of the set Ω and using the first order differentiability of the function $f(\cdot)$ and of the matrix function $F(\cdot)$ and $G(\cdot)$, the Kuhn-Tucker necessary optimality condition for problem (4.26) are given as the existence of some $\bar{U} \leq 0$ such that $F(x_{k+1}+G_{x_{k+1},x_k}) \leq$

0 and

$$\nabla f(x_{k+1}) + \langle \bar{U}, \nabla F(x_{k+1}) + \nabla G(x_{k+1}, x_k) \rangle = 0, \tag{4.28a}$$

$$\langle \bar{U}, F(x_{k+1}) + G(x_{k+1}, x_k) \rangle = 0. \tag{4.28b}$$

As a stationary point $x_{k+1} = x_k$, the above conditions coincide with the optimality conditions for the original nonconvex problem because $G(x_{k+1}, x_{k+1}) = 0$ and $\nabla G(x_{k+1}, x_{k+1}) = 0$.

Notice that at a stationary solution $x_{k+1} = x_k$ and the value of the convexifying potential functional $G(x_{k+1}, x_k)$ in (4.26) reduces to zero, guaranteeing the feasibility of the original problem. This completes the proof. □

4.3.2.2 Convexification of the Dynamic Simualtion Problem

Denote

$$F(K, Z) = -\begin{bmatrix} Z^{-1} & \tilde{A} & \tilde{A}_e & \tilde{B} & \tilde{B}_e \\ \tilde{A}^T & Z & 0 & 0 & 0 \\ \tilde{A}_e^T & 0 & E_x^{-1} & 0 & 0 \\ \tilde{B}^T & 0 & 0 & U & 0 \\ \tilde{B}_e^T & 0 & 0 & 0 & E_u^{-1} \end{bmatrix} \leq 0. \tag{4.29}$$

Let $H(Z, Z_0)$ be a convexifying potential function such that $F(K, Z) + H(Z, Z_0) \leq 0$. A choice of a convexifying potential function may be found as below where $lin(Z^{-1}, Z_0)$ represents the linearizzation of Z^{-1} about Z_0

$$\begin{aligned} H(Z, Z_0) &= Z^{-1} - lin(Z^{-1}, Z_0) \\ &\approx Z^{-1} - (2Z_0^{-1} - Z_0^{-1} Z Z_0^{-1}). \end{aligned} \tag{4.30}$$

Then, from equation (4.29) and equation (4.30) we have

$$F(K, Z) + H(Z, Z_0) =$$

$$-\begin{bmatrix} 2Z_0^{-1} - Z_0^{-1}ZZ_0^{-1} & \tilde{A} & \tilde{A}_e & \tilde{B} & \tilde{B}_e \\ \tilde{A}^T & Z & 0 & 0 & 0 \\ \tilde{A}_e^T & 0 & E_x^{-1} & 0 & 0 \\ \tilde{B}^T & 0 & 0 & U & 0 \\ \tilde{B}_e^T & 0 & 0 & 0 & E_u^{-1} \end{bmatrix} \leq 0. \tag{4.31}$$

One can select an initial Z_0 such that $F(K,Z) + H(Z,Z_0) < 0$ is satisfied. Then, one iterate the procedure below until a converged Z_k is found

$$Z_{k+1} = \underset{Z \epsilon \mho_k}{\operatorname{argmin}} \alpha, \tag{4.32}$$

where

$$\mho_k \stackrel{\Delta}{=} \{Z : F(K,Z) + H(Z,Z_0) \leq 0, (4.25a), (4.25c)\} \tag{4.33}$$

A general algorithm for finding the optimal simulation model at prespecified simulation model size γ and finite precision environment of word-length $beta$ is given below:

Algorithms 4.3.2. *Initialize with an initial Z_0 to make $F(K,Z) + H(Z,Z_0) \leq 0$, and a threshold ϵ.*

1. *Update*

$$Z_{k+1} = \underset{Z \epsilon \mho_k}{\operatorname{argmin}} \alpha,$$

$$\mho_k \stackrel{\Delta}{=} \{Z : F(K,Z) + H(Z,Z_0) \leq 0, (4.25a), (4.25c)\},$$

2. *If $||\alpha_k - \alpha_{k-1}|| \leq \epsilon$, declare convergence; otherwise, return to Step 1 and set $k \leftarrow k+1$.*

4.3.3 Nonlinear Dynamic System Simulation

In reality, a well-linearized dynamics of the system to simulate may not be available. We may only have access to the non-linear dynamics of the system to simulate. Let us consider a general system as the following:

$$\dot{x}(t) = f(x(t), u(t)) \tag{4.34a}$$

$$y(t) = g(x(t), u(t)), \tag{4.34b}$$

We want to find the most optimal simulation system that matches the outputs of (4.34). The theorem 4.3.1 developed in section 4.2 is only applicable to linear systems. An extension to dynamic system simulations of non-linear systems is necessary.

In Chapter 3 section 3.3 we introduced the generalized QMC theory for system identification applications, and we showed its advantages in system identification in section 3.4. We introduce this method again for the purpose of linearization for the non-linear system (4.34).

We first discretize the system (4.34) using the zero-order-hold (ZOH) method. A conceptual drawing of disretization using the ZOH method is shown in Figure 4.1. Hold the input $u(t)$ at discrete control u_k at sampling period Δt

$$u(t) = u_k, \quad k\Delta t \le t < (k+1)\Delta t. \tag{4.35a}$$

Denote y_k as the discretized states and outputs of the system (4.34) with sampling period Δt

$$x_k = x(k\Delta t), \tag{4.35b}$$

$$y_k = y(k\Delta t). \tag{4.35c}$$

Next, define Markov parameters(H_i) and Covariance parameters (R_i) of system (4.34) as the

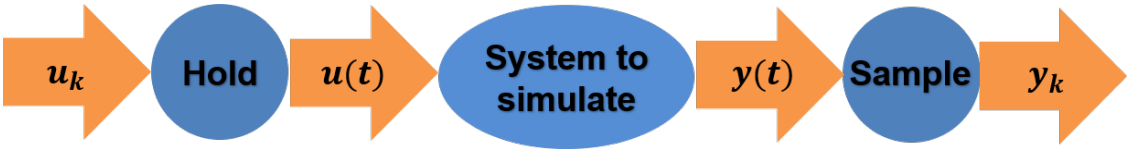

Figure 4.1: A discretization framework using the zero-order hold (ZOH) method.

cross-correlations and auto-correlations as follows:

$$H_i = E(y_{k+i}^T u_k), \tag{4.36a}$$

$$R_i = E(y_{k+i}^T y_k). \tag{4.36b}$$

Using Algorithm 3.4.1, we find a linear approximation system (4.37) that matches $\{H_i, R_i | i = 0, 1, \ldots, q-1\}$:

$$\hat{x}_{k+1} = \hat{A}\hat{x}_k + \hat{B}u_k, \tag{4.37a}$$

$$\hat{y}_k = \hat{C}\hat{x}_k + \hat{D}u_k, \tag{4.37b}$$

One may proceed with the simulation problem of non-linear systems using Algorithm 4.3.2 by replacing the non-linear dynamics (4.1) with this approximation system.

4.3.4 An Illustrative Example

In this section we introduce an example to demonstrate our method. We find the most optimal simulation model with implementation of finite word-length effects.

Assume a linear model given as the format (4.1), where

$$A = \begin{bmatrix} 0.0673 & 0.0589 & 0.0641 & 0.0410 & 0.0237 & 0.0100 \\ -0.6875 & -0.3817 & -0.2456 & -0.0216 & 0.0210 & 0.0162 \\ -0.2787 & -0.3539 & -0.5766 & -0.7079 & -0.3442 & -0.1328 \\ 1.1390 & 0.7089 & 0.6199 & 0.3092 & -0.3626 & -0.1470 \\ 0.6304 & 0.4828 & 0.6183 & 0.8003 & 0.8921 & -0.0445 \\ 0.0954 & 0.0820 & 0.1271 & 0.2288 & 0.4884 & 0.9952 \end{bmatrix}, \quad B = \begin{bmatrix} -0.0859 \\ -0.1393 \\ 1.1390 \\ 1.2608 \\ 0.3817 \\ 0.0416 \end{bmatrix},$$

$$C = \begin{bmatrix} 0.5000 & 0.2799 & 0.1749 & 0.1175 & 0.0904 & 0.0700 \end{bmatrix}, \qquad D = 0. \tag{4.38}$$

Denote β_u, β_y and β_x as fractional bits of float-pointing arithmeticat inputs, outputs and states respectively. Let $\beta_u = \beta_y = \beta_x = \beta$ where $\beta = 0, \cdots, 6$, and $Q = I$.

4.3.4.1 dynamic simulation Results

Let $\beta = 4$. Construct the error system (4.11) and find simulation models in form of (4.3) using algorithm (1) for simulation model size $\gamma = 1, 2, \ldots, 6$. The optimized α for each case are presented in the Table 4.1. This result has also been plotted in Figure 4.2 for the case of Fractional bit $\beta = 4$. The optimal simulation model size occurs at $\gamma = 3$. This tells us that a simulation model of size 3 gives the best simulation performance in a finite precision environment of float-pointing arithmetic of fractional bits $\beta = 4$. Such a $3rd$ order model is given below:

$$A_s = \begin{bmatrix} 0.5258 & 0.5230 & 0.1437 \\ -0.4918 & -0.2707 & -0.1882 \\ 0.4406 & -0.4955 & 0.4523 \end{bmatrix}, \qquad B_s = \begin{bmatrix} 0.5647 \\ 0.7589 \\ 0.2452 \end{bmatrix},$$

$$C_s = \begin{bmatrix} 0.1924 & 0.1924 & 0.1924 \end{bmatrix}, \qquad D_s = 0. \tag{4.39}$$

Table 4.2 shows the eigenvalues of the simulation system of size 6. This simulation is not the optimal, its error covariance scalar is $3.3117e^{-3}$ as shown in Table 4.1. However, one may notice that the $4th$, $5th$ and $5th$ eigenvalues are nearly negligible. This essentially indicates that only 3 eigenvalues are required for this simulation case, and a model size of 3 will give satisfying

Table 4.1: Error covariance scalar α for simulation model at different sizes $\gamma = 1, \ldots, 6$ in float-pointing arithmetic with fractional bit $\beta = 4$.

γ	α
1	0.0164
2	$3.8239e^{-3}$
3	$3.2877e^{-3}$
4	$3.2906e^{-3}$
5	$3.2916e^{-3}$
6	$3.3117e^{-3}$

simulation performance. This converges with our result in Table 4.1.

Table 4.2: Eigenvalues of the simulation system for $\beta = 4, \gamma = 6$.

Index	Eigenvalues
1	0.6252
2	$0.0378 + 0.1357i$
3	$0.0378 - 0.1357i$
4	0.0007
5	0.0000015
6	−0.0001

Figure 4.2 shows how different fractional bits affect the optimal simulation model size. It shows that for a float-pointing arithmetic fractional bit $\beta = 0$, and optimal simulation model size is $\gamma = 2$. The optimal size increases to $\gamma = 3$ for $\beta = 2$ and $\beta = 4$, and increases to $\gamma = 4$ for $\beta = 6$. It is expected that if we increase the fractional bits $beta$, the optimal simulation model size will keep increasing till the full model size of the physics, which is $\gamma = 6$ in this specific case.

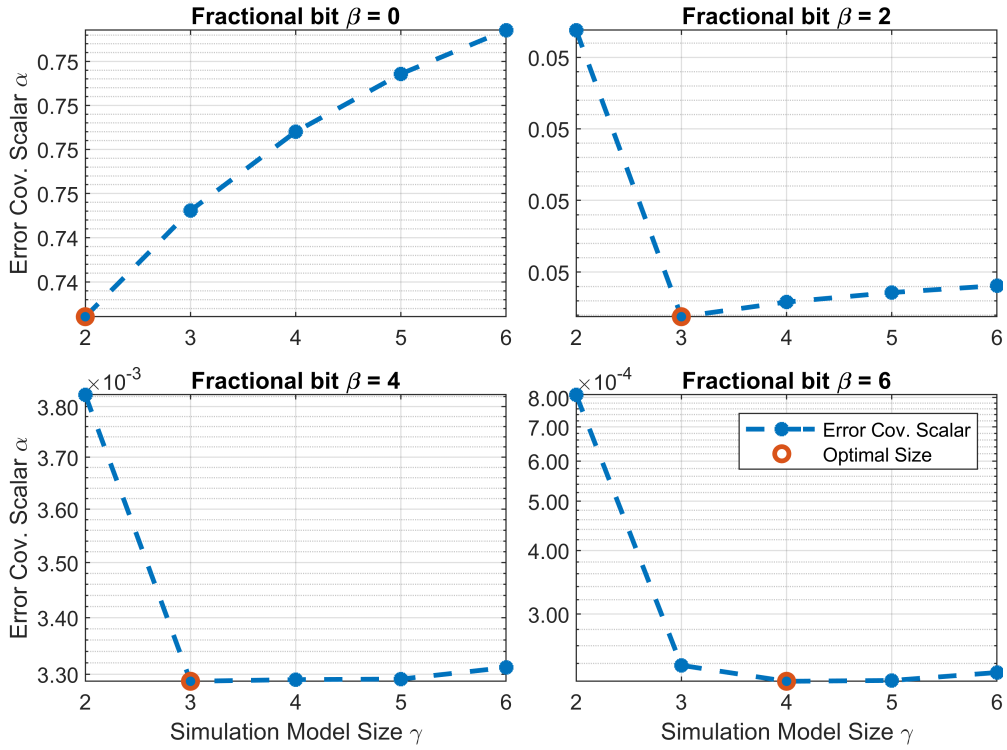

Figure 4.2: Error covariance scalar α for simulation models at different sizes $\gamma = 1, \ldots, 6$ in float-pointing arithmetic with fractional bit $\beta = 0, 2, 4, 6$.

4.3.4.2 Error Covariance of the Physics System

We are also interested in studying what is the error covariance scalar if we put the physics system directly into the finite precision environment. Consider the physics system (4.1) and its implementation with finite precision errors (4.2). Combine them together to get the following assembly plant:

$$\tilde{x}_{k+1} = \tilde{A}\tilde{x}_k + \tilde{A}_e e_{x_k} + \tilde{B}u_k + \tilde{B}_e e_{u_k} \tag{4.40a}$$

$$\tilde{y}_k = \tilde{C}\tilde{x}_k + \tilde{C}_e e_{x_k} + \tilde{D}_e e_{u_k} - e_{y_k} \tag{4.40b}$$

where

$$\tilde{x}_k = \begin{bmatrix} x_k \\ \check{x}_k \end{bmatrix}, \tilde{A} = \begin{bmatrix} A & 0 \\ 0 & A \end{bmatrix}, \tilde{A}_e = \begin{bmatrix} 0 \\ A \end{bmatrix}, \tilde{B} = \begin{bmatrix} B \\ B \end{bmatrix}, \tilde{B}_e = \begin{bmatrix} 0 \\ B \end{bmatrix}, \tag{4.40c}$$

$$\tilde{y}_k = y_k - \check{y}_k, \tilde{C} = \begin{bmatrix} C & -C \end{bmatrix}, \tilde{C}_e = -C, \tilde{D}_e = -D. \tag{4.40d}$$

The error covariance for performing computational simulation over the physics system in a finite precision environment is given below:

$$\tilde{Y} = \tilde{C}\tilde{X}\tilde{C}^T + \tilde{C}_e E_x \tilde{C}_e^T + \tilde{D}_e E_u \tilde{D}_e^T + E_y, \tag{4.41}$$

where $\tilde{X}$ is the solution to the equation below:

$$\tilde{X} = \tilde{A}\tilde{X}\tilde{A}^T + \tilde{A}_e E_x \tilde{A}_e^T + \tilde{B}U\tilde{B}^T + \tilde{B}_e E_u \tilde{B}_e^T. \tag{4.42}$$

Let $\check{\alpha}$ be the smallest scalar that satisfies $\check{\alpha}Q \geq \tilde{Y}$. $\check{\alpha}$ is the performance scalar of computational simulation for the physics system in a finite precision environment.

Let $\beta = 0, \ldots, 6$, construct the error system (4.2) and compute their corresponding error covariance scalar $\check{\alpha}$. We compare these results with the optimal error covariance scalar α from simulation systems in section 4.3.4.1. The result is attached in table 4.3. It clearly shows that in any of the finite precision $\beta = 0, \ldots, 6$, the error covariance scalar of the simulation model α, is superior to that of the physics model. This result shows that implementing a physics model directly into the computational simulation may lead to a very poor simulation performance.

Table 4.3: Comparison of error covariance scalars for physics system $\breve{\alpha}$ and optimal simulation system α in finite precision environment of float-pointing arithmetic, fractional bits $\beta = 0, \cdots, 6$.

β	$\breve{\alpha}$	α
0	1.0077	0.7414
1	0.2519	0.1999
2	0.0630	0.0517
3	0.0157	0.0131
4	0.0039	0.0033
5	$9.8413E^{-4}$	$8.5841E^{-4}$
6	$2.4603E^{-4}$	$2.2128E^{-4}$

4.4 Simulation Design by Truncation of Modes

In section 4.3 we attacked the system simulation problem with finite precision effects using a feedback control technique. The problem is transformed into three linear matrix inequalities (LMIs) and one nonconvex constraint. After convexification, we can numerically evaluate the problem using LMI toolbox. However, this approach only guarantees local optimum, where the final solution depends on the choice of initial guess. Yet, a general criterion on how to make a good initial guess is not available. In this section, we confine the system of interest to flexible structures and attack this problem using a different approach.

4.4.1 Problem Statement

Assume the system to simulate is a flexible structure, where (4.43) denotes as its dynamics.

$$\dot{x} = f(x, u), \tag{4.43a}$$

$$y = g(x, u). \tag{4.43b}$$

Let (4.44) be the state-space realization in its modal coordinate, where l is the number of modes included.

$$\dot{x}_l = A_l x_l + B_l u, \tag{4.44a}$$

$$y_l = C_l x_l + D_l u. \tag{4.44b}$$

With the existence of finite precision effects, (4.44) becomes the following when implemented in computation simulations

$$\breve{\dot{x}}_l = A_l(\breve{x} + e_x) + B_l(u + e_u), \tag{4.45a}$$

$$\breve{y}_l = C_l(\breve{x} + e_x) + D_l(u + e_u) + e_y. \tag{4.45b}$$

Denote $\tilde{y} = y - \breve{y}_l$ to be the error between outputs of the system to simulate and the reduced-modes system with finite precision effects. We are interested in finding the smallest mode number l

that satisfies an output covariance upper-bound constraint (4.46) where α is a pre-specified positive scalar, and Q is a given weighting matrix.

$$E(\tilde{y}\tilde{y}^T) \leq \alpha Q \tag{4.46}$$

4.4.2 Problem Formulation

Let's start this problem by first discretizing and linearizing the flexible structure system (4.44). This is similar to the section (4.3.3) where non-linear dynamics are identified to linear state-space realizations using q-Markov Covariance Equivalent (QMC) method. Denote the system (4.47) as the linearized physics we would like to match

$$\hat{x}_{k+1} = \hat{A}\hat{x}_k + \hat{B}u_k, \tag{4.47a}$$

$$\hat{y}_k = \hat{C}\hat{x}_k + \hat{D}u_k, \tag{4.47b}$$

where Δt represents the discretization sampling time, u_k and y_k are the discretized input and output

$$u(t) = u_k, \quad k\Delta t \leq t < (k+1)\Delta t, \tag{4.47c}$$

$$y_k = y(k\Delta t). \tag{4.47d}$$

Similarly, denote the system (4.48) as the discretized reduced-modes system of modes number l

$$x_{l_{k+1}} = \check{A}_l x_{l_k} + \check{B}_l u_k, \tag{4.48a}$$

$$y_{l_k} = \check{C}_l x_{l_k} + +\check{D}_l u_k, \tag{4.48b}$$

where u_k, x_{l_k} and y_{l_k} are the discretized input, state and output

$$u(t) = u_k, \quad k\Delta t \leq t < (k+1)\Delta t, \tag{4.48c}$$

$$x_{l_k} = x_l(k\Delta t), \tag{4.48d}$$

$$y_{l_k} = y_l(k\Delta t). \tag{4.48e}$$

Implement (4.48) in finite precision environment to get system (4.49)

$$\breve{x}_{l_{k+1}} = \breve{A}_l(\breve{x}_{l_k} + e_{x_k}) + \breve{B}_l(u_k + e_{u_k}), \tag{4.49a}$$

$$\breve{y}_{l_k} = \breve{C}_l(\breve{x}_{l_k} + e_{x_k}) + \breve{D}_l(u_k + e_{u_k}) + e_{y_k}, \tag{4.49b}$$

where $e_{x_k}, e_{y_k}, e_{u_k}$ are modelled as random variables satisfying a uniform distribution with variance E_x, E_y, E_u respectively as depicted in section (4.2)

$$E(e_{x_k}) = 0, E(e_{x_k}e_{x_k}^T) = E_x, \tag{4.49c}$$

$$E(e_{u_k}) = 0, E(e_{u_k}e_{u_k}^T) = E_u, \tag{4.49d}$$

$$E(e_{y_k}) = 0, E(e_{y_k}e_{y_k}^T) = E_y, \tag{4.49e}$$

Augment systems (4.47) and (4.49) to get the following error system

$$\tilde{x}_{l_{k+1}} = \tilde{A}_l\tilde{x}_{l_k} + \tilde{A}_{l_e}e_{x_k} + \tilde{B}_l u_k + \tilde{B}_{l_e}e_{u_k}, \tag{4.50a}$$

$$\tilde{y}_{l_k} = \tilde{C}_l\tilde{x}_{l_k} + \tilde{C}_{l_e}e_{x_k} + \tilde{D}_l u_k + \tilde{D}_{l_e}e_{u_k} - e_{y_k}, \tag{4.50b}$$

where

$$\tilde{x}_{l_k} = \begin{bmatrix} \hat{x}_k \\ \breve{x}_{l_k} \end{bmatrix}, \tilde{y}_{l_k} = \hat{y}_k - \breve{y}_{l_k}, \tag{4.50c}$$

$$\tilde{A}_l = \begin{bmatrix} \hat{A} & 0 \\ 0 & A_l \end{bmatrix}, \tilde{A}_{l_e} = \begin{bmatrix} 0 \\ A_l \end{bmatrix}, \ \tilde{B}_l = \begin{bmatrix} \hat{B} \\ \breve{B}_l \end{bmatrix}, \tilde{B}_{l_e} = \begin{bmatrix} 0 \\ \breve{B}_l \end{bmatrix}, \tag{4.50d}$$

$$\tilde{C}_l = \begin{bmatrix} \hat{C} & -\breve{C}_l \end{bmatrix}, \tilde{C}_{l_e} = -\breve{C}_l, \tilde{D}_l = \hat{D} - \breve{D}_l, \tilde{D}_{l_e} = -\breve{D}_l, \tag{4.50e}$$

Notice that for a specific modes number l, its corresponding modal coordinate realization

$\{A_l, B_l, C_l, D_l\}$ is known. Thus he augmented plant (4.50) is also known for a pre-specified l. The error covariance $\tilde{Y}_l$ of (4.50) is computable once l is specified as follows:

$$\tilde{Y}_l = \tilde{C}_l \tilde{X}_l \tilde{C}_l^T + \tilde{C}_{l_e} E_x \tilde{C}_{l_e}^T + \tilde{D}_l U \tilde{D}_l^T + \tilde{D}_{l_e} E_u \tilde{D}_{l_e}^T + E_y, \tag{4.51a}$$

$$\tilde{X}_l = \tilde{A}_l \tilde{X}_l \tilde{A}_l^T + \tilde{A}_{l_e} E_x \tilde{A}_{l_e}^T + \tilde{B}_l U \tilde{B}_l^T + \tilde{B}_{l_e} E_u \tilde{B}_{l_e}^T. \tag{4.51b}$$

Algorithms 4.4.1. *Let a positive weighting matrix Q be given. Find the linear approximation system of (4.43) using QMC method. Initialize with $k = 1$.*

1. *Find the modal coordinate system with modes number $l = k$ and discretize to get (4.45).*
2. *Construct the error plant (4.50), and compute the error covariance scalar α_k which satisfies $E(\tilde{y}_l \tilde{y}_l^T) < \alpha_k Q$.*
3. *If $\alpha_k - \alpha_{k-1} > 0$, stop; otherwise set $k \leftarrow k + 1$ and return to step 1.*

4.4.3 A Flexible Structure Example

Section 3.5.1 describes a formulation of an cantilever beam with different mode shapes. In this specific example, we select the cantilever beam with following material properties: $EI = 1, \rho = 1, L = 1$, and an damping coefficient $c = 0.1$. We consider the true physics has 1 deflection output at $r_1 = 0.8L$, 1 force input at $r_2 = L$, and 16 mode shapes. Frequencies of all mode shapes are listed in Table 4.4, and frequencies responses are plotted in Figure 4.3. High-frequency modes are essentially difficult to excite, and their magnitudes become insignificant compared to low-frequency modes. The corresponding state-space realization is the following:

$$\dot{x}_l = A_l x_l + B_l u, \tag{4.52a}$$

$$y_l = C_l x_l + D_l u. \tag{4.52b}$$

where

$$A_l = diag\left(\begin{bmatrix} 0 & 1 \\ -\omega_1^2 & -2c\omega_1 \end{bmatrix}, \cdots, \begin{bmatrix} 0 & 1 \\ -\omega_l^2 & -2c\omega_l \end{bmatrix}\right), \tag{4.52c}$$

$$B_l = \begin{bmatrix} 0 & \Phi_1(r_1)^T & \cdots & 0 & \Phi_N(r_1)^T \end{bmatrix}^T, \tag{4.52d}$$

$$C_l = \begin{bmatrix} \Phi_1(r_1) & 0 & \cdots & \Phi_N(r_1) & 0 \end{bmatrix}, \tag{4.52e}$$

$$D_l = 0, \tag{4.52f}$$

where $\Phi_i(r_i)$ represents the mode shape function (4.52g), the constant $\mathcal{C}$ is determined by the initial condition at $t = 0$, and β_i are solutions to make the following condition satisfied

$$\Phi_i(r) = \mathcal{C}[cosh(\beta_i r) - cos(\beta_i r) - k_i\{sinh(\beta_i r) - sin(\beta_i r)\}], \tag{4.52g}$$

$$k_i = \frac{cosh(\beta_i L) + cos(\beta_i L)}{sinh(\beta_i L) + sin(\beta_i L)}, \tag{4.52h}$$

$$cos(\beta_i L)cosh(\beta_i L) = -1. \tag{4.52i}$$

We consider the fixed-pointing arithmetic, fractional bits $\beta = [0, 1, 2, 4, 8, 16, 32, 64]$, as the finite precision environment. We calculated the error covariance scalar α with reduced-mode systems considering mode numbers $l = 1, \cdots, 16$. Figure 4.4a displays the results for $\beta = [0, 1, 2, 4]$ and Figure 4.4b displays the results for $\beta = [8, 16, 32, 64]$. The result shows that the optimal number of modes to include in the simulation model is 1 for $\beta = [0, 1, 2, 4, 8]$, 7 for $\beta = 16$, 12 for $\beta = 32$, and 16 for $\beta = 64$. This result demonstrates that reduced-mode models may have better simulation performances than the full-size model with the existence of finite precision effects.

Table 4.4: Mode shape frequencies for the cantilever beam.

Mode Index i	Mode Frequency $\omega_i(rad/s)$
1	3.5160
2	22.0345
3	61.6972
4	120.9019
5	199.8595
6	298.5555
7	416.9908
8	555.1652
9	713.0790
10	890.7318
11	1088.1237
12	1305.2555
13	1542.1258
14	1798.7353
15	2075.0840
16	2371.1728

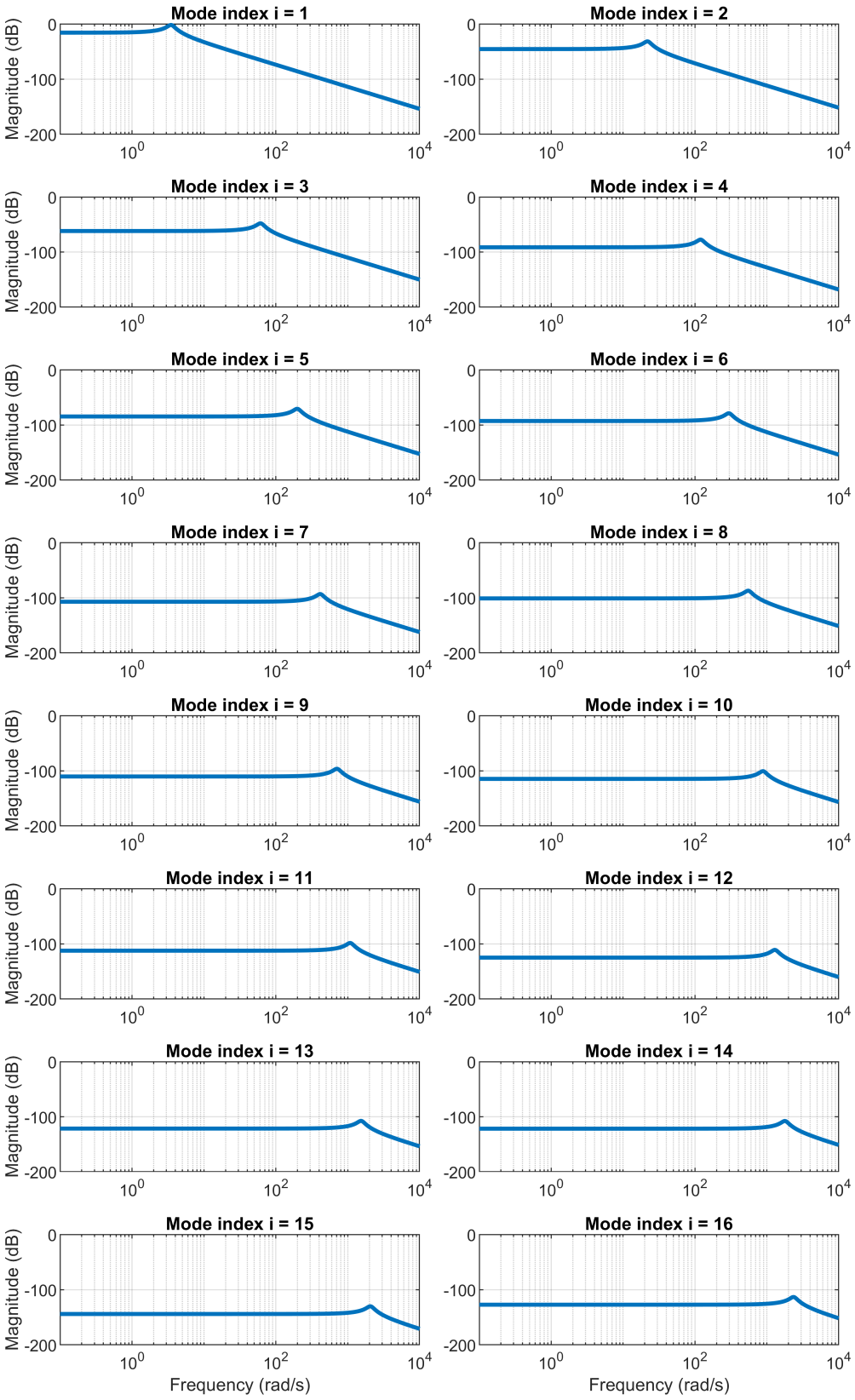

Figure 4.3: Frequency responses for the 16 modes.

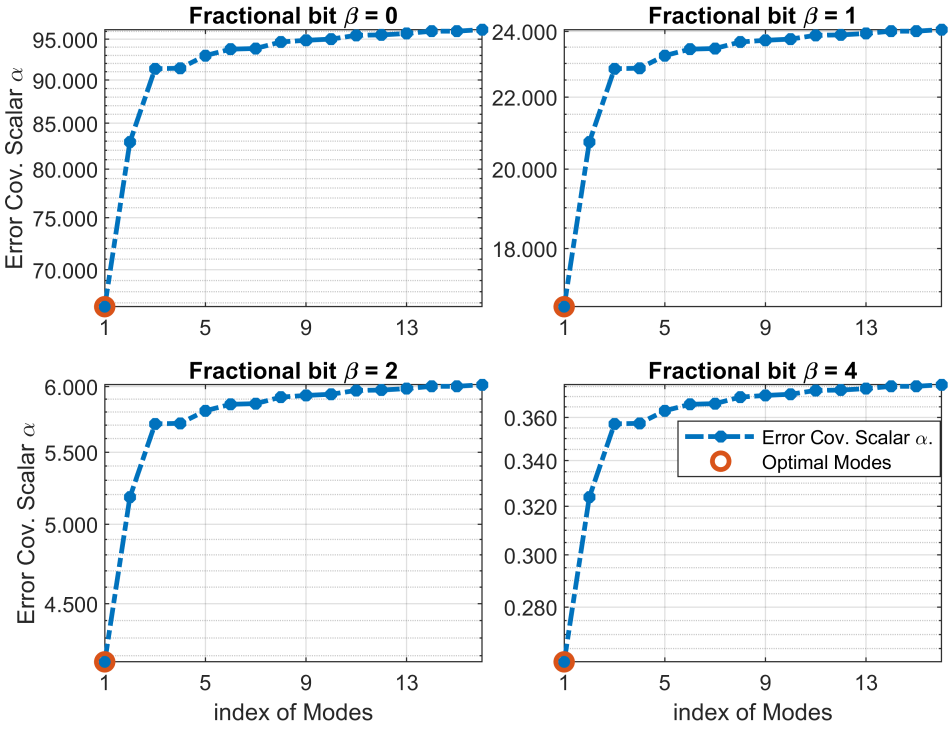

(a) Error covariance scalar plots for fixed-point arithmetic, fractional bits $\beta = 0, 1, 2, 4$.

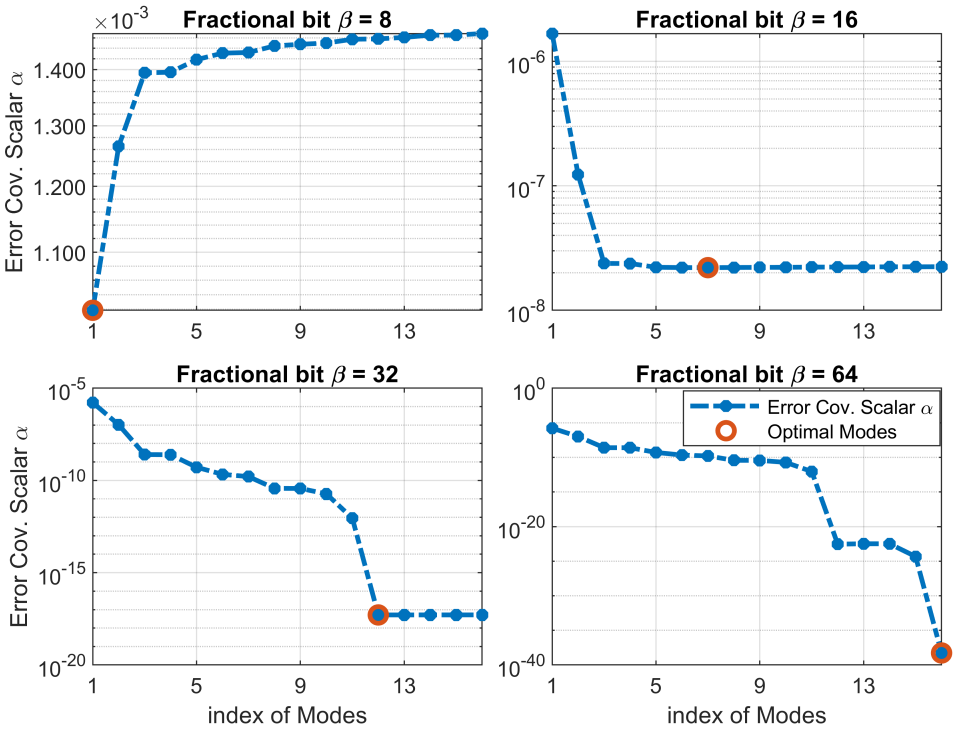

(b) Error covariance scalar plots for fixed-point arithmetic, fractional bits $\beta = 8, 16, 32, 64$.

Figure 4.4: Error covariance scalars for fixed-point arithmetic with different fractional bits.

4.5 Conclusion

This chapter develops a general approach for computational simulations of dynamic systems that considers finite precision. First, the problem is mathematically formulated, where the simulation performance is defined as the error covariance of an assembled system integrating the physics system and the simulation system. The purpose is to minimize the norm of the error covariance through the integration of signal processing and model reduction. The problem yields to a set of linear matrix inequalities (LMIs) plus a coupling non-convex constraint. A convexification algorithm has been applied to guarantee local optimum so that the problem is solvable through the LMI toolbox. A methodology that extends the approach to computational simulation applications of nonlinear systems is provided. An illustrative example has been conducted at the end. Its result demonstrates that one should reduce the simulation model to the optimal size in order to get the most optimal simulation performance.

5. MARKOV DATA-BASED REFERENCE TRACKING CONTROL AND ITS APPLICATION TO A TENSEGRITY AIRFOIL

This chapter presents a data-based control design for reference tracking applications, which requires only the first $N + 1$ Markov parameters of a system. This design finds the optimal control sequence, which minimizes a quadratic cost function consisting of tracking error and input increments over a finite interval $[0, N]$. This design is employed on a tensegrity morphing airfoil whose topology has been described in detail in this chapter. A NACA 2412 airfoil with specified morphing targets is chosen to verify the developed design. The principle developed in this paper is also applicable to other structural control problems.

5.1 Problem Formulation

Assume the system to control may be represented by the following state-space realization:

$$x_{k+1} = Ax_k + Bu_k + B_w w_k, \tag{5.1a}$$

$$y_k = Cx_k + Du_k + v_k, \tag{5.1b}$$

where A, B, C and D are state-space coefficient matrices, u_k is the control input, w_k is the system disturbance and v_k is the sensor noise. Consider a trajectory reference signal r_k, which we would like the output signal y_k to track. Denote the following two terms:

$$e_k = r_k - y_k, \tag{5.2a}$$

$$\Delta u_k = u_k - u_{k-1}, \tag{5.2b}$$

where e_k is the tracking error between the reference signal y_k, and Δu_k is the input increment between two concussive inputs.

Notice that system (5.1) may be written as the following [65]:

$$\breve{x}_{k+1} = \breve{A}\breve{x}_k + \breve{B}\Delta u_k + \breve{B}w_k, \tag{5.3a}$$

$$y_k = \breve{C}\breve{x}_k + \breve{D}\Delta u_k + v_k, \tag{5.3b}$$

where

$$\breve{A} = \begin{bmatrix} A & B \\ 0 & I \end{bmatrix}, \breve{B} = \begin{bmatrix} B \\ I \end{bmatrix}, \breve{B}_w = \begin{bmatrix} B_w \\ 0 \end{bmatrix}, \tag{5.4}$$

$$\breve{C} = \begin{bmatrix} C & D \end{bmatrix}, \breve{D} = D, \breve{x}_k = \begin{bmatrix} x_k \\ u_{k-1} \end{bmatrix}. \tag{5.5}$$

We are interested in finding an optimal control sequence u_k over a finite horizon $[0, N]$ that minimizes a quadratic weighted cost function (5.6) using Markov parameters of (5.1) only, where J is a function consisting of tracking errors and input increments, and S, Q, R, T are related weight matrices.

$$J = \frac{1}{2} e_N^T S e_N + \frac{1}{2} \sum_{k=0}^{N-1} (e_k^T Q e_k + \Delta u_k^T R \Delta u_k) + \frac{1}{2} \Delta u_N^T T \Delta u_N^T. \tag{5.6}$$

5.2 Model-based Control Law

The cost function (5.6) can be analytically evaluated by taking the partial derivative $\nabla J = 0$. The solution of input increment sequence is given by the theorem below [65].

Theorem 5.2.1. *Suppose a linear system (5.1) is given, and weight matrices S, Q, R, T are known. Suppose a reference signal r_k is specified. A control sequence that minimize the cost function (5.6) is the following:*

$$u_k = \sum_{i=0}^{k} \Delta u_i, \qquad k \in [0, N], \tag{5.7a}$$

where

$$\begin{bmatrix} \Delta u_0 \\ \Delta u_1 \\ \vdots \\ \Delta u_N \end{bmatrix} = \mathbf{K}\left(\begin{bmatrix} r_0 \\ r_1 \\ \vdots \\ r_N \end{bmatrix} - \begin{bmatrix} \breve{C} \\ \breve{C}\breve{A} \\ \vdots \\ \breve{C}\breve{A}^N \end{bmatrix} \breve{x}_0\right), \tag{5.7b}$$

$$\mathbf{K} = (\breve{\mathbf{H}}^T \breve{\mathbf{Q}} \breve{\mathbf{H}} + \breve{\mathbf{R}})^{-1} (\breve{\mathbf{Q}} \breve{\mathbf{H}})^T, \tag{5.7c}$$

$$\breve{\mathbf{H}} = \begin{bmatrix} \breve{D} & 0 & \cdots & \cdots & 0 \\ \breve{C}\breve{B} & \breve{D} & \ddots & \ddots & \vdots \\ \breve{C}\breve{A}\breve{B} & \breve{C}\breve{B} & \ddots & \ddots & \vdots \\ \vdots & \vdots & \ddots & \ddots & \vdots \\ \breve{C}\breve{A}^{N-1}\breve{B} & \breve{C}\breve{A}^{N-2}\breve{B} & \cdots & \breve{C}\breve{B} & \breve{D} \end{bmatrix}, \tag{5.7d}$$

$$\breve{\mathbf{Q}} = \begin{bmatrix} Q & \cdots & \cdots & 0 \\ \vdots & \ddots & \ddots & \vdots \\ \vdots & \ddots & Q & \vdots \\ 0 & \cdots & \cdots & S \end{bmatrix}, \tag{5.7e}$$

$$\breve{\mathbf{R}} = \begin{bmatrix} R & \cdots & \cdots & 0 \\ \vdots & \ddots & \ddots & \vdots \\ \vdots & \ddots & R & \vdots \\ 0 & \cdots & \cdots & T \end{bmatrix}. \tag{5.7f}$$

Proof. The cost function (5.6) may be rewritten as the following:

$$\begin{aligned} J = {} & \frac{1}{2}\vec{\mathbf{r}}^T \breve{\mathbf{Q}} \vec{\mathbf{r}} - \vec{\mathbf{r}}^T \breve{\mathbf{Q}} \breve{\mathbf{C}} \vec{\mathbf{x}} - \vec{\mathbf{r}}^T \breve{\mathbf{Q}} \breve{\mathbf{D}} \Delta\vec{\mathbf{u}} + \frac{1}{2}\vec{\mathbf{x}}_k^T \breve{\mathbf{C}}^T \breve{\mathbf{Q}} \breve{\mathbf{C}} \vec{\mathbf{x}} \\ & + \vec{\mathbf{x}}_k^T \breve{\mathbf{C}}^T \breve{\mathbf{Q}} \breve{\mathbf{D}} \Delta\vec{\mathbf{u}} + \frac{1}{2}\Delta\vec{\mathbf{u}}^T \breve{\mathbf{D}}^T \breve{\mathbf{Q}} \breve{\mathbf{D}} \Delta\vec{\mathbf{u}} + \frac{1}{2}\Delta\vec{\mathbf{u}}^T \breve{\mathbf{R}} \Delta\vec{\mathbf{u}}, \end{aligned} \tag{5.8a}$$

where

$$\vec{\mathbf{x}} = \begin{bmatrix} \breve{x}_0 \\ \breve{x}_1 \\ \vdots \\ \breve{x}_N \end{bmatrix}, \vec{\mathbf{r}} = \begin{bmatrix} \breve{r}_0 \\ \breve{r}_1 \\ \vdots \\ \breve{r}_N \end{bmatrix}, \Delta\vec{\mathbf{u}} = \begin{bmatrix} \Delta u_0 \\ \Delta u_1 \\ \vdots \\ \Delta u_N \end{bmatrix}, \tag{5.8b}$$

$$\breve{\mathbf{C}} = \begin{bmatrix} \breve{C} & \cdots & \cdots & 0 \\ \vdots & \ddots & \ddots & \vdots \\ \vdots & \ddots & \breve{C} & \vdots \\ 0 & \cdots & \cdots & \breve{C} \end{bmatrix}, \breve{\mathbf{D}} = \begin{bmatrix} \breve{D} & \cdots & \cdots & 0 \\ \vdots & \ddots & \ddots & \vdots \\ \vdots & \ddots & \breve{D} & \vdots \\ 0 & \cdots & \cdots & \breve{D} \end{bmatrix}. \tag{5.8c}$$

Notice the following:

$$\vec{\mathbf{x}} = \mathbf{A_1} x_0 + \mathbf{A_2}\Delta\vec{\mathbf{u}}, \tag{5.9a}$$

where

$$\mathbf{A_1} = \begin{bmatrix} I \\ \breve{A} \\ \vdots \\ \breve{A}^N \end{bmatrix}, \mathbf{A_2} = \begin{bmatrix} 0 & 0 & \cdots & 0 \\ \breve{B} & 0 & \ddots & 0 \\ \vdots & \ddots & \ddots & \vdots \\ \breve{A}^{N-1}\breve{B} & \breve{A}^{N-1}\breve{B} & \cdots & 0 \end{bmatrix}, \tag{5.9b}$$

Substitute (5.8b) into (5.8a) and take partial derivative over the vector $\Delta\vec{\mathbf{u}}$ give the following:

$$\begin{aligned} \Delta J = &-(\breve{\mathbf{Q}}\breve{\mathbf{C}}\mathbf{A_2} + \breve{\mathbf{Q}}\breve{\mathbf{D}})^T\vec{\mathbf{r}} + (\breve{\mathbf{Q}}\breve{\mathbf{C}}\mathbf{A_2} + \breve{\mathbf{Q}}\breve{\mathbf{D}})^T\breve{\mathbf{C}}\mathbf{A_1}x_0 \\ &+ ((\breve{\mathbf{C}}\mathbf{A_2} + \breve{\mathbf{D}})^T\breve{\mathbf{Q}}(\breve{\mathbf{C}}\mathbf{A_2} + \breve{\mathbf{D}}) + \breve{\mathbf{R}})\Delta\vec{\mathbf{u}}. \end{aligned} \tag{5.10}$$

Notice

$$\breve{\mathbf{C}}\mathbf{A_2} + \breve{\mathbf{D}} = \breve{H}, \tag{5.11}$$

Set $\Delta J = 0$ gives the following result:

$$\begin{bmatrix} \Delta u_0 \\ \Delta u_1 \\ \vdots \\ \Delta u_N \end{bmatrix} = \mathbf{K} \left(\begin{bmatrix} r_0 \\ r_1 \\ \vdots \\ r_N \end{bmatrix} - \begin{bmatrix} \breve{C} \\ \breve{C}\breve{A} \\ \vdots \\ \breve{C}\breve{A}^N \end{bmatrix} \breve{x}_0 \right), \tag{5.12}$$

$$\mathbf{K} = (\breve{\mathbf{H}}^T \breve{\mathbf{Q}} \breve{\mathbf{H}} + \breve{\mathbf{R}})^{-1} (\breve{\mathbf{Q}} \breve{\mathbf{H}})^T. \tag{5.13}$$

□

5.3 Markov Parameters

Markov parameters of a system convey its transient properties and can be evaluated via many approaches. Let's start our discussion with the deterministic definitions of Markov parameters for the system (5.1):

$$H_0 = 0, H_i = CA^{i-1}B, i = 1, 2, \cdots, \tag{5.14a}$$

$$M_0 = 0, M_i = CA^{i-1}B_w, i = 1, 2, \cdots. \tag{5.14b}$$

There are quite a few methods to evaluate Markov parameters H_i and M_i without knowing the dynamics of (5.1). The most straightforward method would be an impulse experiment, as Markov parameters are equivalent to the impulse responses of a system. Another method would be the white noise which utilizes its stochastic definition (5.15). A least-square method to determine Markov parameters of a system employing input/output information is also given in [50].

$$H_i = E(y_{k+i} u_k^T) = \lim_{N \to \infty} \frac{1}{N} \sum_{k=0}^{N-1} y_{k+i} u_k^T, \tag{5.15a}$$

$$M_i = E(y_{k+i} w_k^T) = \lim_{N \to \infty} \frac{1}{N} \sum_{k=0}^{N-1} y_{k+i} w_k^T. \tag{5.15b}$$

Let's define the following Markov parameters $\breve{H}_1$ and $\breve{M}_i$ for the reconstructed system (5.3):

$$\breve{H}_0 = 0, \breve{H}_i = \breve{C}\breve{A}^{i-1}\breve{B}, i = 1, 2, \cdots, \tag{5.16a}$$

$$\breve{M}_0 = 0, \breve{M}_i = \breve{C}\breve{A}^{i-1}\breve{B}_w, i = 1, 2, \cdots. \tag{5.16b}$$

One may numerically evaluate $\breve{H}_i$ and $\breve{M}_i$ using information of H_i and M_i, as stated in the Lemma 5.3.1.

Lemma 5.3.1. *Markov parameters of (5.3) and (5.1) satisfy the following relationships:*

$$\breve{H}_i = \sum_{j=0}^{i} H_j, \tag{5.17a}$$

$$\breve{M}_i = M_i. \tag{5.17b}$$

Proof. One may observe the following patterns:

$$\breve{H}_0 = H_0, \tag{5.18a}$$

$$\breve{H}_1 = \breve{C}\breve{B} = CB = H_0 + H_1, \tag{5.18b}$$

$$\breve{H}_2 = \breve{C}\breve{A}\breve{B} = CAB + CB = H_0 + H_1 + H_2, \tag{5.18c}$$

$$\vdots$$

$$\breve{H}_i = \breve{C}\breve{A}^{i-1}\breve{B} = CA^{i-1}B + CA^{i-2}B + \cdots + CB = \sum_{j=0}^{i} H_j, \tag{5.18d}$$

$$\breve{M}_0 = M_0, \tag{5.18e}$$

$$\breve{M}_1 = \breve{C}\breve{B}_w = CB_w = M_1, \tag{5.18f}$$

$$\breve{M}_2 = \breve{C}\breve{A}\breve{B}_w = CAB_w = M_2, \tag{5.18g}$$

$$\vdots$$

$$\breve{M}_i = \breve{C}\breve{A}^{i-1}\breve{B}_w = CA^{i-1}B_w = M_i. \tag{5.18h}$$

□

5.4 Data-Based Control Law

In this section we introduce the complete data-based control law for reference tracking application, which requires Markov parameters $\breve{H}_i$ and $\breve{M}_i$ as defined in (5.16a) and (5.16b).

Theorem 5.4.1. *The data-based control law that minimizes the quadratic weighted cost function (5.6) over a finite horizon* $[0, N]$ *that requires the first* $N + 1$ *Markov parameters (5.14a) and (5.14b) is the following:*

$$u_k = \begin{cases} \Delta u_k & , k = 0 \\ u_{k-1} + \Delta u_k & , k > 0 \end{cases}, \tag{5.19a}$$

$$\begin{bmatrix} \Delta u_k \\ \Delta u_{k+1} \\ \vdots \\ \Delta u_N \end{bmatrix} = \mathbf{K}_k \left(\begin{bmatrix} r_k \\ r_{k+1} \\ \vdots \\ r_N \end{bmatrix} - \vec{\bar{\mathbf{x}}}_k \right), \tag{5.19b}$$

where

$$\mathbf{K}_k = (\breve{\mathbf{H}}_k^T \breve{\mathbf{Q}}_k \breve{\mathbf{H}}_k + \breve{\mathbf{R}}_k)^{-1} (\breve{\mathbf{Q}}_k \breve{\mathbf{H}}_k)^T, \tag{5.19c}$$

$$\vec{\bar{\mathbf{x}}}_k = \begin{cases} 0 & , \ k = 0 \\ \begin{bmatrix} -\mathbf{F}_k & I \end{bmatrix} \vec{\bar{\mathbf{x}}}_{k-1} + \mathbf{B}_k \Delta u_k + \mathbf{F}_k y_{k-1} & , \ k > 0 \end{cases}, \tag{5.19d}$$

$$\breve{\mathbf{H}}_k = \begin{bmatrix} \breve{H}_0 & 0 & \cdots & \cdots & 0 \\ \breve{H}_1 & \breve{H}_0 & \ddots & \ddots & \vdots \\ \breve{H}_2 & \breve{H}_1 & \ddots & \ddots & \vdots \\ \vdots & \vdots & \ddots & \ddots & \vdots \\ \breve{H}_{N-k} & \breve{H}_{N-k-1} & \cdots & \breve{H}_1 & \breve{H}_0 \end{bmatrix}, \tag{5.19e}$$

$$\breve{\mathbf{Q}}_k = \begin{bmatrix} Q & \cdots & \cdots & 0 \\ \vdots & \ddots & \ddots & \vdots \\ \vdots & \ddots & Q & \vdots \\ 0 & \cdots & \cdots & S \end{bmatrix}, \tag{5.19f}$$

$$\breve{\mathbf{R}}_k = \begin{bmatrix} R & \cdots & \cdots & 0 \\ \vdots & \ddots & \ddots & \vdots \\ \vdots & \ddots & R & \vdots \\ 0 & \cdots & \cdots & T \end{bmatrix}, \tag{5.19g}$$

$$\mathbf{F}_k = \mathbf{M}_k \mathbf{P}_k \mathbf{N}_k^T (V + \mathbf{N}_k \mathbf{P}_k \mathbf{N}_k^T)^{-1}, \tag{5.19h}$$

$$\mathbf{B}_k = \begin{bmatrix} \breve{H}_1 \\ \breve{H}_2 \\ \vdots \\ \breve{H}_{N-k+1} \end{bmatrix}, \tag{5.19i}$$

$$\mathbf{M}_k = \begin{bmatrix} \breve{M}_2 & \breve{M}_3 & \cdots & \breve{M}_{k+1} \\ \breve{M}_3 & \iddots & \iddots & \breve{M}_{k+2} \\ \vdots & \iddots & \iddots & \vdots \\ \breve{M}_{N-k+2} & \breve{M}_{N-k+3} & \cdots & \breve{M}_{N+1} \end{bmatrix}, \tag{5.19j}$$

$$\mathbf{N}_k = \begin{bmatrix} \breve{M}_1 & \breve{M}_2 & \cdots & \breve{M}_k \end{bmatrix}, \tag{5.19k}$$

$$\mathbf{P}_k = (\mathbf{W}_{k-1}^{-1} + \mathbf{T}_{k-1}^T \mathbf{V}_{k-1}^{-1} \mathbf{T}_{k-1})^{-1}, \tag{5.19l}$$

$$\mathbf{W}_{k-1} = diag(W), \quad W = E(w_k^T w_k), \tag{5.19m}$$

$$\mathbf{V}_{k-1} = diag(V), \quad V = E(v_k^T v_k), \tag{5.19n}$$

$$\mathbf{T}_{k-1} = \begin{bmatrix} \breve{M}_0 & \breve{M}_1 & \cdots & \cdots & \breve{M}_{k-1} \\ 0 & \breve{M}_0 & \ddots & \ddots & \breve{M}_{k-2} \\ \vdots & \ddots & \ddots & \ddots & \vdots \\ \vdots & \ddots & \ddots & \ddots & \breve{M}_1 \\ 0 & \cdots & \cdots & 0 & \breve{M}_0 \end{bmatrix}. \tag{5.19o}$$

Proof. Define the following variable:

$$\vec{\bar{\mathbf{x}}}_k = \begin{bmatrix} \breve{C} \\ \breve{C}\breve{A} \\ \vdots \\ \breve{C}\breve{A}^{N-k} \end{bmatrix} \breve{x}_k, \tag{5.20}$$

Then, we can write the following:

$$\breve{x}_{k+1} = \breve{A}\breve{x}_k + \breve{B}\Delta u_k + \mathbf{L}_k(y_k - \breve{C}\breve{x}_k), \tag{5.21}$$

where $\breve{x}_k$ is the estimation of the state $\breve{x}_k$, and L_k stands for the gain of the estimator. The following relation can be established [42]:

$$\begin{aligned} \vec{\bar{\mathbf{x}}}_k &= \begin{bmatrix} \breve{C}\breve{A} \\ \breve{C}\breve{A}^2 \\ \vdots \\ \breve{C}\breve{A}^{N-k+1} \end{bmatrix} \breve{x}_{k-1} + \begin{bmatrix} \breve{C}\breve{B} \\ \breve{C}\breve{A}\breve{B} \\ \vdots \\ \breve{C}\breve{A}^{N-k}\breve{B} \end{bmatrix} \Delta u_{k-1} + \begin{bmatrix} \breve{C} \\ \breve{C}\breve{A} \\ \vdots \\ \breve{C}\breve{A}^{N-k} \end{bmatrix} \mathbf{L}_{k-1}(y_{k-1} - \breve{C}\breve{x}_{k-1}) \\ &= \begin{bmatrix} -\begin{bmatrix} \breve{C} \\ \breve{C}\breve{A} \\ \vdots \\ \breve{C}\breve{A}^{N-k} \end{bmatrix} \mathbf{L}_{k-1} & I \end{bmatrix} \begin{bmatrix} \breve{C} \\ \breve{C}\breve{A} \\ \vdots \\ \breve{C}\breve{A}^{N-(k-1)} \end{bmatrix} \breve{x}_{k-1} + \begin{bmatrix} \breve{C}\breve{B} \\ \breve{C}\breve{A}\breve{B} \\ \vdots \\ \breve{C}\breve{A}^{N-k}\breve{B} \end{bmatrix} \Delta u_{k-1} + \begin{bmatrix} \breve{C} \\ \breve{C}\breve{A} \\ \vdots \\ \breve{C}\breve{A}^{N-k} \end{bmatrix} \mathbf{L}_{k-1} y_{k-1} \end{aligned}$$

$$= \begin{bmatrix} -\mathbf{F}_k & I \end{bmatrix} \vec{\tilde{\mathbf{x}}}_{k-1} + \mathbf{B}_k \Delta u_{k-1} + \mathbf{F}_k y_{k-1}, \tag{5.22}$$

where

$$\mathbf{F}_k = \begin{bmatrix} \breve{C} \\ \breve{C}\breve{A} \\ \vdots \\ \breve{C}\breve{A}^{N-k} \end{bmatrix} \mathbf{L}_{k-1}, \quad \mathbf{B}_k = \begin{bmatrix} \breve{C}\breve{B} \\ \breve{C}\breve{A}\breve{B} \\ \vdots \\ \breve{C}\breve{A}^{N-k}\breve{B} \end{bmatrix}. \tag{5.23}$$

The solution of the estimator gain can be expressed as the following [66]:

$$\mathbf{L}_{k-1} = \breve{A}\mathbf{Y}_{k-1}\breve{C}^T(V + \breve{C}\mathbf{Y}_{k-1}\breve{C}^T)^{-1}, \tag{5.24}$$
$$\mathbf{Y}_{k-1} = \mathbf{D}_{k-1}\mathbf{P}_k\mathbf{D}_{k-1}^T,$$

where:

$$\mathbf{D}_{k-1} = \begin{bmatrix} \breve{B}_w & \breve{A}\breve{B}_w & \cdots & \breve{A}^{k-1}\breve{B}_w \end{bmatrix}, \tag{5.25a}$$

$$\mathbf{P}_k = (\mathbf{W}_{k-1}^{-1} + \mathbf{T}_{k-1}^T\mathbf{V}_{k-1}^{-1}\mathbf{T}_{k-1})^{-1}, \tag{5.25b}$$

$$\mathbf{W}_{k-1} = diag(W), \quad W = E(w_k^T w_k), \tag{5.25c}$$

$$\mathbf{V}_{k-1} = diag(V), \quad V = E(v_k^T v_k), \tag{5.25d}$$

$$\mathbf{T}_{k-1} = \begin{bmatrix} \breve{D} & \breve{C}\breve{B}_w & \cdots & \cdots & \breve{C}\breve{A}^{k-2}\breve{B}_w \\ 0 & \breve{D} & \ddots & \ddots & \breve{C}\breve{A}^{k-3}\breve{B}_w \\ \vdots & \ddots & \ddots & \ddots & \vdots \\ \vdots & \ddots & \ddots & \ddots & \breve{C}\breve{B}_w \\ 0 & \cdots & \cdots & 0 & \breve{D} \end{bmatrix}. \tag{5.25e}$$

Applying Eq. (5.24) one may get the following expression:

$$\mathbf{F}_k = \mathbf{M}_k \mathbf{P}_k \mathbf{N}_k^T (V + \mathbf{N}_k \mathbf{P}_k \mathbf{N}_k^T)^{-1}, \tag{5.26a}$$

where:

$$\mathbf{M}_k = \begin{bmatrix} \breve{C}\breve{A}\breve{B}_w & \breve{C}\breve{A}^2\breve{B}_w & \cdots & \breve{C}\breve{A}^k\breve{B}_w \\ \breve{C}\breve{A}^2\breve{B}_w & \iddots & \cdots & \breve{C}\breve{A}^{k+1}\breve{B}_w \\ \vdots & \iddots & \iddots & \vdots \\ \breve{C}\breve{A}^{N-k+1}\breve{B}_w & \breve{C}\breve{A}^{N-k+2}\breve{B}_w & \cdots & \breve{C}\breve{A}^N\breve{B}_w \end{bmatrix}, \tag{5.26b}$$

$$\mathbf{N}_k = \begin{bmatrix} \breve{C}\breve{B}_w & \breve{C}\breve{A}\breve{B}_w & \cdots & \breve{C}\breve{A}^{k-1}\breve{B}_w \end{bmatrix}. \tag{5.26c}$$

□

5.5 Tensegrity Morphing Airfoil

5.5.1 Tensegrity

A tensegrity structure is a pre-stressed and stable structure composed of compressive members (bars or struts), and tensile members (strings or cables) [67]. Evidence from biological systems perhaps elucidates that tensegrity concepts yield the most efficient structures. For example, the molecular structure of cell surface, DNA bundles, spider fibers, and human elbows are all examples of internal tensegrity structures [68–71]. During its development, the tensegrity system has shown its advantages in properties lightweight, deployability, energy absorption, and promoting the integration of structural and control [72–80].

Due to the many benefits of tensegrity systems, control and robotics communities have developed many soft robots using the tensegrity paradigm in recent years. For example, Baines et al. presented their tensegrity rolling robots by soft membrane actuators [81]. Wang et al. derived a nonlinear dynamics-based control, and a decoupled data-based (D2C) LQR control law around the linearized open-loop trajectories [82]. Goyal et al. developed tensegrity robotics with gyro

actuators [83]. Begey et al. demonstrated two approaches, X-shaped tensegrity mechanisms and an analogy with scissor structures, to design tensegrity-based manipulators [84].

Compared with rigid airfoils, morphing airfoils are gaining significant interest from various researchers due to their advantage of excellent flexibility to different flight regimes. Although current approaches, such as flaps, slats, aileron, and wing-let, can help achieve the desired control objective, most of these efforts break the streamlined airfoil shape, which aerodynamics engineers carefully design. Other emerging methods, such as shape memory alloys and piezoelectric actuators, can also smoothly fulfill the morphing targets—however, most of them work at relatively low bandwidth and require heavy supporting equipment. A few attempts have been made to integrate topology design and control design towards a system point of view. For example, Chen et al. presented a design of tensegrity morphing airfoil and a nonlinear control approach to class-k tensegrity structures [85]. Shintake et al. designed a fish-like robot with tensegrity systems, driven by a waterproof servomotor [86]. This chapter also tries to demonstrate structural control with an application of reference tracking control for a tensegrity morphing airfoil by a data-based approach.

5.5.2 Airfoil Configuration

We connect the discrete points in a pattern similar to the structure of the vertebra. Figure 5.1 shows the procedure of discretization. Figure 5.2 gives the notation of nodes, bars, and strings of a tensegrity airfoil with any complexity q, where q represents the number of horizontal bars in a tensegrity structure. The discrete points on the surface of the airfoil (nodes $\boldsymbol{n}_{q+1}, \boldsymbol{n}_{q+2}, \cdots, \boldsymbol{n}_{3q+1}$) are determined by error bound spacing method developed in [85, 87]. They are defined as the maximum errors between the continuous surface shape where each straight-line segment is less than a specified value δ. The coordinate of node $\boldsymbol{n}_i$ ($i = 1, 2, \cdots, q$) is determined by the two nodes that are above or below this point with a same ratio $\mu \in (0, 1)$. The following analytical expression describes this relation:

$$\boldsymbol{n}_i = \mu \boldsymbol{n}_{q+1+i} + (1-\mu)\boldsymbol{n}_{2q+1+i}. \tag{5.27}$$

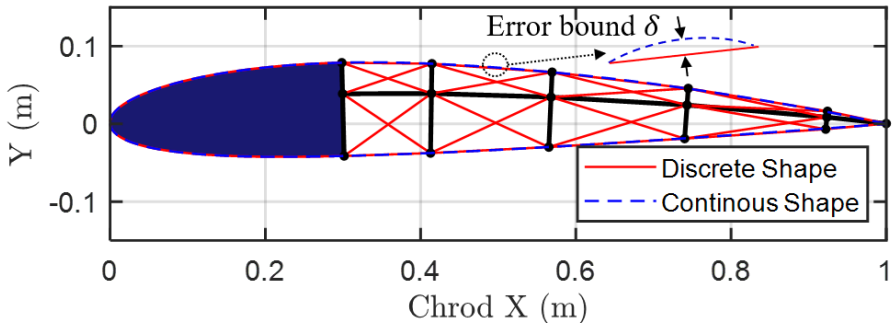

Figure 5.1: Tensegrity airfoil configuration, blue area is the rigid body, black and red lines are bars and strings.

We define N, B, S, C_b, C_s as the matrices for nodes, bars , strings, bar connectivity and string connectivity for a tensegrity airfoil with any complexity q, as shown in (5.28). The nodal matrix N consists of three components, where each column represents the x, y, and z coordinate of each node. C_S and C_B are connectivity matrices of strings and bars consisting of elements 0, -1, and 1, denoting the start and end node of a bar or string, where $\boldsymbol{b}_j$ ($j = 1, 2, \cdots, 3q$) and $\boldsymbol{s}_k$ ($k = 1, 2, \cdots, 6q-4$) are the jth bar and kth string. The bar and string matrices are the multiplications of nodal matrix and connectivity matrices sytisfying $B = NC_b^T$, $S = NC_s^T$. A function $tenseg\_ind2C.m$ is given to convert $C_{b_{in}}$ and $C_{s_{in}}$ to C_b and C_s [88].

$$N = \begin{bmatrix} \boldsymbol{n}_1 & \boldsymbol{n}_2 & \cdots & \boldsymbol{n}_{3q+1} \end{bmatrix}, \boldsymbol{n}_i = \begin{bmatrix} x_i & y_i & z_i \end{bmatrix}^T, \tag{5.28a}$$

$$B = \begin{bmatrix} \boldsymbol{b}_1 & \boldsymbol{b}_2 & \cdots & \boldsymbol{b}_{3q} \end{bmatrix}, \tag{5.28b}$$

$$S = \begin{bmatrix} \boldsymbol{s}_1 & \boldsymbol{s}_2 & \cdots & \boldsymbol{s}_{6q-4} \end{bmatrix}, \tag{5.28c}$$

$$C_{b_{in}} = \begin{cases} [i, i+1], \ 1 \le i \le q \\ [i-q, i+1], \ q+1 \le i \le 2q \\ [i-2q, i+1], \ 2q+1 \le i \le 3q \end{cases}, \tag{5.28d}$$

$$C_{s_{in}} = \begin{cases} [i+1+q, i+2+q],\ 1 \le i \le q-1 \\ [2q+1, q+1] \\ [q+i, i],\ 2 \le i \le q \\ [i, q+2+i],\ 1 \le i \le q-1 \\ [i, 2q+2+i],\ 1 \le i \le q-1 \\ [2q+i, i],\ 2 \le i \le q \\ [i+1+2q, i+2+2q],\ 1 \le i \le q-1 \\ [3q+1, q+1] \end{cases} . \tag{5.28e}$$

The nonlinear tensegrity dynamics using a finite element method is employed as the black box system to do the system identification, which is in the following vector form [89]:

$$\boldsymbol{M}\ddot{\boldsymbol{n}} + \boldsymbol{D}\dot{\boldsymbol{n}} + \boldsymbol{K}\boldsymbol{n} = \boldsymbol{f}_{ex} - \boldsymbol{g}, \tag{5.29}$$

$$\boldsymbol{M} = \frac{1}{6}(|\boldsymbol{C}|^T \hat{\boldsymbol{m}} |\boldsymbol{C}| + \lfloor |\boldsymbol{C}|^T \hat{\boldsymbol{m}} |\boldsymbol{C}| \rfloor) \otimes \mathbf{I}_3, \tag{5.30}$$

$$\boldsymbol{K} = (\boldsymbol{C}^T \hat{\boldsymbol{x}} \boldsymbol{C}) \otimes \mathbf{I}_3, \tag{5.31}$$

$$\boldsymbol{g} = \frac{g}{2}(|\boldsymbol{C}|^T \boldsymbol{m}) \otimes \begin{bmatrix} 0 & 0 & 1 \end{bmatrix}^T. \tag{5.32}$$

Here $\boldsymbol{n} \in \mathbb{R}^{3n_n}$ is the nodal coordinate vector for the whole structure where $\boldsymbol{n} = \begin{bmatrix} \boldsymbol{n}_1^T & \boldsymbol{n}_2^T & \cdots & \boldsymbol{n}_{3q+1}^T \end{bmatrix}^T$, connectivity matrix $\boldsymbol{C} = \begin{bmatrix} C_b^T & C_s^T \end{bmatrix}^T$, $\boldsymbol{M}$, $\boldsymbol{D}$, and $\boldsymbol{K}$ are mass, damping, and stiffness matrices, $\boldsymbol{m}$ is the mass vector of bars and strings ($\hat{\boldsymbol{m}}$ is a diagonal matrix), $\boldsymbol{f}_{ex}$ represents the external force on the structure nodes, and $\boldsymbol{g}$ represents the gravity vector where g is gravity constant.

5.5.3 Morphing target

A NACA 2412 is selected. Its chord length is $c = 1$ m where the first 0 ~ 0.3 m is the rigid part. The vertical bar length ratio is selected as $\mu = 1/3$, and error bound $\delta = 0.001$ m for generation of the tensegrity foil's initial generation [90]. This example has five horizontal bars thus $q = 5$. The

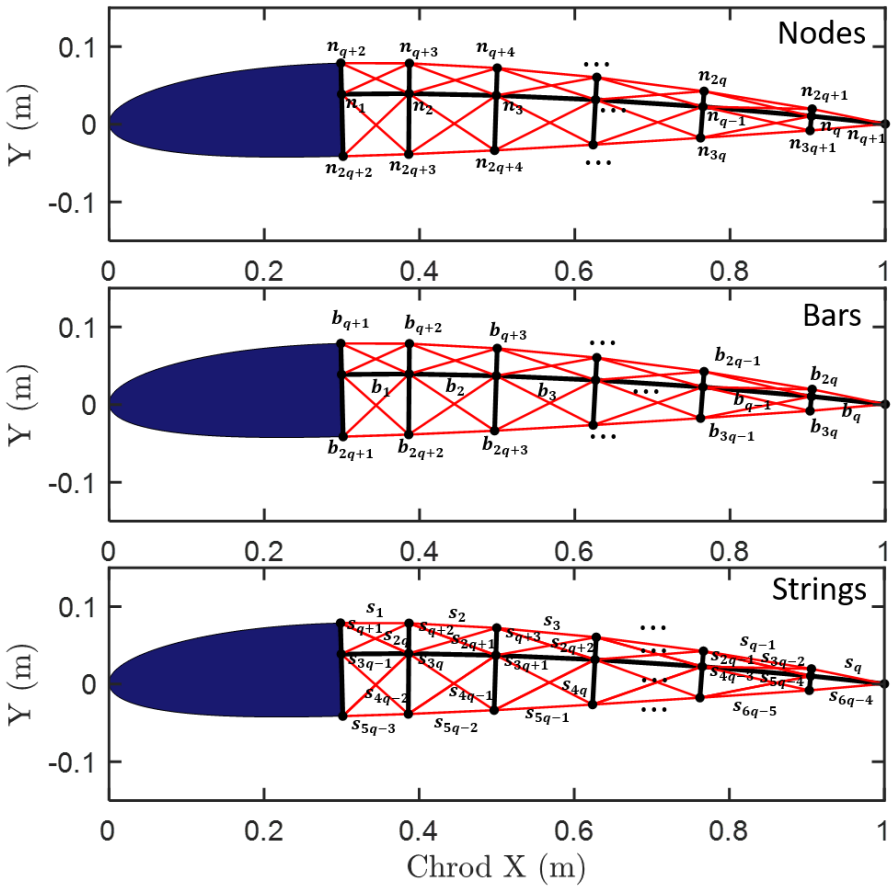

Figure 5.2: Node, bar, and string notations of a tensegrity airfoil with complexity q.

target configuration is generated by rotating the horizontal bars $\boldsymbol{b}_1, \boldsymbol{b}_2, \cdots, \boldsymbol{b}_5$ for angles $\theta_1 = \frac{\pi}{72}$, $\theta_2 = \frac{\pi}{36}$,$\theta_3 = \frac{3\pi}{72}$, $\theta_4 = \frac{\pi}{18}$ $\theta_5 = \frac{5\pi}{72}$. The rotation motions are assumed linear and lengths of every bar are assumed unchanged during deformation. Vertical bars remain perpendicular to the horizontal bars. Figure 5.3 depicts the initial configuration and target configuration.

5.5.4 Data experiment and results

A black box system that contains the dynamics of the tensegrity airfoil shown has been constructed, which accepts 26 input signals and returns 26 output signals. Its Markov parameters have been evaluated via black box experiments Eq. (5.15), and control sequences have been computed using Eq. (5.19) to track a reference configuration. Figure 5.4 shows the configuration of the morphing airfoil at $T = 0s, 0.5s$ and $1s$. Figures 5.5 and 5.6 show the node errors in x and y

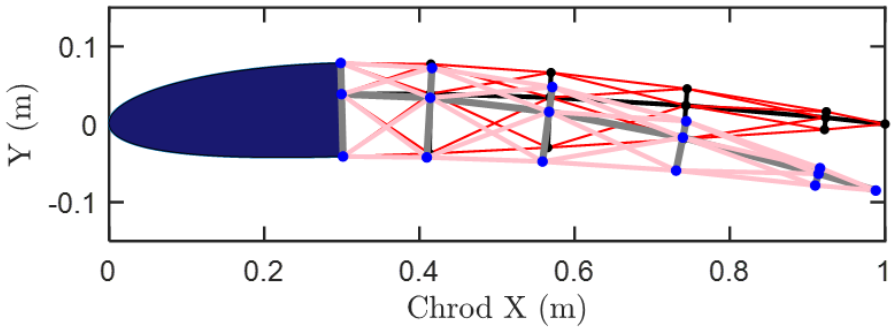

Figure 5.3: Initial and morphing configuration of the tensegrity NACA 2412 airfoil, top one (bars in black, strings in red, and nodes in black) is the initial state, and the bottom one (bars in grey, strings in pink, and nodes in blue) is the morphing target.

coordinates during the control process. These errors decrease and converge to zero as the control process approaches the final step. A bump occurs at the beginning of the control process. This is because the state estimator takes effect at the second step, and the control algorithm takes effect at the third step. Figure 5.7 shows the change of the string lengths during the control process. The result demonstrates a successful morphing control for the tensegrity airfoil.

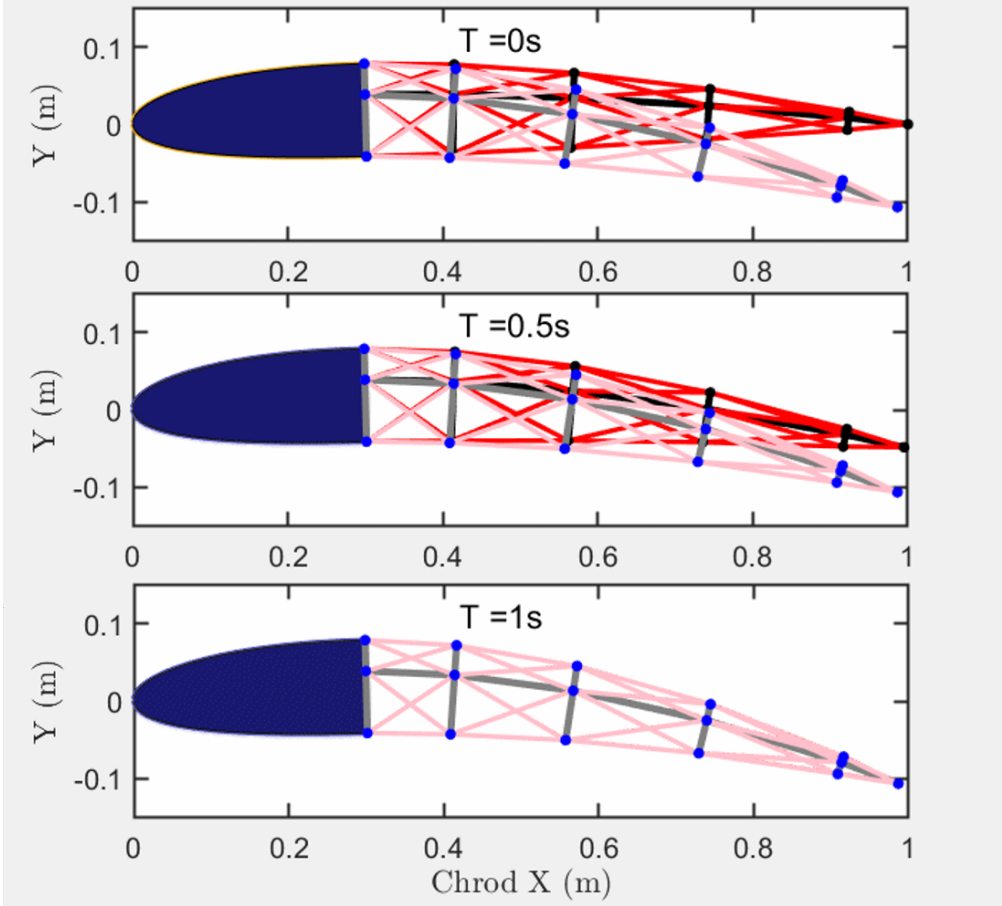

Figure 5.4: Time history of the tensegrity morphing airfoil at T = 0s, 0.5s, and 1s.

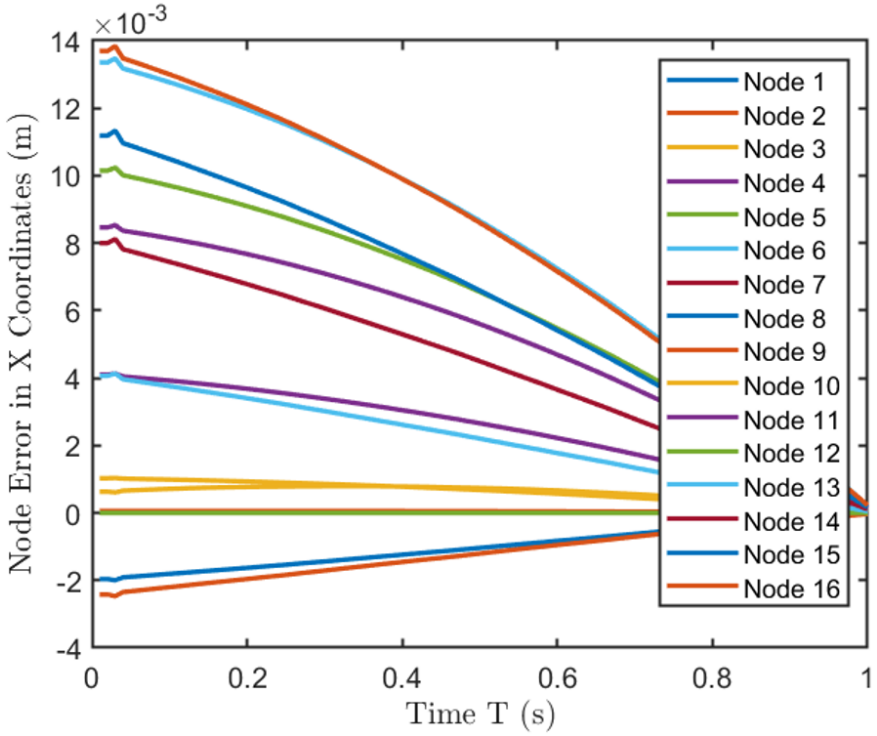

Figure 5.5: Node error in x coordinate during control process.

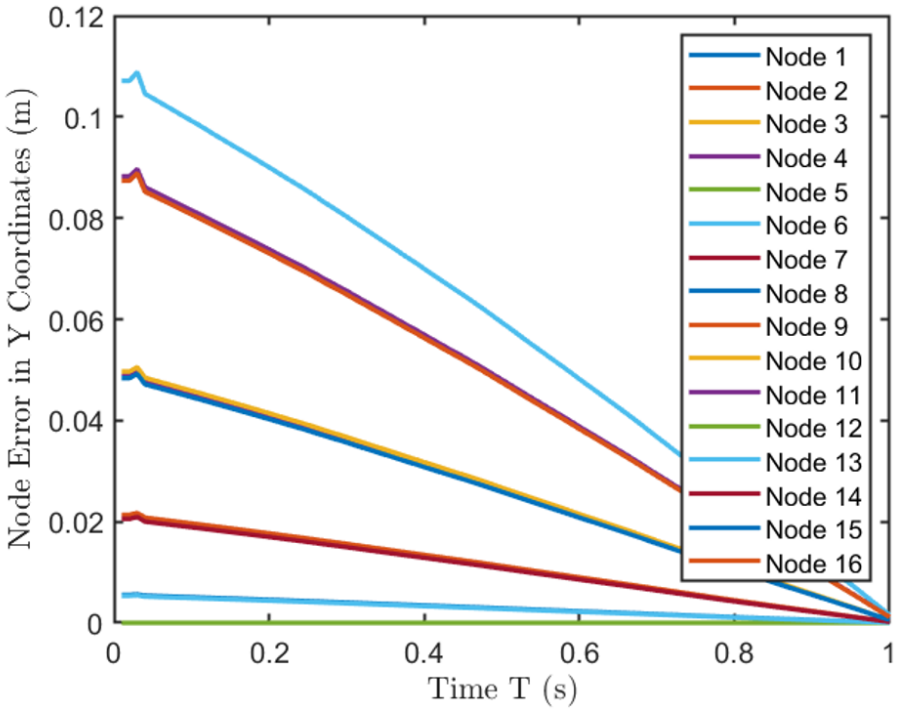

Figure 5.6: Node error in y coordinate during control process.

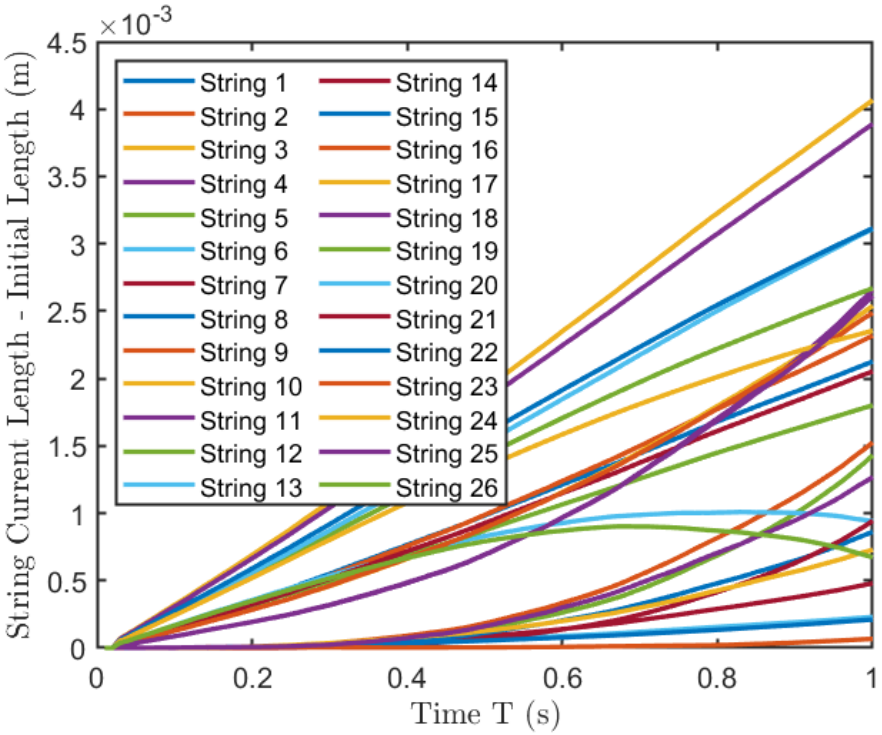

Figure 5.7: String length time history, string current length minus string initial length v.s. time.

5.6 Conclusions

This chapter presents an optimal data-based reference tracking controller design that uses the knowledge of the first $N + 1$ Markov parameters. This design finds an optimal control sequence minimizing a quadratic cost function concerning tracking error and input increments. The only necessary knowledge, Markov parameters, can be evaluated from the input/output experimental data from the system one aims to control. Accordingly, this design does not require any explicit information regarding the dynamics of the system to control. Result demonstrates a successful reference tracking control of a tensegrity morphing airfoil.

6. SUMMARY AND CONCLUSIONS

This dissertation delivers innovative contributions to the system identification problem using the q-Markov Covariance Equivalent (QMC) method, the simulation problem considering finite precision effects, and the data-based control problem for reference tranking applications.

The identification of unstable or marginally stable systems using the QMC method has been addressed in Chapter 2. Existing QMC methods do not apply to unstable or marginally stable system identifications. We repaired this deficiency by introducing the closed-loop observer dynamics into a unique formulation of the QMC dynamics. By feeding the outputs into the states, the observer system is guaranteed asymptotically stable via pole placements. This unique QMC formulation enables us to find an approximation system with identical nature of stability to the system one aims to identify. A method to reconstruct state-space QMC systems from observer QMC systems is presented.

The identification problem of finding the best QMC solution which matches the pre-specified data set using minimal data has been addressed in Chapter 3. Parametrization of existing QMC methods finds all solutions that match the given data set. We propose a new selection criterion to find the most efficient QMC, then prove it matches the transfer function of the system to identify. Combining with the unstable QMC formulation in Chapter 2, we propose a general QMC theorem and a generalized algorithm for system identification using QMC methods.

The system simulation problem of finding the most optimal simulation model with the existence of round-off errors, disturbance, and measurement noise has been addressed in Chapter 4. First, We transform this problem into a set of linear matrix inequalities (LMIs) along with a coupling non-convex constraint. A convexifying algorithm is applied to the non-convex constraint. Solving the problem via the LMI toolbox guarantees the convergence of the local optimum. Next, focus on the simulation applications of flexible structures in modal coordinates. We find the simulation model with the optimal size via truncation of modes. By introducing the QMC method, We further extend both methods to dynamic simulations of a non-linear system.

The system control problem of finding an optimal control sequence using a data-based technique for reference tracking applications has been addressed in Chapter 5. This control sequence minimizes a weighted quadratic cost function over a finite horizon $[0, N]$, and requires only information of Markov parameters up to $N + 1$. We apply this data-based technique on the control of a 2D tensegrity morphing airfoil for demonstration.

REFERENCES

[1] J.-N. Juang, *Applied system identification*. Prentice-Hall, Inc., 1994.

[2] M. Ohlberger and S. Rave, "Reduced basis methods: Success, limitations and future challenges," *arXiv preprint arXiv:1511.02021*, 2015.

[3] B. Ho and R. E. Kálmán, "Effective construction of linear state-variable models from input/output functions," *at-Automatisierungstechnik*, vol. 14, no. 1-12, pp. 545–548, 1966.

[4] J. N. Juang and R. S. Pappa, "An eigensystem realization algorithm for modal parameter identification and model reduction," *Journal of Guidance, Control, and Dynamics*, vol. 8, no. 5, pp. 620–627, 1985.

[5] P. J. Schmid, "Dynamic mode decomposition of numerical and experimental data," *Journal of Fluid Mechanics*, vol. 656, pp. 5–28, 2010.

[6] K. Liu and R. Skelton, "A new formulation of q-markov covariance equivalent realization," *Applied mathematics and computation*, vol. 53, no. 1, pp. 83–95, 1993.

[7] K. Liu and R. E. Skelton, "Q-markov covariance equivalent realization and its application to flexible structure identification," *Journal of Guidance, Control, and Dynamics*, vol. 16, no. 2, pp. 308–319, 1993.

[8] S. B. Kim, B. Spencer Jr, and C.-B. Yun, "Frequency domain identification of multi-input, multi-output systems considering physical relationships between measured variables," *Journal of Engineering Mechanics*, vol. 131, no. 5, pp. 461–472, 2005.

[9] J.-N. Juang, J. Cooper, and J. Wright, "An eigensystem realization algorithm using data correlations (era/dc) for modal parameter identification," 1987.

[10] B. Anderson and R. Skelton, "The generation of all q-markov covers," *IEEE transactions on circuits and systems*, vol. 35, no. 4, pp. 375–384, 1988.

[11] A. M. King, U. B. Desai, and R. E. Skelton, "A generalized approach to q-markov covariance equivalent realizations for discrete systems," *Automatica*, vol. 24, no. 4, pp. 507–515, 1988.

[12] K. Liu, R. Skelton, and J. Sharkey, "Modeling hubble space telescope flight data by q-markov cover identification," in *1992 American Control Conference*, pp. 1961–1965, IEEE, 1992.

[13] K. Liu and R. Skelton, "Identification and control of nasa's aces structure," in *1991 American Control Conference*, pp. 3000–3006, IEEE, 1991.

[14] K. Liu, R. Skelton, and L. Peterson, "Q-markov cover identification with frequency partition for modal analysis of hubble telescope flight data," in *9th Conference International Modal Analysis Conference (IMAC)*, vol. 1, pp. 750–756, 1991.

[15] G. Zhu, K. M. Grigoriadis, and R. E. Skelton, "Covariance control design for the hst," *NASA STI/Recon Technical Report A*, vol. 95, pp. 519–538, 1993.

[16] M. Moonen, B. De Moor, L. Vandenberghe, and J. Vandewalle, "On-and off-line identification of linear state-space models," *International Journal of Control*, vol. 49, no. 1, pp. 219–232, 1989.

[17] J.-S. Lew, J.-N. Juang, and R. W. Longman, "Comparison of several system identification methods for flexible structures," *Journal of Sound and Vibration*, vol. 167, no. 3, pp. 461–480, 1993.

[18] R. E. Skelton and G. Shi, "Iterative identification and control using a weighted q-markov cover with measurement noise," *Signal Processing*, vol. 52, no. 2, pp. 217–234, 1996.

[19] G. G. Zhu, R. E. Skelton, and P. Li, "Q-markov cover identification using pseudo-random binary signals," *International Journal of Control*, vol. 62, no. 6, pp. 1273–1290, 1995.

[20] F. Li and R. E. Skelton, "q-markov covariance equivalent realizations in fixed and floating point computations," *International Journal of Control*, vol. 81, no. 4, pp. 607–625, 2008.

[21] M. Majji, "Time varying covariance equivalent realizations," in *2018 Annual American Control Conference (ACC)*, pp. 283–287, IEEE, 2018.

[22] C. Mullis and R. Roberts, "Synthesis of minimum roundoff noise fixed point digital filters," *IEEE transactions on Circuits and Systems*, vol. 23, no. 9, pp. 551–562, 1976.

[23] S. Hwang, "Minimum uncorrelated unit noise in state-space digital filtering," *IEEE Transactions on Acoustics, Speech, and Signal Processing*, vol. 25, no. 4, pp. 273–281, 1977.

[24] D. Williamson and R. E. Skelton, "Optimal q-markov cover for finite wordlength implementation," *Mathematical systems theory*, vol. 22, no. 1, pp. 255–273, 1989.

[25] P. Benner and P. Goyal, "Balanced truncation model order reduction for quadratic-bilinear control systems," *arXiv preprint arXiv:1705.00160*, 2017.

[26] T. Reis and T. Stykel, "Balanced truncation model reduction of second-order systems," *Mathematical and Computer Modelling of Dynamical Systems*, vol. 14, no. 5, pp. 391–406, 2008.

[27] K. Liu and R. Skelton, "Optimal controllers for finite wordlength implementation," in *1990 American Control Conference*, pp. 1935–1940, IEEE, 1990.

[28] G. Zhu, K. M. Grigoriadis, and R. E. Skelton, "Covariance control design for hubble space telescope," *Journal of Guidance, Control, and Dynamics*, vol. 18, no. 2, pp. 230–236, 1995.

[29] M. Gevers and G. Li, *Parametrizations in control, estimation and filtering problems: accuracy aspects*. Springer Science & Business Media, 2012.

[30] G. Obinata and B. D. Anderson, *Model reduction for control system design*. Springer Science & Business Media, 2012.

[31] H. T. Odum and E. C. Odum, *Modeling for all scales: an introduction to system simulation*. Elsevier, 2000.

[32] M. Rosenblum, S. A. Herrod, E. Witchel, and A. Gupta, "Complete computer system simulation: The simos approach," *IEEE Parallel & Distributed Technology: Systems & Applications*, vol. 3, no. 4, pp. 34–43, 1995.

[33] F. Li and R. E. Skelton, "Simulation study via output feedback control design," in *2004 43rd IEEE Conference on Decision and Control (CDC) (IEEE Cat. No. 04CH37601)*, vol. 1, pp. 784–789, IEEE, 2004.

[34] F. Li, *Economic resource allocation in system simulation and control design*. University of California, San Diego, 2006.

[35] R. K. Lim and M. Q. Phan, "Identification of a multistep-ahead observer and its application to predictive control," *Journal of guidance, control, and dynamics*, vol. 20, no. 6, pp. 1200–1206, 1997.

[36] M. G. Safonov and T.-C. Tsao, "The unfalsified control concept and learning," *IEEE Transactions on Automatic Control*, vol. 42, no. 6, pp. 843–847, 1997.

[37] H. Zhang, L. Cui, X. Zhang, and Y. Luo, "Data-driven robust approximate optimal tracking control for unknown general nonlinear systems using adaptive dynamic programming method," *IEEE Transactions on Neural Networks*, vol. 22, no. 12, pp. 2226–2236, 2011.

[38] J. L. Proctor, S. L. Brunton, and J. N. Kutz, "Dynamic mode decomposition with control," *SIAM Journal on Applied Dynamical Systems*, vol. 15, no. 1, pp. 142–161, 2016.

[39] R. Wang, K. S. Parunandi, D. Yu, D. Kalathil, and S. Chakravorty, "Decoupled data-based approach for learning to control nonlinear dynamical systems," *IEEE Transactions on Automatic Control*, 2021.

[40] L. Ljung, "System identification, theory for the user, information and system science series," *Englewood Cliffs*, 1987.

[41] K. Furuta, M. Wongsaisuwan, and H. Werner, "Dynamic compensator design for discrete-time lqg problem using markov parameters," in *Proceedings of 32nd IEEE Conference on Decision and Control*, pp. 96–101, IEEE, 1993.

[42] G. Shi and R. E. Skelton, "Markov data-based lqg control," *J. Dyn. Sys., Meas., Control*, vol. 122, no. 3, pp. 551–559, 2000.

[43] W. Aangenent, M. Steinbuch, de Jager (AG), D. Kostic, and A. Lefeber, *Data-based LQG control*. Technische Universiteit Eindhoven, 2003.

[44] H. Kwakernaak and R. Sivan, *Linear optimal control systems*, vol. 1. Wiley-interscience New York, 1972.

[45] F. L. Lewis, D. Vrabie, and V. L. Syrmos, *Optimal control*. John Wiley & Sons, 2012.

[46] J. A. Gubner, *Probability and random processes for electrical and computer engineers*. Cambridge University Press, 2006.

[47] R. Bracewell, "Pentagram notation for cross correlation. the fourier transform and its applications," *New York: McGraw-Hill*, vol. 46, p. 243, 1965.

[48] C. Wang, "Kernel learning for visual perception," *PhD thesis*, 2019.

[49] D. Luenberger, "An introduction to observers," *IEEE Transactions on Automatic Control*, vol. 16, no. 6, pp. 596–602, 1971.

[50] J. N. Juang, M. Phan, L. G. Horta, and R. W. Longman, "Identification of observer/kalman filter markov parameters-theory and experiments," *Journal of Guidance, Control, and Dynamics*, vol. 16, no. 2, pp. 320–329, 1993.

[51] M. Majji, J. N. Juang, and J. L. Junkins, "Observer/kalman-filter time-varying system identification," *Journal of Guidance, Control, and Dynamics*, vol. 33, no. 3, pp. 887–900, 2010.

[52] M. Phan, L. G. Horta, J. N. Juang, and R. W. Longman, "Linear system identification via an asymptotically stable observer," *Journal of Optimization Theory and Applications*, vol. 79, no. 1, pp. 59–86, 1993.

[53] A. M. Lyapunov, "The general problem of the stability of motion," *International journal of control*, vol. 55, no. 3, pp. 531–534, 1992.

[54] M. Q. Phan, *Identification of linear systems by an asymptotically stable observer*, vol. 3164. National Aeronautics and Space Administration, 1992.

[55] R. E. Skelton, T. Iwasaki, and K. Grigoriadis, "A unified algebraic approach to linear control design," 2013.

[56] G. Strang, G. Strang, G. Strang, and G. Strang, *Introduction to linear algebra*, vol. 3. Wellesley-Cambridge Press Wellesley, MA, 1993.

[57] T. Kailath, A. H. Sayed, and B. Hassibi, *Linear estimation*. No. BOOK, Prentice Hall, 2000.

[58] J. O. Smith, *Introduction to digital filters: with audio applications*, vol. 2. Julius Smith, 2007.

[59] J. L. Junkins, *Introduction to dynamics and control of flexible structures*. Aiaa, 1993.

[60] J. G. Proakis, *Digital signal processing: principles algorithms and applications*. Pearson Education India, 2001.

[61] K. Liu, R. E. Skelton, and K. Grigoriadis, "Optimal controllers for finite wordlength implementation," *IEEE Transactions on Automatic Control*, vol. 37, no. 9, pp. 1294–1304, 1992.

[62] J. Gallier *et al.*, "The schur complement and symmetric positive semidefinite (and definite) matrices (2019)," *URL https://www. cis. upenn. edu/jean/schur-comp. pdf*, 2020.

[63] F. Zhang, *The Schur complement and its applications*, vol. 4. Springer Science & Business Media, 2006.

[64] M. De Oliveira, J. F. Camino, and R. E. Skelton, "A convexifying algorithm for the design of structured linear controllers," in *Proceedings of the 39th IEEE Conference on Decision and Control (Cat. No. 00CH37187)*, vol. 3, pp. 2781–2786, IEEE, 2000.

[65] J. B. Rawlings, D. Q. Mayne, and M. Diehl, *Model predictive control: theory, computation, and design*, vol. 2. Nob Hill Publishing Madison, WI, 2017.

[66] K. Furuta and M. Wongsaisuwan, "Closed-form solutions to discrete-time lq optimal control and disturbance attenuation," *Systems & control letters*, vol. 20, no. 6, pp. 427–437, 1993.

[67] R. E. Skelton and M. C. De Oliveira, *Tensegrity systems*, vol. 1. Springer, 2009.

[68] N. Wang, K. Naruse, D. Stamenović, J. J. Fredberg, S. M. Mijailovich, I. M. Tolić-Nørrelykke, T. Polte, R. Mannix, and D. E. Ingber, "Mechanical behavior in living cells

consistent with the tensegrity model," *Proceedings of the National Academy of Sciences*, vol. 98, no. 14, pp. 7765–7770, 2001.

[69] T. Liedl, B. Högberg, J. Tytell, D. E. Ingber, and W. M. Shih, "Self-assembly of three-dimensional prestressed tensegrity structures from dna," *Nature nanotechnology*, vol. 5, no. 7, pp. 520–524, 2010.

[70] A. H. Simmons, C. A. Michal, and L. W. Jelinski, "Molecular orientation and two-component nature of the crystalline fraction of spider dragline silk," *Science*, vol. 271, no. 5245, pp. 84–87, 1996.

[71] G. Scarr, "A consideration of the elbow as a tensegrity structure," *International Journal of Osteopathic Medicine*, vol. 15, no. 2, pp. 53–65, 2012.

[72] M. Chen and R. E. Skelton, "A general approach to minimal mass tensegrity," *Composite Structures*, p. 112454, 2020.

[73] S. Ma, M. Chen, and R. E. Skelton, "Design of a new tensegrity cantilever structure," *Composite Structures*, p. 112188, 2020.

[74] M. Chen, R. Goyal, M. Majji, and R. E. Skelton, "Deployable tensegrity lunar tower," *arXiv preprint arXiv:2009.12958*, 2020.

[75] K. Yıldız and G. A. Lesieutre, "Deployment of n-strut cylindrical tensegrity booms," *Journal of Structural Engineering*, vol. 146, no. 11, p. 04020247, 2020.

[76] K. Garanger, I. del Valle, M. Rath, M. Krajewski, U. Raheja, M. Pavone, and J. J. Rimoli, "Soft tensegrity systems for planetary landing and exploration," *arXiv preprint arXiv:2003.10999*, 2020.

[77] M. R. Sunny, C. Sultan, and R. K. Kapania, "Optimal energy harvesting from a membrane attached to a tensegrity structure," *AIAA journal*, vol. 52, no. 2, pp. 307–319, 2014.

[78] M. Chen, R. Goyal, M. Majji, and R. E. Skelton, "Design and analysis of a growable artificial gravity space habitat," *Aerospace Science and Technology*, vol. 106, p. 106147, 2020.

[79] W.-Y. Li, H. Nabae, G. Endo, and K. Suzumori, "New soft robot hand configuration with combined biotensegrity and thin artificial muscle," *IEEE Robotics and Automation Letters*, vol. 5, no. 3, pp. 4345–4351, 2020.

[80] A. P. Sabelhaus, A. H. Li, K. A. Sover, J. R. Madden, A. R. Barkan, A. K. Agogino, and A. M. Agogino, "Inverse statics optimization for compound tensegrity robots," *IEEE Robotics and Automation Letters*, vol. 5, no. 3, pp. 3982–3989, 2020.

[81] R. L. Baines, J. W. Booth, and R. Kramer-Bottiglio, "Rolling soft membrane-driven tensegrity robots," *IEEE Robotics and Automation Letters*, vol. 5, no. 4, pp. 6567–6574, 2020.

[82] R. Wang, R. Goyal, S. Chakravorty, and R. E. Skelton, "Model and data based approaches to the control of tensegrity robots," *IEEE Robotics and Automation Letters*, vol. 5, no. 3, pp. 3846–3853, 2020.

[83] R. Goyal, M. Chen, M. Majji, and R. E. Skelton, "Gyroscopic tensegrity robots," *IEEE Robotics and Automation Letters*, vol. 5, no. 2, pp. 1239–1246, 2020.

[84] J. Begey, M. Vedrines, and P. Renaud, "Design of tensegrity-based manipulators: Comparison of two approaches to respect a remote center of motion constraint," *IEEE Robotics and Automation Letters*, vol. 5, no. 2, pp. 1788–1795, 2020.

[85] M. Chen, J. Liu, and R. E. Skelton, "Design and control of tensegrity morphing airfoils," *Mechanics Research Communications*, vol. 103, p. 103480, 2020.

[86] J. Shintake, D. Zappetti, T. Peter, Y. Ikemoto, and D. Floreano, "Bio-inspired tensegrity fish robot," in *2020 IEEE International Conference on Robotics and Automation (ICRA)*, pp. 2887–2892, IEEE, 2020.

[87] M. Chen, *Soft Robotics By Integrating Structure, Materials, Fluids, Control Design, and Signal Processing Using the Tensegrity Paradigm*. PhD thesis, 2021.

[88] R. Goyal, M. Chen, M. Majji, and R. E. Skelton, "Motes: Modeling of tensegrity structures," *Journal of Open Source Software*, vol. 4, no. 42, p. 1613, 2019.

[89] S. Ma, M. Chen, and R. E. Skelton, "Tensegrity system dynamics based on finite element method," *Composite Structures*, under view.

[90] E. S. Saxena and M. R. Kumar, "Design of naca 2412 and its analysis at different angle of attacks, reynolds numbers, and a wind tunnel test," *International Journal of Engineering Research and General Science*, vol. 3, no. 2, pp. 193–200, 2015.